U.PORTO
FEUP FACULDADE DE ENGENHARIA
UNIVERSIDADE DO PORTO

U.PORTO
INSTITUTO DE CIÊNCIAS
BIOMÉDICAS ABEL SALAZAR
UNIVERSIDADE DO PORTO

Multifunctional Cell-Instructive Pectin Hydrogels for Wound Healing Applications

Eduardo Filipe Mendes Capitão

Dissertation for the Degree of Master of Science in Bioengineering at Faculdade de Engenharia da Universidade and Instituto de Ciências Biomédicas Abel Salazar da Universidade do Porto

Multifunctional Cell-Instructive Pectin Hydrogels for Wound Healing Application

Eduardo Filipe Mendes Capitão

Dissertation for the Degree of Master of Science in Bioengineering at Faculdade de Engenharia da Universidade and Instituto de Ciências Biomédicas Abel Salazar da Universidade do Porto

Integrated Master in Bioengineering

Supervisor: Aureliana Sousa

Co-Supervisor: Cristina Barrias

July 2020

© Eduardo Filipe Mendes Capitão, July 2020

“We have the best chance of
communicating our thoughts
if we are sincere and speak
from the heart,
without hidden intent.”

Wu Wei, I Ching

Page intentionally left in blank

Acknowledgements

First, I have to thank to Prof. Pedro Granja, Biofabrication Group Leader, for accepting me in the former Biomaterials for Multistage Drug and Cell Delivery (Biocarrier) group and considerer my nursing background an asset to the group.

I have to thank Filipa for taking the lead as my supervisor, for openness to my thoughts and acceptance of my ideas, allowing me to explore them. Thank you for your guidance through this process, your support, your kindness, your friendship and your comprehension with my constantly changing work schedule and my inability to meet deadlines.

I would like to thank Sara Neves for helping me in the beginning of this journey and introduce me to an all new world of biomaterial's sciences and share with me her expertise.

To Mariana Neves, thank you for your friendship, your availability to helping me, even in the most nonsense questions that constantly blocked my rational thinking.

To Manuel Barros, thank you for friendship and your availability to help and technical support provided.

I would like to thank to Cassilda Reis, for welcoming me in her lab, for your teaching's, your support and for being always available to help.

To Marco Araújo for the help in chemical stuff and chemical analysis.

To Rafaela Presa e Filipa Serôdio, thank you for all the support, teamwork and companionship.

Thank you to the support of all members of the Biofabrication group.

I would like to thank to Prof. Cristina Barrias and all members of the Bioengineered 3D Microenvironments group, for good work environment and cooperative spirit.

I would like to thank with all my heart to my family, mom, dad, sisters and brother, for always supporting my decisions and choices, for give strength to carry on with this journey. To my nephews Filipa, Joana e Tiago for always making laugh and happy and in touch with my inner child.

To my best friend and traveler companion Vítor Sousa, thank you for support, for being there when I needed and helping me relax when I most needed.

Thank you all

The work described here was financially supported by FEDER - Fundo Europeu de Desenvolvimento Regional funds through the COMPETE 2020 - Operacional Programme for Competitiveness and Internationalisation (POCI), Portugal 2020, and

Portuguese funds through FCT - Fundação para a Ciência e a Tecnologia/ Ministério da Ciência, Tecnologia e Ensino Superior in the framework of the Project SkinPrint: **PTDC/BBB-ECT/2145/2014**.

Abstract

The development of wound healing strategies and skin-replacing constructs has been a major issue tackled by Tissue Engineering (TE) in the development of treatment strategies and scaffolds for skin tissue engineering constructs, over the years. Wound healing is a complex, highly biochemically regulated process which is dependent on the perfect interaction and communication between skin cells, immune cells and growth factors. Wounds are associated with increased morbidity, painful treatments, high costs thus impacting negatively the patient's overall quality of life. Considering the current available wound healing treatment options, hydrogel-based therapies are one of the most successful and versatile option enabling physical and chemical modification of biomaterials to adapt to each patient needs´.

Hydrogels are 3D hydrophilic, cross-linked polymeric networks, with soft texture, high absorption capacity of water and wound exudate, mainly composed by water, mimicking the ECM structure. Pectin is a natural polymer (polysaccharide), derived from plant cell wall, which forms a complex branched macromolecule. Pectin was already successfully used to produce hydrogels allowing the fine tune of the physical and mechanical properties and the possibility of being functionalized with different molecules and peptides. Catechol-based hydrogels mimic the adhesion mechanism of the marine mussel's that has the ability to firmly adhere to surfaces, through the secretion of mussel adhesive proteins. This strong adhesion is mediated by amino acid 3,4-dihydroxyphenylalanine (DOPA) that undergoes oxidative chemical cross-linking, establishing chemical interactions with surfaces providing the adhesion properties.

The aim of this work is the development of pectin hydrogels functionalized with dopamine. This strategy is envisaged to allow improved mechanical and adhesive properties for wound healing applications. Using carbodiimide chemistry system, we were able to successfully engraft dopamine molecules within the pectin structure. The dopamine-grafted pectin was structural and chemically characterized. Furthermore, the hydrogels produced with these newly synthetized polymers were characterized in terms of viscoelastic properties, gelation and adhesive properties. The results showed that the dopamine modified hydrogels have an increased stiffness with the increasing of the elastic components of the shear modulus (G'), depending on the concentration of dopamine in the hydrogels. The gelation properties were optimized, introducing a nanoparticulated calcium source (CalEssence® 70), and the results reveal an instantaneous gelation profile with this optimization. Concerning the adhesive properties of the hydrogel, the adhesion tests performed did not allow the obtention of conclusive

results. The dopamine modified hydrogels were cultured with HDNFs over 14 days, and cell viability, metabolic activity and morphology were assessed at different time points. Overall, dopamine modified pectin hydrogels provide favorable microenvironment for 3D cell culture, supporting cell adhesion, viability and proliferation for up to 14 days.

Altogether, the obtained results, suggest that this dopamine functionalized pectin hydrogel is able to fulfil the needs of a promising injectable hydrogel system, with instantaneous *in-situ* gelation, providing the platform for the future development of improved wound healing hydrogels.

Page intentionally left in blank

Table of Contents

Acknowledgements vii

Abstract ix

Abbreviation List xv

List of figures xvi

List of tables xviii

Introduction 19

1 Skin Anatomy and Physiology 19

2 Biology of Wound Healing 21

2.1 Haemostasis 21

2.2 Inflammation 22

2.3 Proliferation – Granulation Tissue Formation 23

2.4 Remodeling – Scar Formation 23

3 Regenerative Medicine and Skin Tissue Engineering for Wound Healing 26

4 Hydrogel-Based Strategies for Wound Healing 31

5 Pectin Structure and Wound Healing Applications 33

6 Mussel Inspired Catechol - Functionalized Hydrogels 35

6.1 Mussel Adhesive Proteins 35

6.2 Catechol-Based Hydrogel Synthesis 36

6.3 Catechol-Based Hydrogel Medical Applications 37

7 Problem Statement and Aim of this Work 41

Materials and Methods 42

1 Pectin Purification 42

2 Contaminants Assessment 42

2.1 Protein quantification 42

2.2 Polyphenol quantification 43

3 Preparation of Pectin hydrogels functionalized with RGD substitution 43

3.1 UV-Vis RGD pectin quantification 44

4 Preparation of Pectin hydrogels functionalized with Dopamine substitution 44

4.1 1H-NMR Dopamine Analysis 44

4.2 UV-Vis Dopamine Quantification 45
4.3 Measurement of FTIR Spectra 45

5 Preparation of functionalized Pectin hydrogel matrices - Rheological and mechanical properties characterization 45

5.1 Determination of Linear Viscoelastic Region (LVR) – Amplitude and Frequency Sweeps....46
5.2 Gelation Kinetics....47

6 Adhesion Studies 47

7 Scanning Electron Microscopy (SEM) 48

8 In Vitro Studies 48

8.1 Human Dermal Neonatal Fibroblasts (hDNFs) Culture 48
8.2 hDNFs culture with Functionalized Pectin Hydrogels....48
8.3 Cell metabolic activity and viability 49
8.4 Cell morphology and fibronectin deposition....49

9 Statistical Analysis 50

Results and Discussion 52

1 Pectin purification, functionalization and characterization 52

1.1 Pectin purification 52
1.2 Pectin functionalization with RGD peptide....53
1.3 Pectin functionalization with Dopamine 55
1.3.1 Pectin coupling with DOPA – Optimization....56
1.3.2 Preparation and physico-chemical characterization of Pectin coupling with DOPA 63
1.3.3 Rheological characterization ad internal gelation properties of Pectin functionalized hydrogel matrices 66

2 Adhesive Properties 72

3 Morphological and Structural characterization of the functionalized pectin hydrogels with Scanning Electron Microscopy (SEM) 75

4 In vitro cell culture of dopamine modified pectin hydrogels 76

4.1 Viability and metabolic activity of pectin functionalized hydrogels embedded with hDNFs....77
4.2 Morphology and ECM deposition of hDNFs loaded Pectin Hydrogels 79

Conclusions and Future Work 85

References 87

Supplementary Material 98

Annexes **99**

Abbreviation List

3D – Three - dimensional
AMPs - Antimicrobial peptides
BLK_PEC – Blank Pectin
BSA – Bovine serum albumin
Ca^{2+} - Calcium
$CaCO_3$ – Calcium Carbonate
DFU - Diabetic foot ulcers
DM – Degree of methylation
DMEM - Dulbecco's Modified Eagle Medium
DOPA – 3,4-dihydroxyphenylalanine
DOPA_PEC – Dopamine Pectin
ECM – Extracellular Matrix
EGF - Epidermal growth factor
EPC - Endothelial progenitor cells
EPS - Extracellular polymeric substance
F-actin – Filamentous actin
FBS – Fetal Bovine Serum
FGF - Fibroblast growth factor
FN – Fibronectin
GDL - Gluconic acid δ-lactone
HBOT - Hyperbaric oxygen therapy
HBSS – Hank's Balanced Salt Solution
hDNFs – Human Dermal Neonatal Fibroblasts
HG – Homogalacturonan
HM – High methoxyl
HUVEC's - Human Umbilical Vein Endothelial Cells
IL-3 - Interleukin-3
IL-4 – Interleukin 4
IL-6 - Interleukin-6
iPSCs – Induced Pluripotent Stem Cells
LM – Low methoxyl
LVR – Linear viscoelastic region
MAPs - Mussel Adhesive Proteins
MMPs - Matrix metalloproteinases
MSCs – Mesenchymal stem cells
NPWT - Negative Pressure Wound Therapy
PDA - Polydopamine
PDGF - Platelet derived growth factor
PEG – Polyethylene glycol
PFA – Paraformaldehyde
PHMB - Polyhexamethylene Biguanide
PLGA – Poly lactic-co-glycolic acid
PU - Pressure ulcers
PU – Polyurethane
PUR_PEC – Pure Pectin
RAW_PEC – Raw pectin
RCTs - Randomized Controlled Trials
RG-I - Rhamnogalacturonan-I
RG-II - Rhamnogalacturonan-II
RGD – Arginine-glycine-aspartic acid
RGD_PEC – RGD Pectin
ROS - Reactive oxygen species
RT – Room temperature
SDF-1 – Stromal cell-derived factor
TCPS – Tissue Culture Plate Surface
TGF-β - Transforming growth factor - β
TGF-α - Transforming growth factor - α
TNF - Tumor Necrose Factor
uPAR - Urokinase Plasminogen Activator Receptor
UV-VIS – UV-Visible
VEGF - Vascular endothelial growth factor
VLU - Vascular leg ulcers

List of figures

Figure 1. Schematic representation of Skin Structure. 21
Figure 2. Overview of acute wound healing phases.. 24
Figure 3. The role of MSCs in the treatment of chronic wounds 27
Figure 4. Different sources of stem cells for wound healing applications 28
Figure 5. Summary of tissue engineering strategies. 28
Figure 6. Hydrogel-based delivery system for wound healing and skin tissue regeneration. 31
Figure 7. (A) Schematic representation of Pectin fundamental structure and main domains and monosaccharidic composition; (B) “Egg box” gelation mechanism of pectin 33
Figure 8. Anatomy of Mytilus edulis mussel and byssus structures. 35
Figure 9. Oxidative Reactions and Possible Cross-Linking Pathways of DOPA 36
Figure 11. Functionalization of pectin with RGD by carbodiimide chemistry 54
Figure 12. RGD Coupling efficiency - UV-Vis Quantification 55
Figure 13. Schematic representation of Carbodiimide chemistry used to functionalization of Pectin with Dopamine. 56
Figure 14. DOPA quantification by UV-VIS 57
Figure 15. ^{1}H-NMR spectra of the formulations tested for pectin dopamine carbodiimide coupling reaction, comparatively to pectin and dopamine spectra 59
Figure 16. Reactionary mechanism of the formation of N-acylurea as a carbodiimide intermediary 60
Figure 17. Schematic representation of hydrophobic interactions between poly(ether)sulfone from Milipore® filters and DOPA/Polydopamine (PDA) of Pectin functionalized with Dopamine. 62
Figure 18. UV-VIS quantification of DOPA. 63
Figure 19. ^{1}H-NMR Spectra of dopamine, pectin (PEC_BLK) and Dopamine conjugated pectin (DOPA_PEC) 64
Figure 20. Comparative Fourier Transform Infra-Red (FTIR) spectra of pure Pectin and DOPA functionalized Pectin in comparison with Dopamine. 65
Figure 21. Gelation scheme using the internal gelation methodology 67
Figure 22. Representative graphs of frequency and amplitude strain sweeps.. 68
Figure 23. Viscoelastic properties (elastic (G’) and viscous (G’’)) components of the shear moduli of DOPA_PEC , BLK_PEC and DOPA_BLK 69
Figure 24. Representative graphs of the Gelation kinetics over time 70

Figure 25. Experimental setting for Adhesion studies 72
Figure 26. Adhesive properties (Adhesiveness (N) and Work of Adhesion (N.sec)) of DOPA_PEC comparatively to BLK_PEC samples 73
Figure 27. Macroscopic observation of Dopamine/PDA oxidative chemical crosslinking over time. 74
Figure 28. Microstructure of functionalized pectin hydrogel matrices. 75
Figure 29. Metabolic Activity (hDNF) embedded within different pectin-functionalized (DOPA and RGD) 3D hydrogel matrices (1.5 %wt) at different timepoints 78
Figure 30. hDNfs morphology when embedded within Blank, DOPA, Blank+DOPA(50/50) hydrogels 79
Figure 31. Morphology and cell proliferation of hDNFs when embedded within different concentrations of Blank and DOPA functionalized pectin hydrogels 80
Figure 32. Morphology and ECM deposition of hDNfs when embedded within DOPA and RGD -functionalized pectin hydrogels 81
Figure 33. Morphology and cell proliferation of hDNFs when embedded within DOPA and RGD -functionalized pectin hydrogels 83

List of tables

Table 1 - Medical Applications of Catechol-based hydrogels 39
Table 2 - Experimental and control conditions studied 47
Table 3 - Primary and Secondary antibodies used in samples immunostaining for confocal visualization 50
Table 4 - UV-VIS and ^{1}H-NMR quantitative analysis of different Carbodiimide reactionary conditions tested for Pectin Dopamine coupling.....58
Table 5 - UV – VIS quantification for the different reactions tested on the optimization stage.....62
Table 6 - Gelation time and mechanical properties of Dopamine pectin and BLK pectin hydrogels, at different pectin concentrations.....71

Introduction

1 Skin Anatomy and Physiology

Skin is the largest organ of human body and represents the first line of protection against pathogens and environmental exposure. It provides essential functions such as, thermoregulation, sensory information transmission related to pain, itch, temperature and touch, prevents from dehydration of the body while allowing the excretion of body metabolites through perspiration and being responsible for the synthesis of vitamin D [1].

As an outer barrier organ, the skin is exposed to external stress factors resulting in frequent disruption of the skin´s protective barrier and cell damage [2]. Therefore, the skin has developed a group of intricate mechanisms to protect itself from mechanical, chemical and biological damage and rapidly restore skin tissue integrity and function after damage, preventing individuals from severe infections [3, 4].

The normal skin structure comprises multiple stratified layers: the epidermis, dermis and subcutaneous fat tissue, often referred as the hypodermis [5]. The outermost layer of the skin, the epidermis, is an avascular tissue, morphologically composed predominantly of multiple layers of keratinocytes [5].The keratinocytes are arranged into distinct layers reflecting sequential levels of differentiation from basal to superficial direction [6]. The lowermost portion of epidermis, the basal layer, is composed of immature proliferating keratinocytes responsible for epidermis self-renewal. As they mature, keratinocytes migrate to the outer portions of epidermis, reaching the external cornified layers, at the final stage of differentiation where they flatten and lose their ability to proliferate, ending up with desquamation in this layer of epidermis [7, 8]. The main cellular components of epidermis besides keratinocytes, includes pigment-producing melanocytes, antigen-presenting Langerhans cells, responsible for the host immune protective responses, and Merkel cells acting as mechanoreceptors and light touch sensors [1, 5]. The major extracellular matrix (ECM) components of the epidermis are keratin and type IV/VII collagen constituting the basement membrane [5].

The regenerative capacity of the epidermis and the hair follicle are attributed to the existence of epidermal stem cells niches, characterized of being relatively quiescent and undifferentiated with the capacity to maintain homeostasis and self-renewal tissue, contributing to wound repair and skin tissue regeneration [6, 8, 9].

The dermis is separated from epidermis trough the basement membrane, is a dense connective tissue, constituted of fibroblasts responsible for the synthesis and production of ECM components, abundant in collagen and elastin fibers, providing

mechanical support and the structural architecture of the skin [1, 5]. Dermis presents a highly dynamic, vascularized layer acting as a support structure to epidermis, providing flexibility and strength to the skin. It is also rich in blood vessels, nerve endings, sweat and sebaceous glands and hair follicles [1, 5]. The major cell types comprising the dermis includes heterogeneous fibroblasts sub-populations, endothelial cells, Langerhans cells, mechanoreceptors cells (such as Meissener corpuscle and Pacinian corpuscle), smooth muscle cells, and hair follicle cells [1, 5, 6]. Besides the specific sub-population of Langerhans cells in dermis, cell types like mast cells and macrophages are also present, playing important roles in immune and inflammatory responses of the dermis [1, 10]. The ECM structure of the dermis is mainly composed by type I collagen, elastin fibers and proteoglycans [5].

The hypodermis is located immediately bellow the dermis connects the upper layers of skin to underlying tissues, consists mostly of adipose cells functioning as energy storage and thermoregulation [1, 5]. Hypodermis also functioning as a complex lipid barrier with high content of stem cells, hormone and growth factors. This tissue layer provides the nerve and blood vessels that nourish the upper layers, and plays a key role in re-epithelization, wound healing and angiogenesis [5, 11]. The main cellular components present in hypodermis are adipocytes and less content in fibroblasts, endothelial cells, smooth muscle cells and some hair follicle cells. Type I collagen and elastin are the major components that gives structure to hypodermis ECM [5].

After skin injury some of the most important skin functions are compromised, specially the protection provided from the skin as a physical barrier. The protective physical barrier of the skin is ensured mainly by the epidermis that provides protection from the environment, through the relatively impermeability of stratum corneum layer [12]. This waterproof barrier is guaranteed either by the arrangement of the keratinocytes in a scaffold-like lattice, bound together by fibrous protein keratohyalin and histidine-rich protein involucrin and intercellular spaces are filled with a lipid-rich laminar structure matrix [12].

The immune functions of the skin is the first line of defense against invading microorganisms, includes the production of antimicrobial peptides (AMPs), resident Langerhans cells, transient epidermal T-cells, and the dryness and desquamation of the outer layer of epidermis preventing the sustained growth of microorganisms [12].

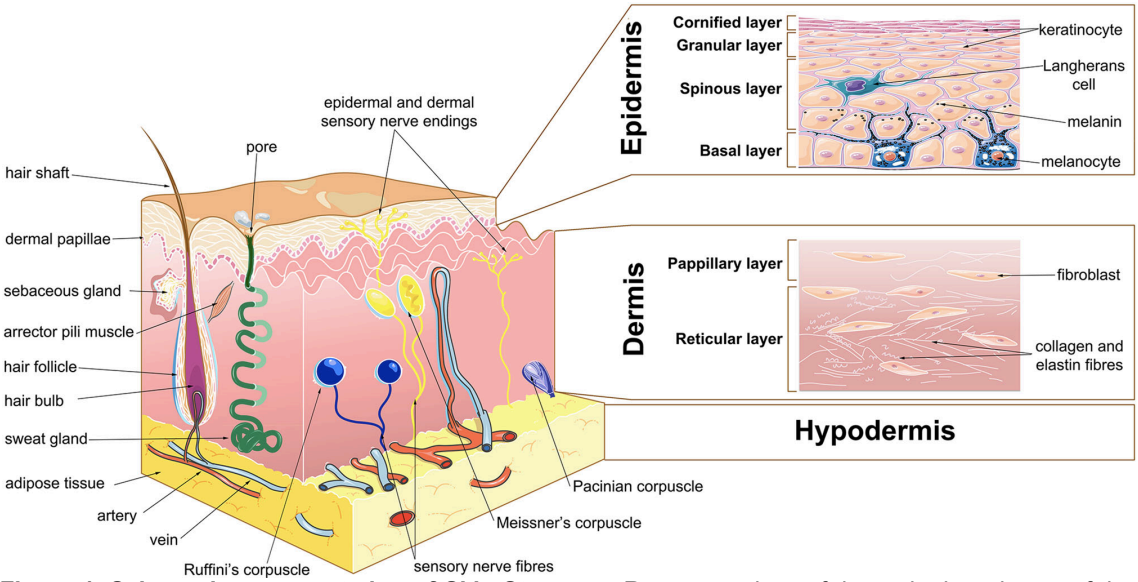

Figure 1. Schematic representation of Skin Structure. Representations of the main three layers of the skin and its cellular components, including skin cells, skin ECM components (collagen and elastin fibers), and specialized elements, such as, sweat glands, hair follicle, skin sensory organs and vascular structures (Adapted from Pereira et al. [1]).

2 Biology of Wound Healing

After skin injury the human body triggers an intricate series of coordinated processes, activating different signaling pathways, involving the communication and interaction between cells, ECM components, cytokines and growth factors in order to repair itself and restore the skin tissue functions [1, 3].

The wound healing process involves a dynamic sequence of temporarily and spatially overlapping phases: haemostasis, inflammation, migration, proliferation (granulation) and remodeling (or maturation), involving the interaction between soluble mediators, blood cells, extracellular matrix and parenchymal cells [13].

2.1 Haemostasis

Immediately after skin injury, haemostasis and inflammation process initiates and last for 1-5 days. Platelets are activated and initiate the primary response and adhere to damaged blood vessels unleashing a hemostatic reaction, starting with the blood-clothing cascade, forming a fibrin cloth, preventing from excessive bleeding and providing protection for the wounded area [14, 15]. During this phase the activated and aggregated platelets, change shape and degranulate, releasing proteins, bioactive lipids, cytokines and growth factors including Interleukin-4 (IL-4), transforming growth factor - β (TGF-β), fibroblast growth factor (FGF), transforming growth factor - α (TGF-α), vascular endothelial growth factor (VEGF), platelet derived growth factor (PDGF) and

epidermal growth factor (EGF).[1, 14] The growth factors released are responsible for attracting inflammatory and vascular cells such as leukocytes, neutrophils and macrophages. The leukocytes are the phagocytic cells, releasing reactive oxygen species (ROS), characterized as antimicrobials by nature, along with proteases that clear the wound of debris, foreign bodies and bacteria [14].

2.2 Inflammation

The inflammation phase is characterized by the phagocytic activity of neutrophils, monocytes and innate immune cells, attracted by the release of chemotactic factors, responsible for cleansing the wound site and helping to coordinate the skin tissue repair mechanism [16]. In order to restore normal tissue architecture and function, the inflammatory phase can be subdivided in three distinct phases.

First, an early pro-inflammatory step, marked by the activity of innate immune cells, mobilizing and recruiting key inflammatory cells, including activated M1 phenotype macrophages [17, 18]. The M1 Macrophages are highly phagocytic cells responsible for the removal of pathogens and debris present in the wound. The macrophages with the M1 phenotype present a pro-inflammatory activity responsible for the production of pro-inflammatory cytokines, such as Tumor Necrose Factor (TNF) and interleukin-6 (IL-6), and other cellular mediators that benefits the initial stages of wound healing.[10, 16] Afterwards, the pro-inflammatory response starts diminishing and key inflammatory cells such as macrophages switch to a reparative phenotype, the M2 phenotype [18].

The activated M2 macrophages are characterized by their anti-inflammatory effect and are produced by the stimuli induced by the phagocytosis of apoptotic neutrophils or the addition of Interleukin-3 (IL-3) or Interleukin-4 (IL-4) [18, 19]. Finally, the releasing of stop inflammatory signals, such as lipoxins and TGF-β, ends inflammatory phase and tissue homeostasis is restored when the inflammatory cells leave the wound site or are eliminated through apoptosis [16].

The variability of the degree and duration of inflammatory responses influences the final outcome. There are positive effects of increasing the inflammatory response, however the negative impact of a prolonged inflammation includes activation of a fibrotic response, defined by the accumulation of excessive amounts of collagenous connective tissue, impairing tissue function [16].

2.3 Proliferation – Granulation Tissue Formation

The proliferation phase starts approximately 3-4 days after injury, and it extends for 2-4 weeks. This phase is characterized by proliferation, phenotypic alteration and migration, of fibroblasts and endothelial cells, ECM deposition and granulation tissue formation [20, 21]. The epithelization and angiogenesis processes lead to the formation of a temporary matrix containing fibrin and fibronectin network. This temporary matrix network supports the formation of the epidermal barrier by the proliferation and differentiation of keratinocytes released from the stem cells reservoirs in the skin [15]. Pro-angiogenic factors such as VEGF, FGF-2, and PDGF are initially produced and released by platelets follow by the resident cells within the wound bed site, through the stimuli provided by the hypoxia secondary to blood vessels disruption [14]. The pro-angiogenic stimuli induce the recruitment of endothelial cells to the wound site, either via degradation of the basement membrane, migration and proliferation from endothelium, either via recruitment of bone marrow derived endothelial progenitor cells (EPC), homing to the adjacent endothelial cells bordering the injury site [20]. The EPC recruitment is mediated by nitric oxide (NO), VEGF and matrix metalloproteinases (MMP), specially MMP-9.[22] The activity of Stromal-derived factor-1 (SDF-1) and more recently Insulin-like growth factor (IGF) are attributed to the engraftment and differentiation of EPC, however further studies are needed to support the underlying mechanisms of recruitment and homing of EPC[14, 23].

Lastly, the macrophages stimulate the fibroblasts attracted from the wound edges or from the bone marrow, and some differentiate into myofibroblasts in response to TGF-α stimuli. Both fibroblasts and myofibroblasts interacts with each other, producing provisional ECM, mainly composed of type III of collagen, fibrin, fibronectin and hyaluronic acid which is progressively replaced by ECM containing type I collagen [20, 24]. Myofibroblasts are a type of contractile cells, responsible for contraction of the wound edges, and in the presence of certain matrix proteins such as ED-A fibronectin and tenascin C, reducing the wound size [20]. Fibroblasts proliferation and the synthesis of ECM forms the granulation tissue that will be perfused by newly formed blood vessels [14, 25].

2.4 Remodeling – Scar Formation

The remodeling is final stage of wound healing and starts 2-3 weeks after injury, persisting for months to years. All cellular and molecular processes activated after injury in the previous stages diminishes and cease [20]. The normal blood supply is

reestablished creates a propitious microenvironment for epidermal and dermal cell migration and proliferation which promotes the wound re-epithelization and restoration of epidermal integrity and this phase is characterized by wound contraction and matrix remodeling. Wound contraction is mainly achieved either by myofibroblasts activity inducing contractile forces transmitted to the ECM, via cytoskeleton-associated and ECM focal adhesion complexes the integrin receptors or fibroblasts motility with consequent matrix rearrangements [14].

This phase involves a dynamic and reciprocal process with slow cycles of ECM synthesis and degradation, occurring in a cell-dependent manner [14]. The majority of the cells, such as endothelial cells, macrophages and myofibroblasts, either undergo programmed death cells (apoptosis) or exit the wound, leaving a mass containing few cells and consists mainly of different types of collagen (I-IV) and other ECM proteins, resulting in the formation of fibrotic scar tissue [20, 26]. The interactions between Epithelial and Mesenchymal cells are probably responsible for the continuously regulation of skin integrity and homeostasis [20, 27]. Over the subsequent 6-12 months, the ECM backbone is actively remodeled changing from a matrix of type III collagen to a matrix structure mainly composed of type I collagen, accomplished by matrix metalloproteinases (MMP) secreted by fibroblasts, macrophages and endothelial cells, strengthening the repaired tissue [20].

Despite this, highly dynamic and intricate process of skin wound healing, the repaired skin tissue never regains the properties of normal uninjured skin [20] (For further information about Wound Healing consult the available Annexes).

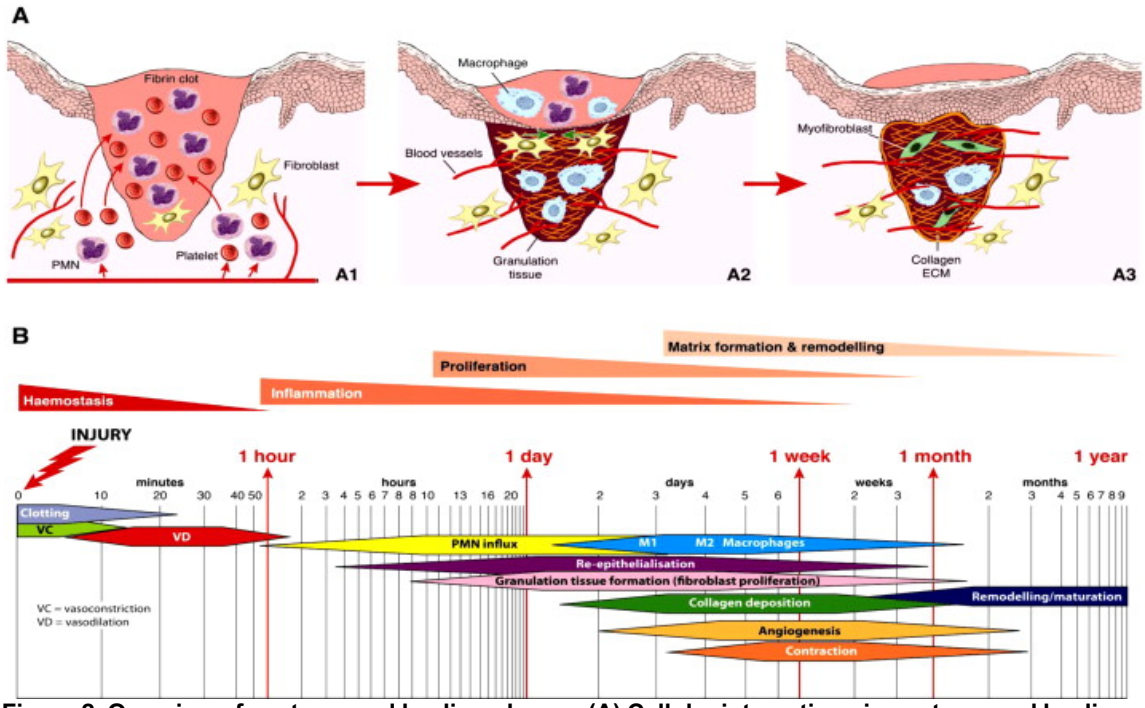

Figure 2. Overview of acute wound healing phases. (A) Cellular interactions in acute wound healing; (B) Overlapping 4-phase model and its timeframe. After skin injury the haemostasis phase starts with

vasoconstriction, clotting cascades and platelets lead to fibrin clot formation. Then vasodilatation induce PMN extravasion and migration to wound site, starting inflammation phase (A1) Inflammatory Macrophages (M1) and reparative type (M2) phagocytes bacteria and wound debris and secrete growth factors, chemokines and cytokines, which recruits fibroblasts and endothelial cells to wound site starting proliferation phase (A2). The cellular proliferation results in ECM deposition, angiogenesis and granulation tissue formation., which forms a provisional ECM scaffold that in remodeling phase (A3) will lead to wound maturation and contraction with eventual scar formation (Adapted from Greaves et al. [21]).

3 Regenerative Medicine and Skin Tissue Engineering for Wound Healing

The tendency is to replace traditional dressings by modern advanced engineered dressings capable of ensure adequate moisture environment, promoting cellular migration and proliferation, combining with the releasing of bioactive substances within the wound bed [1]. Regenerative medicine has been shown a wide variety of potential therapies to overcome the challenges addressing wound healing, which the main purpose is to promote effective healing and tissue repair [28]. These potential therapies can be classified according to:

a) **Growth factors - modulation of signaling pathways**
b) **Stem cell therapy**
c) **Tissue Engineering**
d) **Biomaterials**

Growth factors are biologically active substances (polypeptides) with the ability to interact with specific cell surface receptors, regulating repair processes in the skin tissue [29]. Along with cytokines and chemokines, these growth factors are secreted by cells and capable to regulate wound healing process, via modulation of signaling pathways, promoting cell migration into the wound, epithelization, promote angiogenesis and stimulate matrix formation and remodeling of wounded area [30]. The most studied growth factors with particular impact to wound healing are EGF, TGF-β, FGF, PDGF and recently the Stromal cell-derived factor (SDF-1) which evidence pointed out the association of SDF-1 with regulation of epidermal cell migration and proliferation during wound healing. [28]

Despite the topical application of growth factors have been shown to improve and accelerate wound healing responses, both in vitro and in vivo (animal and human studies), additional studies should be made, focusing on some limitations of the application of growth factors, namely, the resistance to degradation induced by the harsh proteolytic wound environment and the controlled delivery (sustained or transient) when they are required [28].

Stem cells present the key feature of being able to self-renewal and the potentiality to differentiate into different cellular lineages. They can be obtained from different sources and can be derived from various tissues, including embryonic, fetal and adult tissue [28].

Although, adult skin tissue presents an endogenous epidermal stem cells “niche”, able of regenerate skin, these reservoir of cells are not sufficient to provide perfect repair after an extensive deep skin tissue damage [2].

Mesenchymal stem cells (MSCs) have been the most studied stem cells in wound regeneration, owing to its relatively easy isolation from bone marrow, fat tissue and skin and the ability to differentiate into different tissue-specific cell types (multipotency) including skin tissue cell types, such as, keratinocytes and endothelial cells. [28, 31] Many studies of the application of MSCs in wound healing, have identified the potential of MSCs to accelerate wound healing mechanisms, though improvement of angiogenesis via secretion of pro-angiogenic factors and differentiation into endothelial cells, polarization of M2 macrophages, the recruitment of endogenous progenitor stem/progenitor cells, ECM production and remodeling and immunosuppressive effects (Fig. 3) [31].

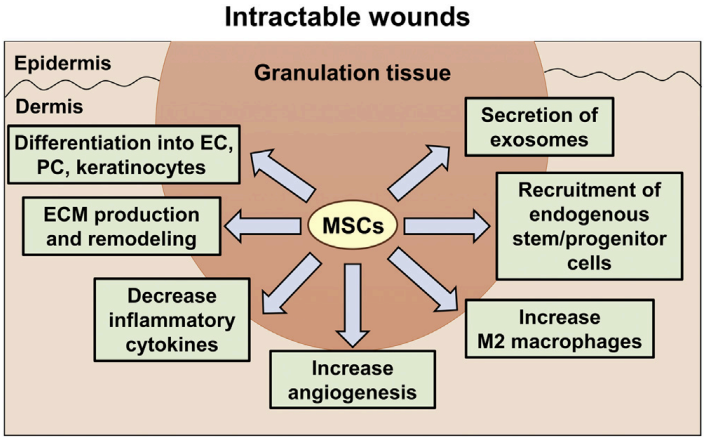

Figure 3. The role of MSCs in the treatment of chronic wounds (Adapted from Motegi et al. [31])

The development of the Induced Pluripotent Stem Cells (iPSCs) technology is relatively recent. iPSCs are obtained from differentiated adult somatic cells that can be reprogrammed, returning to its stem cell-like state. This occurs by the addition of transcription factors, generating pluripotent stem cells with similar characteristics of embryonic stem cells (Fig.4) [8]. Since iPSCs, derived from adult cells by in vitro induction of pluripotency, allowing differentiation into all skin cell types, this technology obviates the ethical dilemmas surrounding embryonic stem cells. Besides that, they are harvested non-invasively and can be transplanted autologously, reducing dramatically the risk of immune rejection. Concerning wound healing, despite of iPSCs showing promising results in acceleration of wound healing and improve healing rates, several optimizations are required, before further translation to the clinical setting [32].

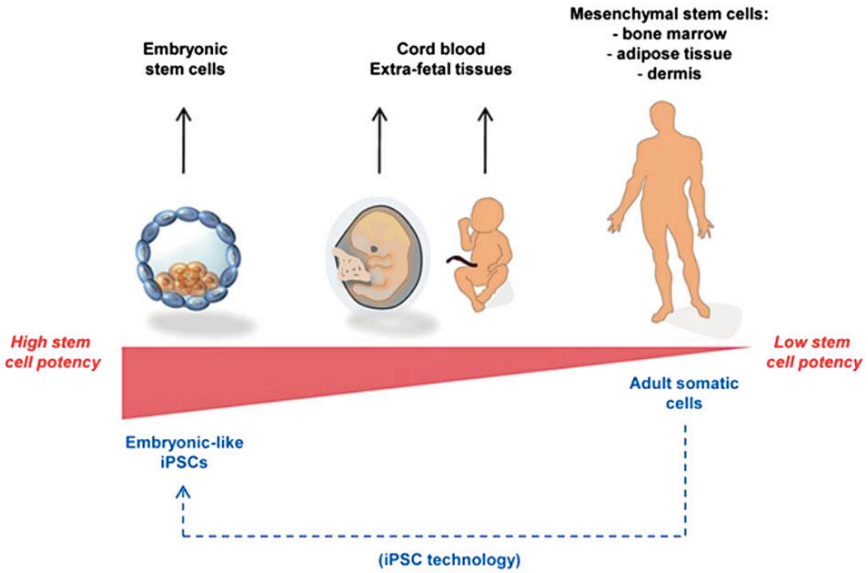

Figure 4. Different sources of stem cells for wound healing applications (Adapted from Nour et al. [33])

Tissue engineering arises from the combination of biological concepts with advanced engineering principles, in order to address the global clinical need for technological solutions, for replacement or regeneration of functionally damaged living tissues or organs [34, 35]. Current skin TE constructs, combines cells, 3D scaffolds and environmental signals (Fig.5), that physiologically mimics the skin 3D structure and its functions [36]. However, translation of these solutions into clinical effective therapies, envisage some difficulties, such as, accurate recapitulation of skin tissue physiology, large-scale production towards the clinical demands and financial costs [34, 36].

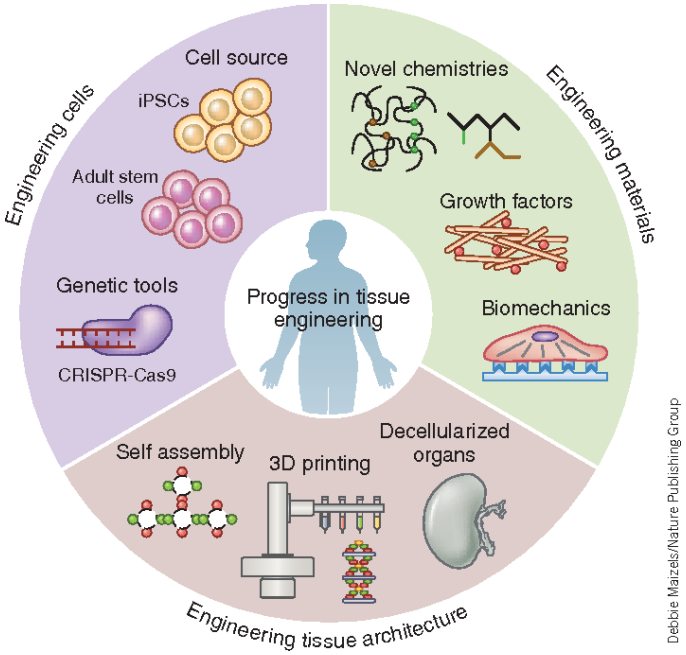

Figure 5. Summary of tissue engineering strategies. The development of new cell sources, new genetic editing tools allows cell manipulation. Optimized chemistry and growth factors delivery systems, allied to the better understanding of cell behavior in native tissues, contributes to improved TE constructs resembling the native tissues. (Adapted from Khademhosseini et al. [36])

The skin presents a high level of structural complexity with specific architectural organization, composed by different cell populations (for example: keratinocytes, fibroblasts, endothelial cells) that constitute the functional structures of the skin, such as blood vessels, lymphatic system, sensory receptors, pigmentation, hair follicles and secretory glands [35].

Biomaterials are widely used in wound healing through the form of wound dressings with the purpose of maintain wound moist environment and protect the wound bed from external environmental aggressions [28]. Cell behavior is highly affected and controlled by tissue ECM supportive scaffolds, which plays an essential role in the promotion of wound healing and tissue homeostasis [37]. Biomaterials based artificial supportive scaffolds can provide provisional platforms for tissue growth, supplying essential growth factors associated with survival, supporting cell attachment and proliferation, promoting tissue formation [35, 37]. Ideal scaffolds are defined as transient structures, characterized by controlled degradation or reabsorption with time, until being fully replaced by tissue. Scaffolds biomaterials offers the possibility of being biofunctionalized with biologically active signals, such as, cell-adhesion peptides and growth factors, mediators of cell attachment and tissue formation [35]. Biomaterials research exploit the application of these biomaterials to actively improve wound healing via immune modulation of healing responses, facilitate cell infiltration within the wound bed, production of ECM and angiogenesis [28].

Biomaterials used in wound dressings can either be from natural or synthetic sources. Natural derived polymers including polysaccharides (e.g. alginates, pectin), proteoglycans and proteins (e.g. collagen, keratin, fibrin) offers an advantage to synthetic polymers because of their properties, such as, similarity to the native skin ECM, chemical structure similarity to natural glycosaminoglycans, biocompatibility, biodegradability and being cell-instructive in nature, due to the presence of cell adhesion domains and/or signaling factors, promoting cell adhesion, support the attachment, proliferation and cell differentiation [33, 35, 38-40]. The main disadvantages of natural polymers are their batch-to-batch variation, which difficult mechanical properties modulation with long-term potential inhibition of cell functions, and inherently immunogenic due to the presence of protein and endotoxins contaminants [28, 40]. Comparatively, synthetic polymers (e.g. polyethylene glycol (PEG), poly-lactic-co-glycolic acid (PLGA), polyurethane (PU)) have the advantage to bypass the immunologic effects and present excellent processing characteristics, in terms of molecular weight, degradation and mechanical properties. Additionally, synthetic polymers have tailored properties, allowing the fine tuning of

properties according to specific application, with the possibility of being easily biofunctionalized to incorporate drugs in the development of bioactive dressings [28, 33, 39].

Currently, there are several scaffolding methods for skin tissue engineering and wound healing with primary goal of mimicking the native skin ECM, we will focus the next sections in hydrogel-based systems which is the scope of this work.

4 Hydrogel-Based Strategies for Wound Healing

The foundations ideal wound management protocols were first described in 1962 by George Winter in a study, where he observed a faster and improved healing in the presence of wound moisture environment. This counteract the established assumption that moisture contributes to wound infection [41]. These findings change the wound management paradigm, towards the usage of hydrocolloids, gels and hydrogels, promoting a moist environment, helping in the debridement instead of dry wound dressings [42].

Hydrogels are 3D hydrophilic, cross-linked polymeric networks, with soft texture, high absorption capacity (more than thousands of times their dry weight) of water and biological fluids (wound exudate) maintaining the shape [40, 42, 43]. Through chemical or physical methods, it's possible to control chain crosslinking, enabling the control of gelation kinetics and making it possible to tailor the hydrogel properties [40].

Hydrogels are compliant and permeable structures, mainly composed by water, which mimics the ECM structure, providing an ideal 3D microenvironment for cells. *Via* physical and chemical modifications of the gel-forming polymers and/or crosslinking strategies, it's possible to modify hydrogels and improve their mechanical and biochemical properties to achieve the most similarity to native ECM. Furthermore, it's possible to incorporate bioactive agents and/or cells within the hydrogel structure, allowing a prolonged controlled delivery system, supporting the delivery of molecules that contributes to wound healing or skin tissue regeneration (Fig. 6) [40, 42, 44].

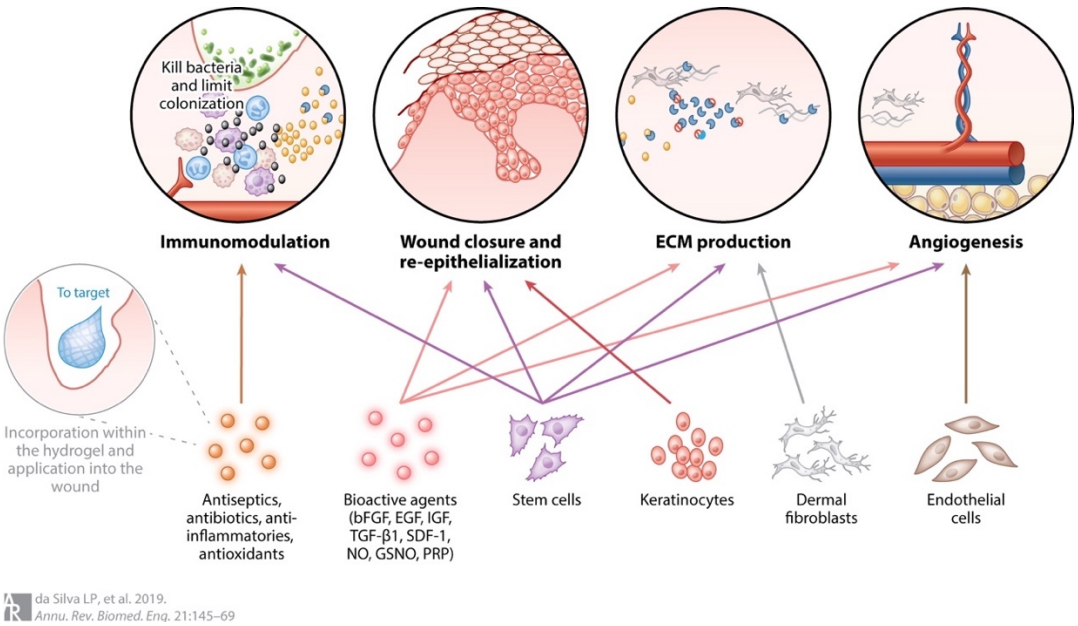

Figure 6. Hydrogel-based delivery system for wound healing and skin tissue regeneration. The rationale of these strategies involves the incorporation of specific mediators to ablate infection (antiseptics,

antibiotics) and resolve inflammation (anti-inflammatories, antioxidants, and stem cells), to accelerate healing (bioactive molecules and cells), and to promote skin regeneration (bioactive molecules and cells). (Adapted from da Silva et al. [42])

There are many ideal key features of a hydrogel that would contribute to improve the hydrogel wound healing ability. These features are compatibility and molecular stability in aqueous solution; biodegradability and biocompatibility, to avoid cumulative or deleterious effects of hydrogel components in the body; the stimuli-responsiveness ability to regulate gel behavior and cell-specific bioactivity to enhance cell activity [45]. Hydrogel-based delivery systems, due to its versatility and endless design possibilities with easy physical and or chemical functionalization, makes them ideal approaches to delivery of bioactive agents to wound site, improving and accelerating wound healing and skin tissue regeneration [42, 45].

5 Pectin Structure and Wound Healing Applications

Pectin is a natural polymer offers the possibility to mutate its characteristics, by grafting desired peptides into biopolymer structure, controlling mechanical properties through control of gelation kinetics (e.g. crosslinking strategy), specific matrices can be constructed [46].

Pectin derived from plant cell wall, it's a biocompatible anionic polysaccharide, composed of at least three polysaccharide domains: the major component the homogalacturonan (HG), rhamnogalacturonan-I (RG-I) and rhamnogalacturonan-II (RG-II) [47], forming a complex branched macromolecule with high molecular weight. (Fig. 7 - A) [47, 48].

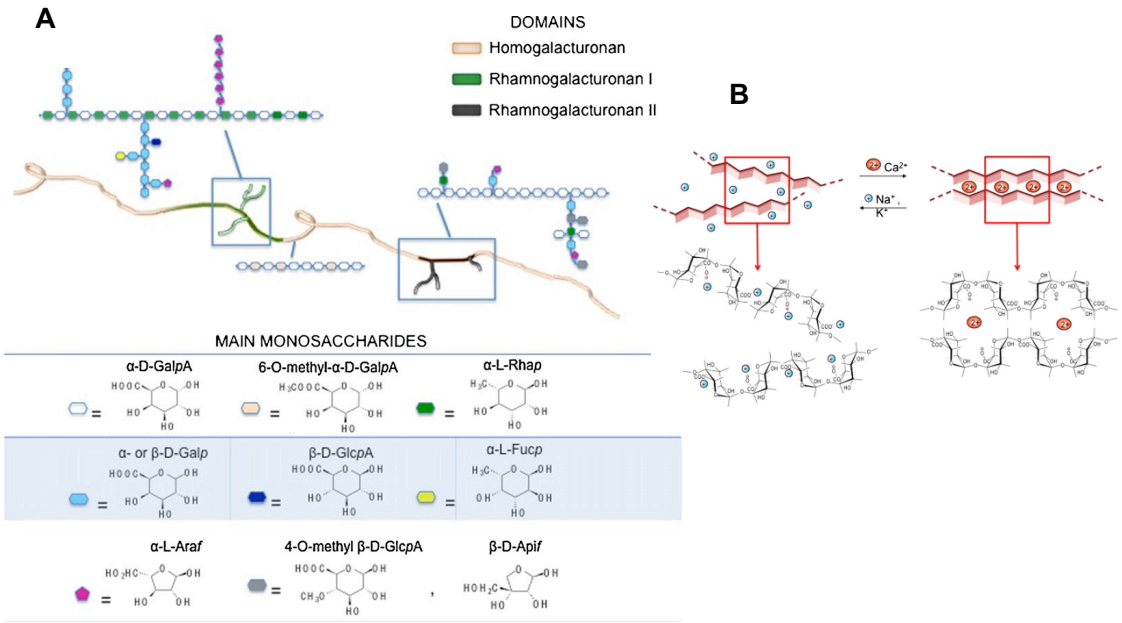

Figure 7. (A) Schematic representation of Pectin fundamental structure and main domains and monosaccharidic composition; (B) "Egg box" gelation mechanism of pectin: the carboxyl groups of pectin backbone form polyelectrolyte complexes with polyvalent cations (Adapted from Munarin, et al. [49]).

The predominant component homogalacturonan, mainly composed of homopolymer of (1-4)-linked-α-D-galacturonic acid (GalA) units, that can be partially esterified on the carboxyl group and by the acetyl group on the secondary hydroxyls. Pectin's are divided into two categories, according to degree of methylation (DM): low methoxyl (LM) pectin (DM < 50%) and high methoxyl (HM) pectin (DM > 50%) [44]. When dissolved LM pectin can form gels, in the presence of strong, positive, divalent metal ions, such as Ca^{2+} ions, Pectin molecules establish strong bonds between the carboxyl groups of the HGA pectin backbone, inducing the "egg box" structure formation (Fig.7-

B). The “egg box” structure is stabilized through electrostatic interactions and ionic bonding. Van der Waals interactions and hydrogen bonds are established within the polymer, stabilizing the egg-boxes formed between neighbored chains forming a flexible network structure [47, 48]. Industrial pectin extraction is mainly from citrus peel waste products using higher temperatures and acidic pH [50]. After the extraction process, contaminants like proteins, polyphenols and endotoxins are still remain in large amounts, compromising its usage for biomedical applications [44]. Therefore, additional purification processes are necessary to guarantee biocompatibility and safety of pectin.

The pectin hydrogels offer interesting advantages for pharmaceutical and biomedical applications, including adaptable physical properties, presenting higher cytocompatibility, high water content and ability to homogeneously immobilize cells, genes, proteins, drugs or growth factors [47, 48, 51-53].

In situ-forming hydrogels suitable for cell-delivery system was explored by Neves et al., optimizing and developing the internal ionotropic gelation of pectin using the slow-gelling calcium carbonate/D-glucono-δ-lactone ($CaCO_3$/GDL). Additionally, in the same study, successfully modified purified pectin with cell adhesion motif arginine-glycine-aspartic acid (RGD) using carbodiimide chemistry and tested RGD pectin in vitro with MSCs cells and *in vivo* model, showing the potential of pectin-based hydrogels for tissue engineering and regenerative medicine [44].

6 Mussel Inspired Catechol - Functionalized Hydrogels

6.1 Mussel Adhesive Proteins

Bioinspired technologies are inspired by nature in the unique capabilities of organisms, such as marine mussels. The adhesion mechanism used by mussels is a biomimetic strategy, currently mimicked for the synthesis of tissue adhesives [43, 54-57].

Marine mussels have the ability to firmly adhere to both organic and inorganic surfaces (e.g. rocks, ships) in the seawater, through the secretion of mussel adhesive proteins (MAPs) by the byssus [43]. The mussel adheres to external surfaces through byssal threads and plaques, which are composed by polyphenolic proteins, collagen and polyphenol oxidase, secreted by the foot gland (Fig. 8). These substances and its structural rearrangement provides water resistance and high strength [58].

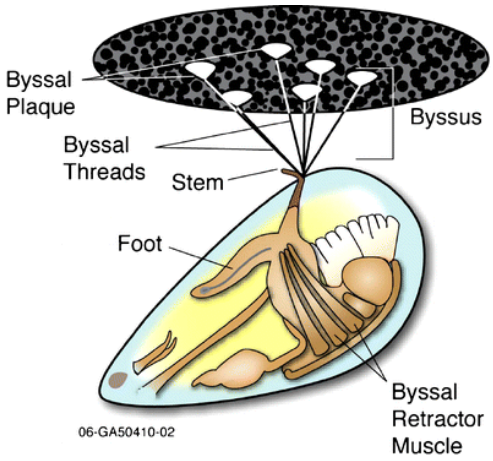

Figure 8. Anatomy of Mytilus edulis mussel and byssus structures. The foot gland secrete the components of byssal threads and plaques, responsible for mussel adhesion to surfaces (Adapted from Silverman et al. [58]).

The strength and efficiency of mussel adhesion are influenced by internal factors, such as, the mussel metabolic status, and also external environmental factors, such as pH, temperature, surface substrate and season [55].

MAPs adhesion mechanisms are not completely understood; however, the mussels' strong adhesive properties are attributed to a catechol group, containing in the amino acid 3,4-dihydroxyphenylalanine (DOPA) found in MAP's structure [54, 59]. Mussel adhesive properties are mediated by the ability of DOPA to establish several type of bonding interaction, such as, formation of bidentate hydrogen bonding, π-π interactions, complex formation with metal (e.g., Fe^{3+}, Cu^{2+}, Ca^{2+} and Ti^{3+}) and metal oxides, and the redox potential of the catechol groups via oxidation to dopa-quinone,

allowing the oxidative cross-linking forming protein network [60]. Although L-DOPA was determined as the key factor of interaction between MAPs and materials surface, the fundamentals of L-DOPA mediated adhesion mechanism and chemical interactions of the adhesion to inorganic and organic substances, has not been yet established [54].

6.2 Catechol-Based Hydrogel Synthesis

The synthesis of catechol-based hydrogels involves three possible chemical reactionary pathways. The mechanistic chemistry behind hydrogels formation depends on the type of chemical intermediary formed. When DOPA is exposed to oxidative chemical cross-linking agent, such as, O_2, $NaIO_4$ and H_2O_2, and enzymes, such as peroxidases, the hydroxyl groups easily give up electrons and DOPA undergoes to series of oxidative chemical reactions, increasing chemical reactivity [43, 61]. Through this oxidative cross-linking process, DOPA grafted within the molecular chains of polymers, can produce a stable polymeric hydrogel with unique features, including strong adhesive capacity, thermosensitivity and pH responsive hydrogels (Fig. 9)

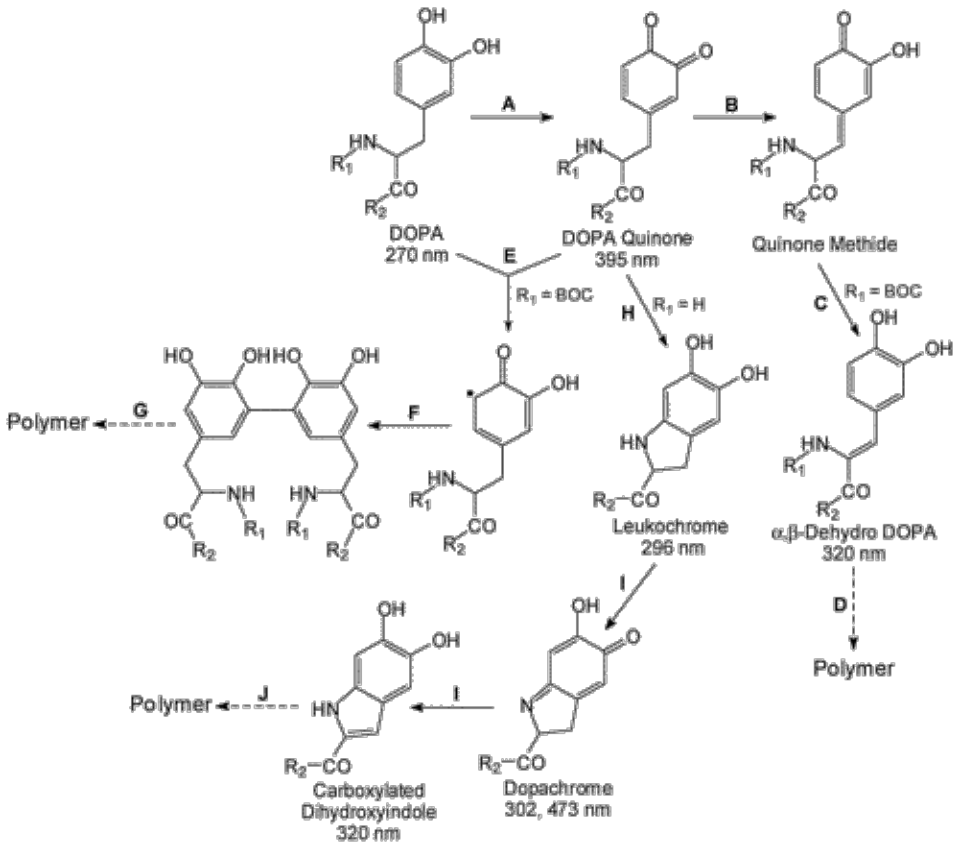

Figure 9. Oxidative Reactions and Possible Cross-Linking Pathways of DOPA (A) Oxidation by catechol oxidase or other oxidizing reagents. (B) Tautomerization of DOPA quinone. (C) Release of α proton. (D) Cross-linking by a pathway similar to that occurring in insect cuticle sclerotization. (E) Aryloxy free radical generation. (F) Phenol coupling. (G) Further oxidation to form cross-linked polymer. (H) Internal cyclization

with R_1 = H. (I) Rearrangement of cyclized DOPA derivatives. (J) Cross-linking by a pathway resembling that occurring in melanin formation. Dashed arrows indicate poorly understood pathways that lead to the formation of cross-linked polymers (Adapted from Lee, et al. [61]).

The properties of catechol-based hydrogels can be fine-tuned variating the type of cross-linking mechanism, controlling the chemical structure of DOPA, the concentration of DOPA grafted into the polymer backbone and the cross-linking reagent concentration [43]. Therefore, according to functionality and chemical properties of catechol-based hydrogels, they can be classified as non-functional, nanocomposite, thermosensitive and pH responsive hydrogels [43].

Independently of the type of hydrogel and its´ tailor-made special properties (such as thermosensitivity or pH-responsiveness), the key property of DOPA functionalized hydrogels are the high adhesive strength and the ability to mimic MAPs strong adhesion to surfaces in the presence of wet environmental conditions. [43]

Lee et al. [60], using a single-molecule assay, studied the interaction between inorganic and organic substrates and the degree of oxidization of DOPA. They concluded that a non-oxidized DOPA molecule has itself a strong, reversible non-covalent interaction with wet metal oxides surface. Oxidized DOPA had a weak interaction with metal oxides, however, it forms highly strong, irreversible covalent bound with organic materials [60].

The adhesive properties of DOPA-functionalized hydrogels in wet environmental conditions, have been used to promote the adhesion to surface of soft biological tissues, tissue-tissue adhesion and cell adhesion [54].

The underlying mechanism regarding the adhesion of catechol-based hydrogels to biological tissue surfaces are attributed to the formation of irreversible covalent bounds, via the oxidative cross-linking of DOPA with the reactive groups (such as, $-NH_2$ and -SH) present in biological tissues [43]. Several factors influence the adhesiveness strength of DOPA-functionalized hydrogels, such as, the dependency on the DOPA oxidation state [62, 63], the influence of pH variation [64], and the increase adhesiveness in higher molecular weight polymers [65].

6.3 Catechol-Based Hydrogel Medical Applications

The development and study of DOPA-based biomaterials offers interesting features, which makes them promising materials with a lot of potential in medical applications. First, they provide effective adhesion in wet environmental conditions present in biological tissue interface, showing advantageous adhesion, hemostasis and healing of wounded tissue. Despite that, the catechol-based tailored hydrogels can be

used as coatings for biological and clinical devices, drug delivery nanoparticles and tissue engineering scaffolds [43]. The table 1 summarizes the medical applications of DOPA-functionalized hydrogels published in literature.

Table 1 - Medical Applications of Catechol-based hydrogels

MEDICAL APPLICATION	REFERENCES	DESCRIPTION	CONCLUSIONS
Tissue adhesion, Hemostasis and Wound Healing	Mehdizadeh et al. [66]	Preparation of injectable citrate-based mussel-inspired bioadhesive (iCMBAs), through one-step reaction of citric acid, PEG and DOPA, for surgical use. The adhesive strength was tested in porcine skin and acellular small intestine submucosa.	iCMBAs formulation showed a 2,5-8,0 folds stronger wet tissue adhesion strength over clinically used fibrin glue, controlled degradability, tissue-like elastomeric mechanical properties and cytocompatibility both in vitro and in vivo.
	Fan et al. [57] and Zhu et al.[56]	Mussel inspired double-crosslink tissue adhesive (DCTA) composed by dopamine-conjugated gelatin macromer, rapid crosslinker (Fe3+) and long term acting crosslinker (genipin).	Comparatively to fibrin glue DCTA presents higher wet tissue adhesion on wet porcine skin and cartilage, fine elasticity, biocompatibility and biodegradability. In rat mastectomy models DCTA successful reduces seroma formation over a period of one week.
	Sun et al. [67]	Development of strategy for surface bFGF-functionalization of electrospun PLGA fibers in aqueus solution, using polydopamine as an adhesive bridge-layer between PLGA fibers and bFGF (PLGA/PDA-bFGF)	bFGF-grafed PLGA fibers have *in vitro* highly enhanced adhesion, viability and proliferation of human dermal fibroblasts; and *In vivo* shortened wound healing time, accelerated epithelialization and promotes skin remodeling.
Antimicrobial Application	Wang et al. [68]	DOPA-modified ε-poly-L-lysine (EPL)-PEG-based hydrogels (PPD hydrogels as wound dressings, crosslinked in situ with horseradish peroxidase.	PPD hydrogels showed rapid integration within the biological tissue and enhanced capacity of *in vivo* hemostasis and wound repair. Additionally, PPD hydrogels showed antimicrobial activity with *Escherichia Coli* and *Staphylococcus aureus*.
	Guo, et al. [69, 70]	Preparation iCMBAs with the introduction of the clinically used and inexpensive anti-fungal agent, 10-undecylenic acid (UA), developing a new family of anti-fungal and anti-bacterial.	The system, not only showed strong wet tissue adhesion strength, but also exhibited excellent *in vitro* cytocompatibility, fast degradation, and strong initial and considerable long-term anti-bacterial and anti-fungal ability.
	Fullenkamp et al. [71]	Hydrogel covalent cross-linked with water-soluble PEG containing reactive catechol moieties, oxidized with silver nitrate.	Hydrogels with sustained silver *in vitro* release (at least 2 weeks), inhibiting bacterial growth and maintain mammalian cell viability. Thin hydrogels films resist bacterial and mammalian cell attachment.
Bone regeneration and Orthopedic Implant Coatings	Rego, et al. [72]	Development of orthopedic implants coating using a Layer-by-Layer (LbL) approach composed by Dopamine carbodiimide conjugates of Bioglass nanoparticles, chitosan and hyaluronic acid.	LbL films containing cathecol groups, enhance cell adhesion and *in vitro* formation of bone-like apatite structure.
	Zhang et al. [73]	Immobilization of bone marrow stem cells in alginate and alginate-dopamine (modified via carbodiimide chemistry) beads and fibers.	Alginate modified with dopamine, increases adhesive properties, enables surface coating with silver nanoparticles for antimicrobial activity; enhance cell viability and proliferation, and *in vitro* osteogenic differentiation of MSCs. This system can be applied to cell encapsulation and regeneration of infected bone defects.

Heparin-Mimetic Coatings	You et al. [74]	Development of mussel-inspired heparin derivative (“hepamine”) via conjugation with dopamine for application in surface poly(urethane) biomaterials.	Poly(urethane) coated with “hepamine” inhibits significantly blood coagulation and platelet adhesion. Simple, one-step surface functionalization.
Drug Delivery	Ren et al. [75]	DOPA-based and poly-DOPA cross-linked injectable hydrogel using a mixture of oxidized quaternized, chitosan, gelatin and DOPA. Dopamine (drug for Parkinson’s disease) and metronidazole (as anti-inflammatory drug) were encapsulated in the hydrogel.	The injectable dopamine-based hydrogels provide an easy approach, which can be used as long-term injectable sustained release system for therapy.
Tissue Engineering Scaffolds	Lee et al. [76]	Preparation of divalent ion-free alginate hydrogels by conjugating dopamine with alginate, via oxidative cross-linking instead of divalent cations cross-linking.	Alginate hydrogels with tunable physical and mechanical properties, enhanced biocompatibility 3D scaffolds for tissue engineering and cell therapy.

7 Problem Statement and Aim of this Work

This work was inspired on personal clinical practical experience as nurse in a highly differentiated polyvalent intensive care unit. Critically ill patients requires complex care in a highly technological sophisticated environment, increasing risk and vulnerability of developing pressure ulcers or pressure-related injuries [77].

Health professionals are constantly faced with the harsh reality of the prevention and treatment of chronic and complex wounds in the hospital setting, outpatient clinic and community setting.

Hydrogels are widely used as treatment strategy for acute and chronic wound, owing to its versatility and adaptability to almost all wound types. Hydrogel-based therapies for wound healing, provides the moisture balance environment and contributes to wound debridement through the activation and recruitment of phagocytic cells to wounded area [41, 42].

The main drawback regarding hydrogels are the weak mechanical properties, stability and weak adhesiveness, especially in heavily exudative wounds or hemorrhage conditions, compromising interfacial adhesion to wounded area [78, 79].

Pectin is a versatile polymer with potential applications for wound healing. Pectin ability to form hydrogels with tunable properties, high-water composition, and the possibility of being functionalized, are key features that make pectin an interesting polymer [80-82]. Comparatively to other natural polymers, such alginate, pectin ramified structure, provides improved mechanical properties and degradation profile, suitable for physiological environment after implantation [48, 83, 84].

Marine Mussel's-inspired functionalization of polymer's, are widely published in literature, as a strategy to improve mechanical properties and adhesiveness in wet environmental conditions, providing potential applications for wound healing [56, 57, 76]. The catechol-based hydrogels are conjugated with dopamine and provide improved adhesion to surfaces in wet condition, by oxidative cross-linking of dopamine [43].

The aim of this work is the development of a cost-effective multifunctional pectin hydrogel suitable for skin tissue engineering specifically for wound healing. Beyond the promotion of ideal wound healing microenvironment and biocompatibility, the hydrogel should hold in same component multi-functionalities, such as, (1) promoting wound healing and skin regeneration, (2) improved mechanical properties, (3) adhesiveness to wound wet environment while proving to perform as a suitable 3D microenvironment for skin cells.

Materials and Methods

1 Pectin Purification

Pectin purification was performed according to the procedure described in Neves et al. [44], with further alterations and optimization of the protocol during pectin purification process. First, using LM citrus pectin (Classic CU701) kindly provided by Herbstreith & Fox (Neuenbürg, Germany), with a GalA content of 86% and a DM of 37% considered as raw pectin (RAWpec), was prepared a 1% (w/V) solution of RAWpec in endotoxin-free water HyClone™ (GE Healthcare, Logan, UT, USA). After complete dissolution of RAWpec, pH was adjusted to 6.0 though the addition of sodium hydroxide (NaOH) solution. Then RAWpec solution was filtrated using membranes with decreasing porosity (0.80 µm (Type AA), 0.45 µm (Type HAWP) and 0.22 µm (Type GSWP) mixed cellulose esters (MCE) membranes (Millipore, Billerica, MA, USA)). After the filtration step, pectin solution was washed with 2% (w/V) of activated charcoal (Sigma-Aldrich, St. Louis, MO, USA) stirred at room temperature (RT) for 1h at 500 to 700 rpm (depending of solution degree of viscosity). The mixture was then submitted to centrifugation cycles, first in the preparatory centrifuge at 12000xg for 1h at 20ºC, and then the ultracentrifuge cycles for 1h, at 4ºC and 27000xg removing carefully the supernatant and reserved until the removal of the majority of the activated charcoal. Finally, the supernatant was filtered using a 0.22 µm membrane (Millipore, Billerica, MA, USA) and the obtained final pectin solution was frozen at -20ºC, lyophilized and stored again at -20ºC until further use. The final lyophilized purified pectin samples were considered PURpec for further contaminants analysis.

2 Contaminants Assessment

2.1 Protein quantification

The amount of protein contaminants present in PURpec was quantified using a Micro BCA Protein Assay Reagent Kit (Pierce Biotechnology, Rockford, IL, USA). For this procedure, two samples were taken from the obtained PURpec and prepared a 0.5% (w/V) pectin solution was prepared in ultrapure water (18 MU, Milli-Q UltraPure Water System, Millipore) (n=3) and the samples were analyzed following the instructions of the manufacturer. For further analysis and comparison, 0.5% (w/V) solutions of RAWpec at pH 6.0 were also prepared and analyzed (n=3).The absorbance was measured at 562

nm using a Synergy MX micro-plate reader (BioTek, Winooski, VT, USA) and the percentage of protein contaminants were determined using a standard curve method.

2.2 Polyphenol quantification

For the polyphenol content analysis in pectin samples the it was used the protocol described by G. Skjak-Bræk et al.[85]. Samples of 1% (w/V) concentration of pectin samples from RAWpec, PURpec. The fluorescence was read at an excitation wavelength of 366 nm and the emission spectrum was recorded between 400 and 500 nm (n=3) using an opaque micro-plate in the Synergy MX micro-plate reader (BioTek, Winooski, VT, USA). For the polyphenols content determination was used the fluorescence values at 445 nm.

3 Preparation of Pectin hydrogels functionalized with RGD substitution

The RGD coupling reaction performed was following the stablished protocol described by Neves, et al, based on carbodiimide chemistry S-NHS/EDC coupling reaction. Purified pectin was weighed and added to MES buffer solution (previously prepared and pH adjusted to ≤ 6.0) in an 1% (w/V) final solution concentration. Then the mixture was stirred overnight at room temperature, to guarantee the complete dissolution of purified pectin and a final 1% (w/V) homogeneous solution. The solution was transferred to ice bath after achieving the argon gas inert environment. Based on 86% of galacturonic acid groups of pure pectin all the reagents were weighted in order to obtain a 1:1 stochiometric molar ratio. Sulfo-NHS and EDC were added in order to activate the carboxylic groups and after 10 minutes the RGD peptide (G4RGDSP). The carbodiimide reaction and coupling RGD reaction was performed in lower controlled temperature in the cold room (4ºC) and Argon gas inert environment always maintained throughout the reaction. The reaction time was 20 hours while stirring. After the reaction was completed, hydroxylamine was added to quench the carbodiimide reaction, and final solution was loaded into dialysis bag with molecular weight of 3 kDa and dialyzed against a decreasing salt solution of type II water and sodium chloride (NaCl) for 3 days and changed every 3-4 times. After dialysis, RGD/pectin solution was stirred for 1 hour with activated charcoal in a ratio of 2 grams for each gram of pectin and then removed during centrifuge cycles of 1200000x*g* at 25ºC for 1 hour, until the activated charcoal is

completely removed. Then the solution was filtered using a 0.22 μm Millipore Sterile bottle top filter and then freeze-dried and stored until further usage.

3.1 UV-Vis RGD pectin quantification

Lyophilized RGD Pectin was weighted and dissolved in MilliQ water to a final concentration of 1% (w/V). A full-spectrum scan was performed in an ultraviolet-visible spectrophometer Synergy MX micro-plate reader (BioTek Instruments, Winooski, VT, USA) and was measured the absorbance at 230 nm. The degree of coupling of pectin with RGD was determined using a standard curve method.

4 Preparation of Pectin hydrogels functionalized with Dopamine substitution

Purified pectin was weighed and added to MES buffer solution (previously prepared and pH adjusted to ≤ 6.0) in an 1% (w/V) final solution concentration. Using light protection flasks, the mixture was stirred overnight at room temperature, to guarantee the complete dissolution of PURpec and a final 1% (w/V) homogeneous solution. Based on 86% of galacturonic acid groups of pectin, Sulfo-NHS and EDC were added in order to activate the free carboxylic groups in a molar ratio 1:1M (100% activation), after 15 minutes the dopamine was added in molar ratio 1:1.5 M. The solution flasks were covered with aluminum foil for light protection and Argon gas inert environment was always maintained throughout the entire reaction time. The reaction time was 9 to 12h hours depending on the brownish macroscopic appearance of the solution. After the reaction was completed, hydroxylamine was added to quench the carbodiimide reaction, and final solution was loaded into dialysis bag with molecular weight cut-off of 3 kDa and dialyzed against a decreasing salt solution of type II water and sodium chloride (NaCl) for 3 days and changed 3-4 times. After dialysis, pectin dopamine solution was stirred for 1 hour with activated charcoal in a ratio of 2 grams for each gram of pectin. In order to remove the remaining activated charcoal, the solution was centrifuged in 1200000 g at 25ºC for 1 hour, until the activated charcoal was completely removed. Then the solution is filtered using a 0.22 μm Millipore Sterile bottle top filter and then freeze-dried and stored until further usage.

4.1 1H-NMR Dopamine Analysis

^{1}H-NMR spectra Dopamine Pectin samples were recorded using a 400 MHz spectrometer AVANCE III (Bruker). The polymer was dissolved (13.3 mg/mL) in deuterated water (D2O, Euriso-top) and transferred to NMR tubes. 3(trimethylsilyl)26propionic 2,2,3,3-d4 acid sodium salt (TSP-d4, Euriso-top) used as internal standard (δ = 0 ppm).

4.2 UV-Vis Dopamine Quantification

Lyophilized Dopamine/Pectin was weighted and dissolved in MilliQ water to a final concentration of 1% (w/V). A full-spectrum scan was performed in an ultraviolet-visible spectrophometer BioTek PowerWave™ XS Microplate Reader equipped with Gen 5 software (BioTek Instruments, Winooski, VT, USA) and was measured the absorbance at 280 nm. The degree of coupling of pectin with RGD was determined using a standard curve method.

4.3 Measurement of FTIR Spectra

Fourier transform infrared (FTIR) spectra were measured directly from lyophilized samples of DOPApec and BLKpec, for further comparison Dopamine Hydrochloride was prepared as pellets with KBr prior to the analysis. Each sample was analyzed using a FTIR spectrophotometer (Perkin-Elmer 200) in a wavelength range of 4000 to 400 cm^{-1} at a rate of 32 scans per spectrum and resolution of 4 cm^{-1} at room temperature and humidity of around 51,5%.

5 Preparation of functionalized Pectin hydrogel matrices - Rheological and mechanical properties characterization

The preparation of *in-situ* crosslinking Dopamine Pectin hydrogel matrices was based on the internal gelation strategy previously described for pectin in the food industry, relying on the $CaCO_3$/GDL system, in which GDL hydrolyses with time, lowering the pH of the solution, and triggering the slow release of Ca^{2+} from $CaCO_3$ molecules. For the preparation of hydrogels, lyophilized Dopamine Pectin was dissolved in 0.9% wt% NaCl (in ultrapure water). Then an aqueous suspension of nanoparticulated $CaCO_3$ (CalEssence 70, Specialty Minerals, Inc.) was thoroughly dispersed into the polymer solution, and a fresh filtered solution od GDL (Sigma-Aldrich) was added. The

$CaCO_3$ and GDL quantities were determined according to stoichiometric ratios reported by Neves et al. [44] defined by the following equations:

Equation (1)

$$R = 2\,[Ca^{2+}]/[COO^{-}]$$

Equation (2)

$$R_{Ca-GDL} = 2\,[Ca^{2+}]/[GDL]$$

The amount of Ca^{2+} to COO^- present (eq. (1)) and the GDL needed for the number of Ca^{2+} in order to have a minimal effect on the final pH of the sample (eq. (2)). For these calculations, the COO^- groups present on pectin were estimated from its DM. These ratios were then optimized for cell immobilization studies under standard cell incubations conditions (37ºC, 5% CO_2).

The rheological properties of pectin gel-precursor solutions and hydrogels were determined using a Kinexus Pro Rheometer (Malvern Instruments, Malvern UK), at 37ºC in a water-vapor saturated environment ensured by the rheometer chamber. For the oscillatory measurements, parallel plate geometries were used.

5.1 Determination of Linear Viscoelastic Region (LVR) – Amplitude and Frequency Sweeps

For the determination of the LVR functionalized pectin hydrogels were previously prepared in final concentration of 1.5 wt% (following the previously described methodology of internal gelation using the $CaCO_3$/GDL gelation system) by placing 20μL of the mixture, directly dispensed between Teflon disc casting, separated by 500 μm in height spacers, placed inside glass petri dishes with 1-2 mL of 0.9% wt% saline solution, and incubate 1h at 37ºC. After incubation period, the pectin hydrogel discs were transferred to a 24 – well plate and incubated (37ºC) in DMEM (Gibco) with 25 mM of N-2-hydroxyethylpiperazine-N-2-ethane sulfonic acid (HEPES, Gibco) at 7.4 pH, to induce swelling. After incubation of the pectin hydrogels discs were punched with 4 mm diameter biopsy punch cylinders, prior the analysis. The LVR was determined using 8 mm diameter sandblasted parallel plate geometries, compressing the gels by 10% of their height (oscillatory measurement gap), and iteratively performing strain amplitude sweep

and frequency sweep measurements. The studied conditions were DOPA_PEC and the control conditions were BLK_PEC and DOPA_PEC/BLK_PEC in a 50/50% ratio.

5.2 Gelation Kinetics

The evolution of the viscoelastic properties of the functionalized pectin gels overtime was assessed with 20 mm diameter sandblasted parallel plate geometries, using the frequency and shear strain values within the LVR. The hydrogel precursor solutions were prepared following the previously described methodology (section 5 and 5.1) and the final addition of $CaCO_3$ and GDL was performed immediately before each measurement to a final concentration of 2, 1.5 and 1 wt% for DOPApec and BLKpec conditions, and to final concentration of 1.5 and 1 wt% for all conditions (Table 2) The time was adjusted, for each assay, in order to match the time at which the GDL was added to the functionalized pectin hydrogel precursor. The assay was performed for 1h until the equilibrium of viscoelastic parameters was achieved.

Table 2 - Experimental and control conditions studied

EXPERIMENTAL	CONTROL
DOPApec	BLKpec
DOPApec + RGDpec (200 μM)	BLKpec + RGDpec (200 μM)
DOPApec (50%) + RGDpec (50%)	BLKpec (50%) + RGDpec (50%)
DOPApec (50%) + BLKpec (50%)	

6 Adhesion Studies

The hydrogels were previously prepared according the internal gelation methodology described in section 5. Alternatively, the hydrogel mixture was poured into a cylindrical Teflon disc casting, to obtained hydrogels with the diameter of 5 mm, and minimal height of 4 mm. After 1h incubation (RT) the samples were carefully removed from the cylindrical disc casting and transferred to 24-well plate with TBS Calcium solution (2xTBS solution (50 mM Tris-Cl; 150 mM NaCl (pH 7.6)) with 15 mM $CaCl_2$) and maintained overnight (4ºC) covered with aluminum foil to protect samples from light. The adhesion studies were performed using TA. XT Plus Texture Analyzer (Stable Micro Systems, UK) with the 5 mm cylindrical probe. Were tested the adhesiveness and work of adhesion performance of 1wt% and 2 wt% DOPA_PEC hydrogels and BLK_PEC in

surfaces of TCPS coverslips (control condition) and Pig Skin (experimental condition). Both samples and surfaces were glued to platform and probe, respectively using two-sided duct tape (Tesa ®, Beiersdorf, Germany) and superglue (Loctite ®, Henkel, Ohio, US). After optimization and testing the both hydrogels (DOPA_PEC and BLK_PEC) and measure the force that both samples can handle without rupture over time, the final experimental conditions were an applying force of 3g (grams) for 5 minutes. The evaluated parameters were the adhesiveness (N), the debonding distance (mm) and time (sec), which allowed the indirect calculation of the work of adhesion (N.sec).

7 Scanning Electron Microscopy (SEM)

The hydrogels were previously prepared according to methodology described in section 5, after 1h incubation (37ºC), the samples were blast freezed in liquid nitrogen and immediately lyophilized. The samples were placed, with a carbon tape, in adequate supports for SEM visualization. Before the visualization the samples were coated with palladium gold. The micro and macroporosity of the scaffolds were assessed through SEM using a High resolution (Schottky) Environmental Scanning Electron Microscope with X-Ray Microanalysis and Electron Backscattered Diffraction analysis: Quanta 400 FEG ESEM/EDAX Genesis X4M.

8 *In Vitro* Studies

8.1 Human Dermal Neonatal Fibroblasts (hDNFs) Culture

hDNFs isolated from neonatal foreskins of heathy male newborns were purchased from ZenBIO. The cells were thawed and maintained in culture at 37ºC in humidified atmosphere with 5% v/v CO_2 in air.

Primary hDNFs used for cell embeddings were cultured in Dermal Fibroblasts Culture Medium (Dulbecco's Modified Eagle Medium (DMEM), Gibco) with 10% v/v Fetal Bovine Serum (FBS, Gibco), 1% v/v Penicillin/Streptomycin (P/S) and 1 % v/v Amphotericin B. The culture medium was changed every 7 days or every cell passage. The cells were trypsinized (0.05 wt% trypsin/ethylenediamine tetra acetic acid (EDTA) solution, Sigma) when they reached 70-80% of confluence. Cells from passages between 10 to 15 were used in this study.

8.2 hDNFs culture with Functionalized Pectin Hydrogels

Cells were trypsinized before reaching confluence and centrifuged. After discarding supernatant, hDNFs were carefully mixed at a final cell density of $8x10^6$ cells per mL with pectin hydrogels precursor solutions and crosslinking agents (as described in section 5). The cell pellet was mixed with precursor solutions of functionalized pectin hydrogels at a final concentration of 1.5 wt%, 20μL of these solution were directly dispensed between 2 teflon disc casting, separated by 500 μm in height spacers, placed inside glass petri dishes with 1-2 mL of 0.9% wt% saline solution (to guarantee proper humidified atmosphere). For completion of gelation process, samples were placed in the incubator (37ºC, 5% CO_2 humidified atmosphere) for 1 hour. After this, cell-loaded discs were transferred to 2-poly(hydroxyethyl methacrylate) (pHEMA)-treated 24 well plate with cell culture medium (DMEM (Gibco) supplemented with 10% FBS (Gibco), 1% v/v Penicillin/Streptomycin (P/S) and 1 % v/v Amphotericin B) and changed after 24 hours. The cell-loaded functionalized pectin hydrogels were cultured for up to two weeks (14 days) and medium changed every week. The table XXXX (see table above) described the studied experimental conditions and respective controls.

8.3 Cell metabolic activity and viability

Metabolic activity was estimated using the resazurin-based assay. At different timepoints (72h, 7 and 14 days), the culture medium was removed from the wells and fresh basal medium with 20 v% resazurin (Sigma) was added. Cell-loaded hydrogels were incubated (37ºC, 5 v% CO_2) for 2h. After incubation period, were transferred 200 μL per well to a black 96-well plate and measured ($\lambda_{ex} \approx 530$ nm, $\lambda_{em} \approx 590$ nm) using a micro-plate reader (Synergy MX, BioTek).

Briefly, media was removed, samples were washed with DMEM without phenol red and then incubated in the Ethidium/Calcein solution for 45 min, at 37°C. This solution was then replaced by DMEM without phenol red. Immediately after incubation, cells were visualized with a confocal laser scanning microscope (CLSM, Leica SP5, Leica Microsystems, Wetzlar, Germany) using LCS software (Leica Microsystems, Wetzlar, Germany). The scanned Z-series were projected onto a single plane and pseudo-colored using ImageJ.

8.4 Cell morphology and fibronectin deposition

For the same defined timepoints (3, 7 and 14 days) as for the cell metabolic activity and viability assays, cell-loaded hydrogels were stained for filamentous actin (F-

actin), fibronectin (FN), and nuclei. Samples were washed several times with Hank's Balanced Salt Solution (HBSS (1X), Gibco) to remove completely traces of phenol red from DMEM medium; fixed for 20 minutes with 4 wt% paraformaldehyde (PFA, Sigma), and permeabilized with 0.1% Triton X-100 (CALBIOCHEM, San Diego, USA) (0.1% v/v in HBSS) for 5 min. Then, samples were incubated for 30 minutes with 1 wt% bovine serum albumin (BSA, VWR International, Pennsylvania, USA) in HBSS. The cell-loaded hydrogels were incubated overnight at 4 ºC with combination of different primary antibodies (Table 3) in humidified atmosphere with BSA (1% w/v in HBSS). After incubation, samples were washed with HBSS and incubated with the conjugated secondary antibodies (Table 3) with BSA solution (1% w/v in HBSS) for at least 40 minutes at RT. Samples were subsequently washed three times with HBSS and nuclei were counterstained with 4',6-diamino-2-phenyl-indole dihydrochloride (DAPI, Sigma, 0.1μg mL^{-1}) (VECTASHIELD, Vector Laboratories), just before confocal visualization (CLSM, Leica SP5, Leica Microsystems, Wetzlar, Germany) using LCS software (Leica Microsystems, Wetzlar, Germany). The scanned Z-series were projected onto a single plane and pseudo-colored using ImageJ.

Adobe Photoshop CC software was used for image adjustments, such as the correction of channel levels, brightness and contrast.

Table 3 - Primary and Secondary antibodies used in samples immunostaining for confocal visualization

Primary Antibody	**Manufacturer**	**Dilution**
Anti-Ki-67 (Rabbit)	Abcam	1:100
Anti-Fibronectin (Rabbit)	Sigma (f3648)	1:400
Secondary Antibody		
Alexa Fluor® 594 (Goat anti-rabbit)	Molecular Probes - Invitrogen	1:1000
Alexa Fluor®647 (Chicken anti-mouse)	Molecular Probes - Invitrogen	1:1000
Additional Markers	**Manufacturer**	**Dilution**
Flash Phalloidin Green 488	BioLegend	1:40

9 Statistical Analysis

Statistical analyses were performed using GraphPad Prism 8.1.2 software. For the quantification data, determination of LVR and metabolic activity measurements, the non-parametric Mann-Whitney test was used. All tests were performed using a 99%

confidence interval. For the adhesion studies, first was applied the D'Agostino & Pearson normality test to analyze the presence of a normal distribution between samples tested. Since data do not present a normal distribution, using one-way ANOVA data were analyzed with Kruskal-Wallis non-parametric test.

Results and Discussion

1 Pectin purification, functionalization and characterization

1.1 Pectin purification

The main drawback regarding pectin is the absence of a commercially available pectin with medical-grade purity. The presence of contaminants, such as, proteins, polyphenols and endotoxins, may compromise the polymer biocompatibility and raises issues regarding *in vivo* studies or future human medical applications.[44] High concentrations of these contaminants in polymers are responsible for immunogenic reactions and probably interfere with *in vivo* applications [86, 87]. Markov, et al., using non purified pectin found that pectin hydrogels have low toxicity rates, even though macrophages and non-specific adsorption of blood plasma proteins seem to increase as pectin concentration in the hydrogels increases [87]. These aspects point out the relevance of establish a purification step, prior to any biomedical application, with aim to prevent its immunogenicity and guarantee the biocompatibility of pectin based biomedical solutions. Therefore, the first step of this work was the implementation of a purification protocol, previously developed and described by Neves, et al [44], aiming the reduction of proteins, polyphenols and endotoxins content, maintaining pectin's structural integrity.

The presence of contaminants in pectin, specifically, proteins and polyphenols, were assessed both for raw pectin and pure pectin (Fig. 10-A).

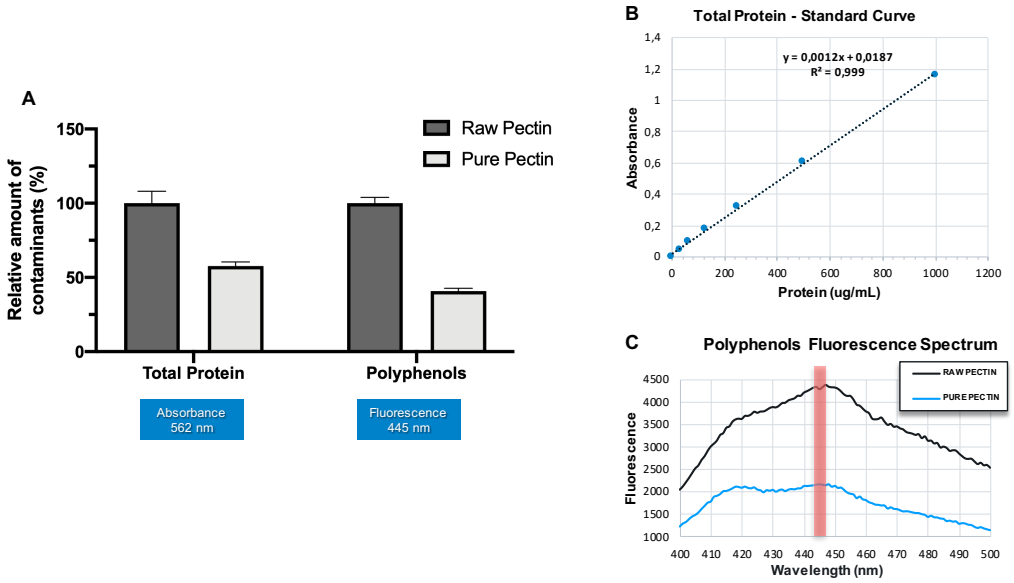

Figure 10. Contaminants assessment of purified pectin. (A) Percentage of reduction of total proteins and polyphenols compared to raw pectin. (B) Total protein content using absorbance readings at 562 nm. (C) Polyphenols content using fluorescence readings at 445 nm.

The purification method reduces the protein content approximately by 42% and polyphenols content by 59%. The contaminants removal rates are consistent with the data published by Neves et al. which the implantation of pectin hydrogels with the removal of 50% of total protein, in murine model, does not induce host immune response and considered biocompatible for this animal model [44].

Despite the advantages of using biopolymers, such as pectin, as inexpensive biomaterials, the degree of contaminants present after extraction, must be removed prior to any application in human body. Several alternative extraction methodologies to conventional heating extraction and purification techniques for contaminants removal, have been described for pectin and other biopolymers [50, 88-92] for biomedical applications. However, most of these techniques, or represents expensive techniques increasing the polymer production costs, or uses high pH and temperature shifts, which are not feasible for pectin, leading to pectin depolymerization, via acid hydrolysis or β-elimination depending on DM and pH of pectin [44, 93, 94].

The purification protocol used was performed at room temperature and at pH of 6.0, wherein pectin is stable in solution and maintain its structural integrity. Using simple and cost-effective methodologies, such as filter membranes, activated charcoal and ultracentrifugation, the major contaminants decrease approximately 50% maintaining the physico-chemical properties of pectin.

Additional strategies need to be implemented to improve pectin purity, increasing contaminants removal, reducing its immunogenicity and improve biocompatibility for future human biomedical applications.

1.2 Pectin functionalization with RGD peptide

Pectin brings together unique biological and physico-chemical features for skin tissue engineering and wound healing applications, such as, high water content, biocompatibility and controlled biodegradability [95]. However, owing to its hydrophobic nature and the absence of cell adhesion biochemical cues in its structure, pectin prevents cell adhesion and protein adsorption [44, 94].

Grafting RGD (Arg-Gly-Asp) sequences in non-adhesives biomaterials, incorporating cell adhesion recognition sites, required for integrins adhesion to ECM cellular components [96, 97]. In this study, RGD-functionalized pectin was synthesized and further used to produce hydrogels matrices for 3D cell culture with HDNF's. Based on the carbodiimide chemistry protocol previously described by Neves et al. [44] (recently optimized for pectin by Biofabrication and Bioengineering 3D

Microenvironments groups), purified pectin was functionalized with RGD containing peptide Arginine - Glycine - Aspartic Acid - Serine - Proline (G4RGDSP) (GenScript) (Fig. 11).

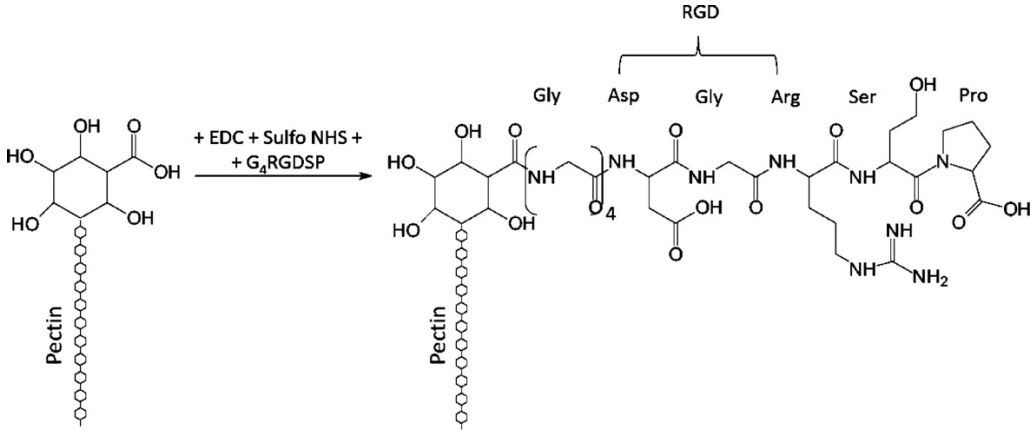

Figure 11. Functionalization of pectin with RGD by carbodiimide chemistry. Pectin was covalently modified with RGD oligopeptide (G4RGDSP) using aqueous carbodiimide chemistry through the activation of free carboxylic groups of pectin (EDC/Sufo-NHS) they will react and bond to RGD. (Adapted from Munarin et al.[52])

The amount of RGD covalently grafted in pectin was estimated by successive dilutions of RGD in 1% (w/v) pectin solution. UV-Visible spectrum of RGD, normalized against blank pectin, (Fig. 12-A), reveal the presence of the characteristic peak around 230 nm, which indicates the successfully grafting of the RGD peptide in pectin backbone.

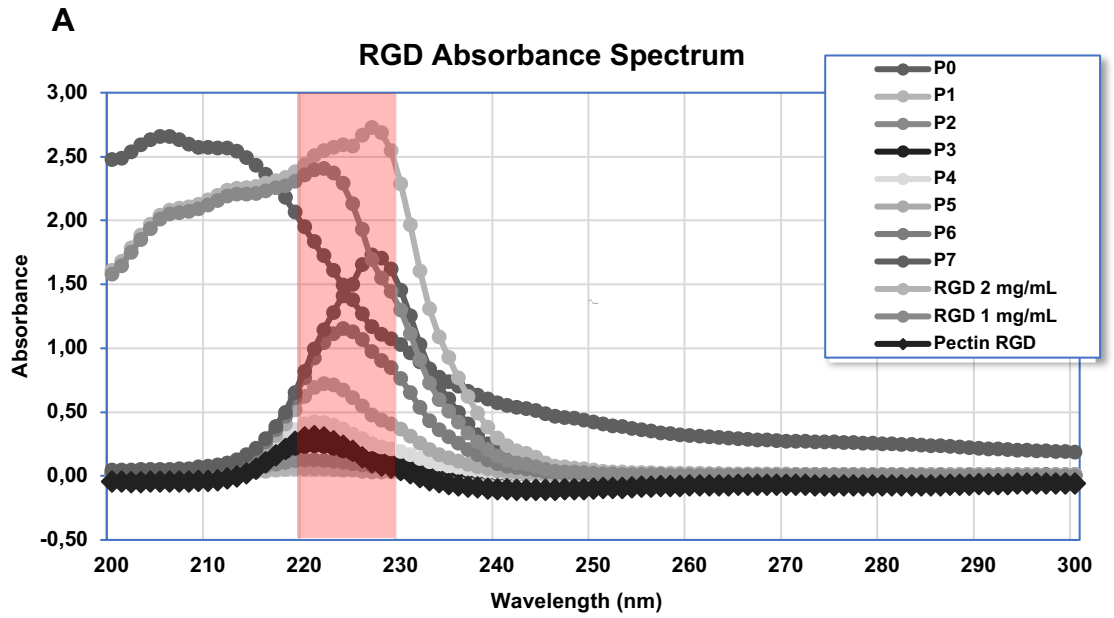

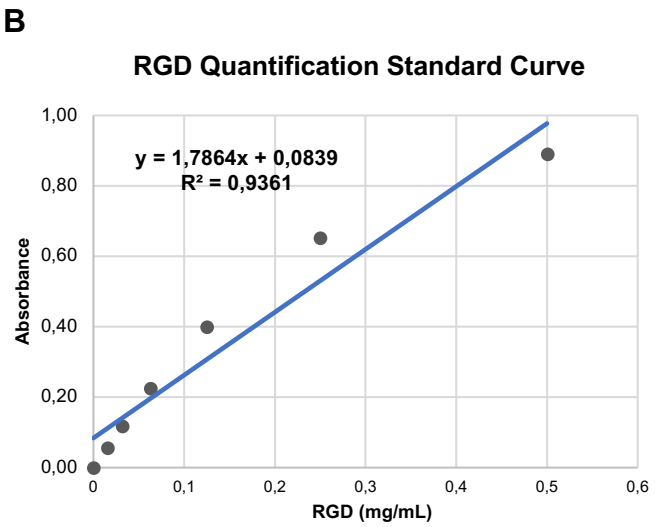

Figure 12. RGD Coupling efficiency - UV-Vis Quantification: (A) UV-Vis absorbance RGD spectrum acquired from wavelength values between 200 to 300 nm. (B) RGD quantification standard curve obtained from absorbance values measured at 230 nm.

In the absorbance spectrum of RGD was observed that as the concentration decreases, the typical RGD peak (230 nm) exhibit a tendency to deviate to the left of the graph and the peak shifts to wavelengths values approximately 221 nm. This deviation is attributed to the effect of pectin overlapping the RGD signal, as RGD concentration decreases. The amount of peptide grafted in pectin estimated, was based on the standard curve method (Fig. 12-B) and takes into account this deviation induced by pectin.

The amount of RGD coupled in pectin was approximately 12 mg of RGD per gram of pectin.

1.3 Pectin functionalization with Dopamine

Hydrogel-based therapies meet the foundations and criteria for an ideal wound healing environment. Hydrogels are versatile, compliant and permeable, cross-linked 3D polymeric structures, mimicking ECM, with high absorption capacity (water and wound exudate), offering endless possibilities for physical and/or chemical modifications, to improve hydrogel similarity to native ECM [40, 42-44].

The main propose our work comprises the development of pectin hydrogel with improved mechanical properties and adhesiveness to wound wet environmental conditions in presence of wound exudate.

In order to obtain hydrogels with these properties one strategy was developed based on the bioinspired model of marine mussels' adhesive properties. This model has been widely explored for other polymer's to create tissue engineering scaffolds [67, 76]

and tissue adhesives with improved mechanical properties and strong adhesive properties in wet environmental conditions under different substrates [56, 57, 66]. During the synthesis of catechol-based hydrogels DOPA are incorporated in the polymer backbone structure, the amount of DOPA grafted and the exposure to an oxidizing cross-linking agent, produces stable hydrogels with improved mechanical properties and strong adhesiveness [43, 61].

The pectin-catechol conjugates were synthesized based on adaptation for pectin of Lee, et al. [76] previously described strategy for alginate.

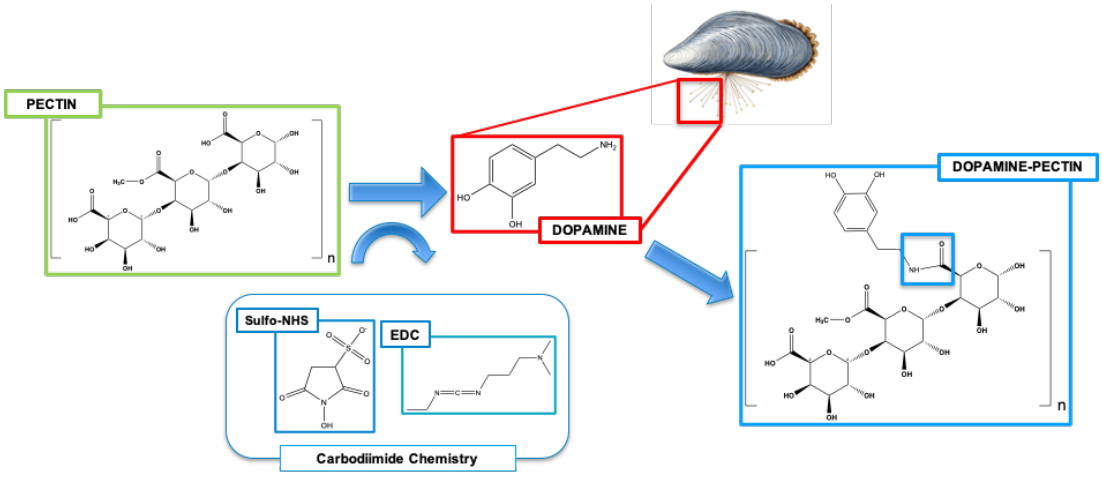

Figure 13. Schematic representation of Carbodiimide chemistry used to functionalization of Pectin with Dopamine.

The pectin functionalization with DOPA was based on a carbodiimide reactionary system (Fig. 13), previously optimized with the goal of obtain higher reaction yield with lowest intermediary formation (n-acylurea) and higher degree of DOPA grafted in pectin without compromise the gelation properties of the polymer.

1.3.1 Pectin coupling with DOPA – Optimization

In an effort to optimize the ideal conditions for pectin functionalization with DOPA as it was never attempted before, different approaches were carried out. Many parameters and variations in the reactionary conditions were performed. Either the variation of the activation rate of pectin free carboxylic groups were DOPA covalently bonds, through the variation of activation reagents (EDC, NHS or Sufo-NHS) or the availability of reacting substance (Dopamine – HCl). After functionalization for each condition, the amount of dopamine grafted in pectin was quantified both by UV-Visible

spectrum quantification and ^{1}H-NMR and compared the obtained results for both analyses.

The UV-Visible spectrum was obtained for wavelength values of 200 to 300 nm and the conjugation efficiency of dopamine to pectin backbone was determined by measure measuring the absorbance at 280 nm (Fig. 14). The aromatic ring structure of conjugated catechol group exhibits absorption peak at this wavelength [76] as seen in figure 14-A. The amount of dopamine in each formulation was calculated using a standard curve obtained by successive dilutions of Dopamine hydrochloride in blank pectin (Fig. 14-B).

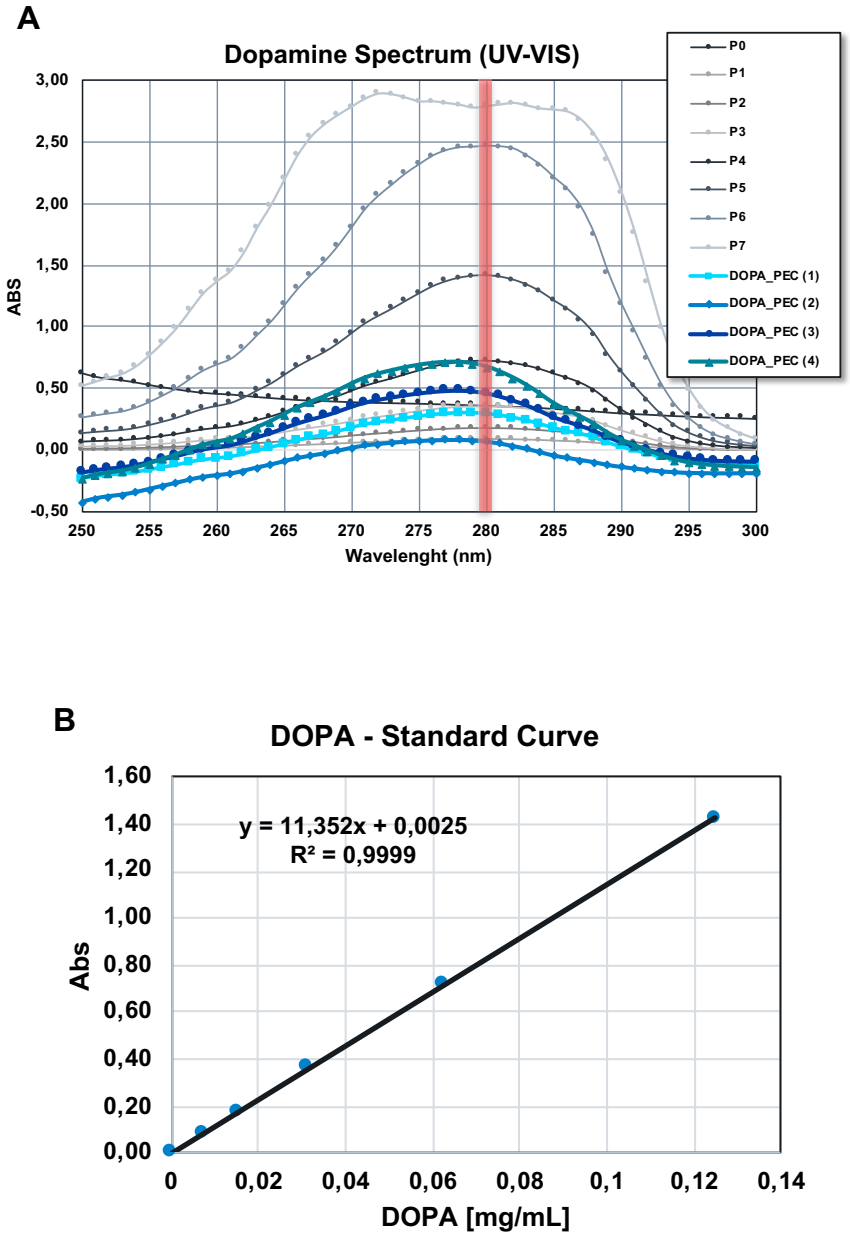

Figure 14. DOPA quantification by UV-VIS. (A) UV-VIS absorbance Dopamine spectrum acquired from 250 to 300 nm and Dopamine quantification determined for absorbance values of 280 nm; (B) Dopamine standard curve according for absorbance readings at 280 nm.

The following table (**table 4)** resumes all the conditional optimization process of the pectin dopamine coupling reaction. In this table for all conditions tested were estimated the amount of dopamine either, through the UV-Visible methodology or through ^{1}H-NMR, and also estimated the amount of intermediary formation with the carbodiimide coupling reaction.

Table 4 - UV-VIS and ^{1}H-NMR quantitative analysis of different Carbodiimide reactionary conditions tested for Pectin Dopamine coupling.

Reaction	Reactionary Conditions			UV-Vis Quantification	^{1}H-NMR Quantification	
	Activation Rate (Free COOH Groups)	Reagent Molar Ratio		Dopamine (mg) per 1 gr Pectin (mg)	Dopamine Degree of Substitution (%)	Intermediary Formation (n-acylurea) (%)
		Carbodiimide Reagents	DOPA			
DOPA_PEC (1)	100%	EDC/NHS (1:1)	(1:1)	3,96	5,66	13,79
DOPA_PEC (2)	200%	EDC/NHS (2:1)	(1:1)	11,01	13,29	19,68
DOPA_PEC (3)	100%	EDC/NHS (1:1)	(1:1.5)	3,34	2,91	9,09
DOPA_PEC (4)	100%	EDC/Sulfo - NHS (1:1)	(1:1.5)	5,13	3,85	12,28

The ^{1}H-NMR spectra were obtained for each formulation and compared against Dopamine hydrochloride and blank pectin spectra (Fig. 15). The successful conjugation efficiency of dopamine in pectin was confirmed by the appearance of characteristic peaks from 6.5 to 7.0 ppm (Fig. 15-a)), correspondent to the hydrogens of the aromatic ring of the catechol group, resulting from the conjugation of Dopamine to pectin carboxylic groups [76, 98]. Likewise, it was observed the appearance of two additional characteristic peaks, the first from 2.75 to 3 ppm (Fig. 15-b)), and the second one the peak from 3 to 3.5 ppm (Fig. 15-c)), corresponding to hydrogens of the aliphatic chain of Dopamine molecule. This final peak was attenuated in the DOPA_PEC conjugates, due to its proximity to the amide bond formation with dopamine coupling. For further analysis it was used the characteristic peak from 6.5 to 7 ppm of the protons of the aromatic ring of Dopamine molecule to quantify the percentage of dopamine conjugated with pectin, allowing the comparison with similar polymers, such alginate.

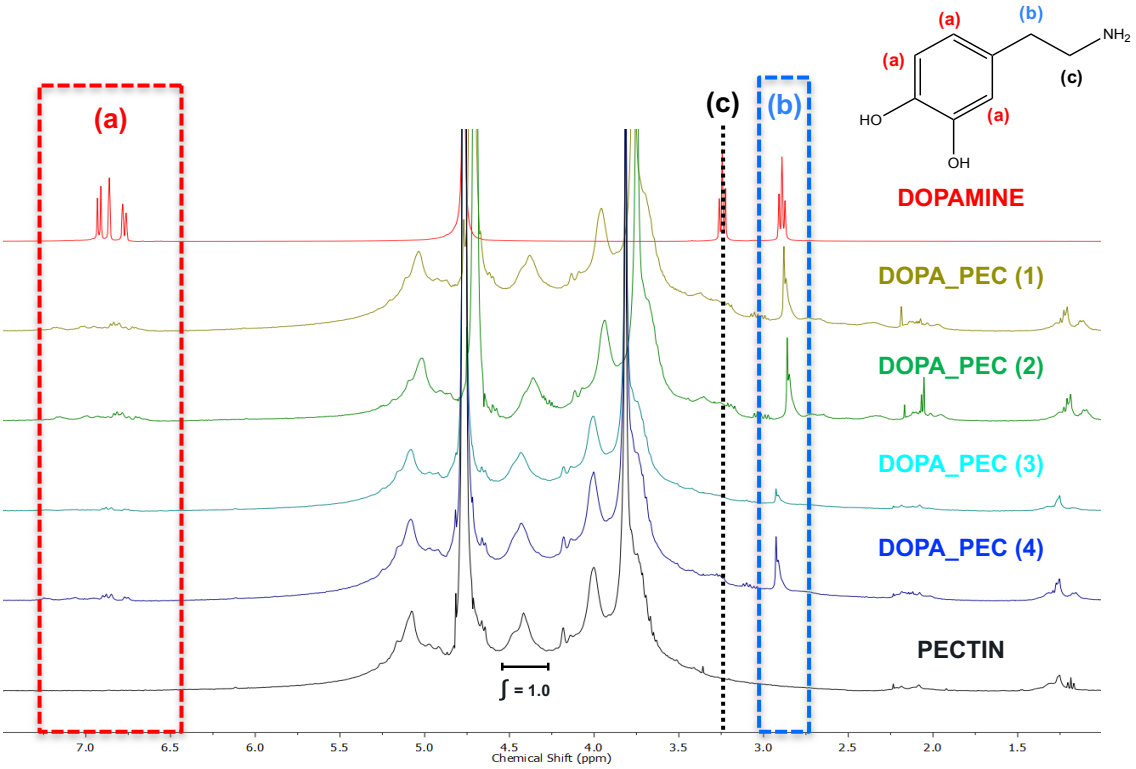

Figure 15. ^{1}H-NMR spectra of the formulations tested for pectin dopamine carbodiimide coupling reaction, comparatively to pectin and dopamine spectra. (a) Characteristic peaks of aromatic ring present in dopamine structure, visible in all DOPA_PEC formulations with variable intensity translating the dopamine coupling degree into pectin molecule. (b) Characteristic peak of the carbon that links the aromatic portion to the aminoethyl portion of dopamine molecule, present in all formulations tested. (c) Characteristic peak representing proton near the amine group, which in case of dopamine pectin conjugates is difficult to evaluate its presence.

The carbodiimide reaction occurs in the free carboxylic groups of galacturonic acid (GalA) molecules of the pectin backbone and the number of reactive groups is dependent on the methylation degree of pectin [44]. The previously purified pectin used for this work (Herbstreith & Fox Classic CU701) has approximately 86% of GalA units, based on the methylation degree, 37% of the carboxylic groups cannot be activated, otherwise pectin structure would be compromised. The calculations for each condition were made in line with this premise.

In the first two conditions, DOPA_PEC (1) and DOPA_PEC (2) there was a variation in the activation rate of the free carboxylic group of pectin, doubling the molar ratio of EDC and NHS, maintaining in both reactions the same amount of Dopamine hydrochloride. Despite DOPA_PEC (2) presents a higher amount of dopamine coupled with pectin (approximately 11 mg of DOPA per gram of pectin), the percentage of intermediary formation, was considerable higher than the DOPA_PEC (1) (approximately 3,96 mg of DOPA per gram of pectin).

The higher intermediary formation rate in DOPA_PEC (2) was probably attributed to the insufficient amount of Dopamine (substrate/nucleophile) to react with the

increased activated carboxylic groups, leading to the formation of N-acylurea. As shown in the scheme of the figure 16, the carbodiimide reaction involves the activation of free carboxylic groups by EDC to origin O-Acylisourea group, which after a nucleophilic attack by free amine groups of the nucleophile (primary amine) forms the cross-linking amide bond and an EDC-related water-soluble residue is liberated. In the absence of the nucleophile, the highly reactive O-acylisourea group can overtime, rearrange to a stable N-acylurea which is a carbodiimide intermediary product [99].

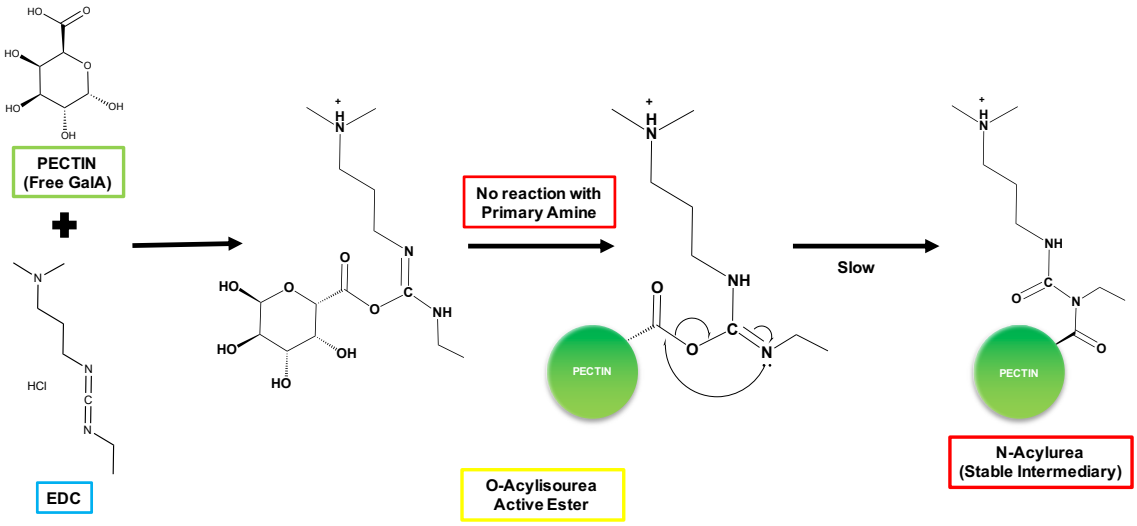

Figure 16. Reactionary mechanism of the formation of N-acylurea as a carbodiimide intermediary. The O-Acylisourea is an unstable active ester, intermediary of the carbodiimide reaction and when it doesn't react with a primary amine (Dopamine), it undergoes to a molecular structural rearrangement process inducing the formation of N-acylurea, which is a stable intermediary of the carbodiimide chemistry.

In the scope of this work, one of the primary aims was development of a biocompatible pectin hydrogel for skin tissue engineering and wound healing. Lai et al, evaluate the properties of carbodiimide-treated gelatin matrices for limbal stem cells niches and concluded that the presence of high amounts of N-acylurea is detrimental for in vitro and in vivo ocular biocompatibility [100]. Thus, for the DOPA_PEC (2) formulation we concluded that doubling the activation rate, was associated with increased intermediary formation (approximately 19,68% intermediary formation), compromising polymer biocompatibility and this strategy was excluded for the final functionalization protocol.

Finally, for the batches DOPA_PEC (3) and DOPA_PEC (4) we evaluate the effect of the increase of the ratio of Dopamine hydrochloride and the advantage of using Sulfo-NHS instead of NHS. The rationale behind the increase of molar ratio of dopamine hydrochloride was an attempt to increase the availability of nucleophile to react with activated carboxylic groups with the objective of increase conjugation ratios with pectin. Dopamine in aqueous solution rapidly undergoes autoxidative processes, reacting first

with the environmental oxygen, giving rise to quinone form and superoxide anion, which will be further converted into different ROS [101]. The dopamine autoxidation is pH-dependent process and the formation of hydroxide ion from a water molecule is responsible to attack amino groups via intramolecular Michael addition, forming an inert intermediate of dopamine [102]. Thus, aiming the increase of the reaction yield, higher amount of dopamine was added to these two batches, with the variation of carbodiimide reaction reagents, DOPA_PEC(3) was activated in the presence of NHS and DOPA_PEC(4) was activated in presence of Sulfo-NHS. NHS and Sulfo-NHS have a stabilizing effect in the carbodiimide coupling reaction, it prevents the hydrolysis of O-acylisourea by the nucleophilic attack of water molecules in solution and reduces the susceptibility of hydrolysis at acidic pH of NHS-activated carboxylic groups [99]. The difference between them relies on the solubility in aqueous solution. Sulfo-NHS is more soluble than NHS and we want to evaluate the effect of the higher solubility in the final yield of the reaction and intermediary formation.

Our results show that DOPA_PEC(4) obtained higher yield, approximately 5,13 mg of Dopamine per gram of pectin, in contrast to 3,34 mg of Dopamine per gram of pectin of DOPA_PEC(3). However, DOPA_PEC(4) shows 12,28% of N-acyulruea formation, which was not significantly higher when compared with 9,09% for the DOPA_PEC(3) batch. When we compared with DOPA_PEC(1) where the activation rate of carboxylic groups was similar, the increase dopamine molar ratio has a beneficial effect over N-acylurea, which was 13,79%.

In agreement with these results, the conditions that satisfy our objectives was the batch DOPA_PEC(4) with carboxylic group activation rate of 100% (stoichiometric ratios of EDC/Sulfo-NHS of 1:1) and molar ratio of 1:1.5 for dopamine.

During the optimization process of carbodiimide coupling of pectin with dopamine, we notice higher variation in dopamine UV-visible quantification within the same batch. In the table 5 we can observe these variations for each batch tested.

Table 5 - UV – VIS quantification for the different reactions tested on the optimization stage.

REACTION	N	Reactionary Conditions			UV-Vis Quantification		
		Activation Rate (Free COOH Groups)	Reagents Molar Ratio		Dopamine (mg)/1 gr Pectin		
			Carbodiimide	Dopamine	Samples	Value (mg)	Average
DOPA_PEC (1)	4	100%	EDC/NHS (1:1)	(1:1)	1.1	4,27	3,96
					1.2	3,29	
					1.3	**1,23**	
					1.4	**7,04**	
DOPA_PEC (2)	3	200%	EDC/NHS (2:1)	(1:1)	2.1	**0,59**	11,01
					2.2	2,68	
					2.3	**29,75**	
DOPA_PEC (3)	5	100%	EDC/NHS (1:1)	(1:1.5)	3.1	6,01	3,34
					3.2	6,66	
					3.3	**0,87**	
					3.4	**2,72**	
					3.5	**0,43**	
DOPA_PEC (4)	4	100%	EDC/Sulfo - NHS (1:1)	(1:1.5)	4.1	**9,50**	5,13
					4.2	**5,42**	
					4.3	2,81	
					4.4	2,77	

All the samples from each batch were quantified with UV-Vis methodology based on the aromatic absorption peak at 280 nm. As shown in the table 5 there is a wide variation between samples from the same batch.

After excluding technical and operator related problems, during the execution of UV-visible protocol and since we obtain consistent inconsistent results after repeating the readings for all batches, we concluded that the filters used in the final filtration step of the protocol were retaining the DOPA_PEC polymer in its structure (Fig. 17).

This phenomenon was probably attributed to retention of Pectin dopamine molecules in PES 0.22 µm filters used for final filtration step before lyophilization.

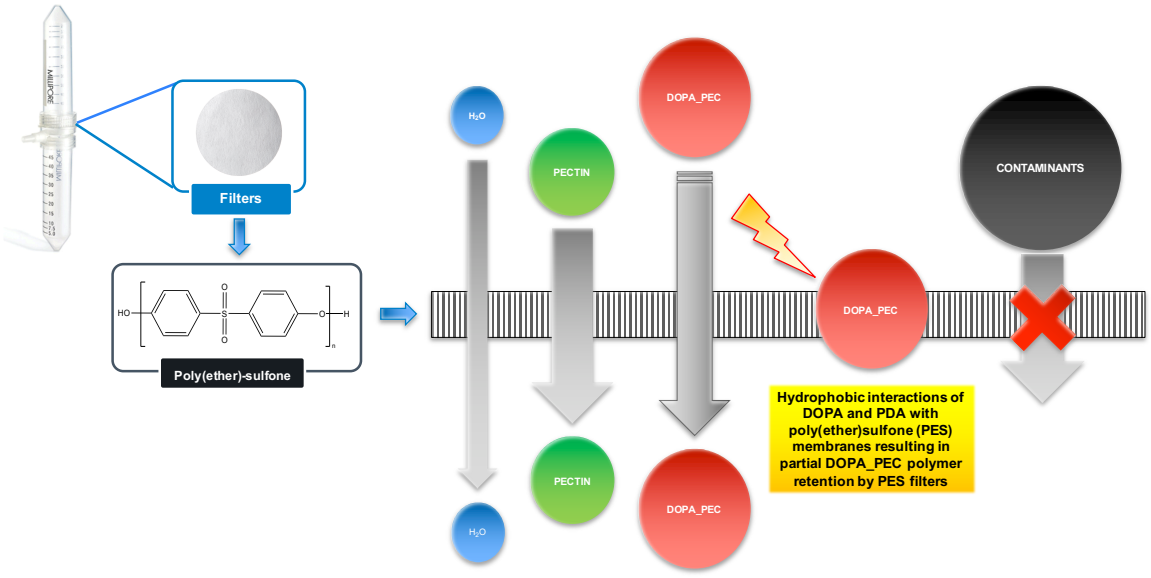

Figure 17. Schematic representation of hydrophobic interactions between poly(ether)sulfone from Milipore® filters and DOPA/Polydopamine (PDA) of Pectin functionalized with Dopamine.

The Milipore® filters used are composed of poly(ether)sulfone (PES) polymer with a porosity of 0.22 µm and were used to remove possible contaminations and residues previously to the lyophilization of the polymer. After extensive search, we found that polydopamine coatings in membranes materials have been widely used in water treatment to produce membranes resistant to fouling during filtration processes, increasing the removal of positively charged contaminants [103, 104]. PES membranes present a hydrophobic nature and polydopamine/dopamine coatings has been used to improve membrane hydrophilicity and hemocompatibility. Dopamine/Polydopamine interacts and adheres to PES through hydrophobic and electrostatic interactions [105]. Based on these findings, we've changed the type of membrane used for the final filtration step of pectin functionalization with dopamine, using mixed cellulose ester (MCE) membranes in alternative to PES filters.

1.3.2 Preparation and physico-chemical characterization of Pectin coupling with DOPA

After conditional optimization, pectin was functionalized with dopamine and we quantified and characterized the final lyophilized polymer using UV-Visible absorbance spectrum, ^{1}H-NMR and ATR-FTIR analysis.

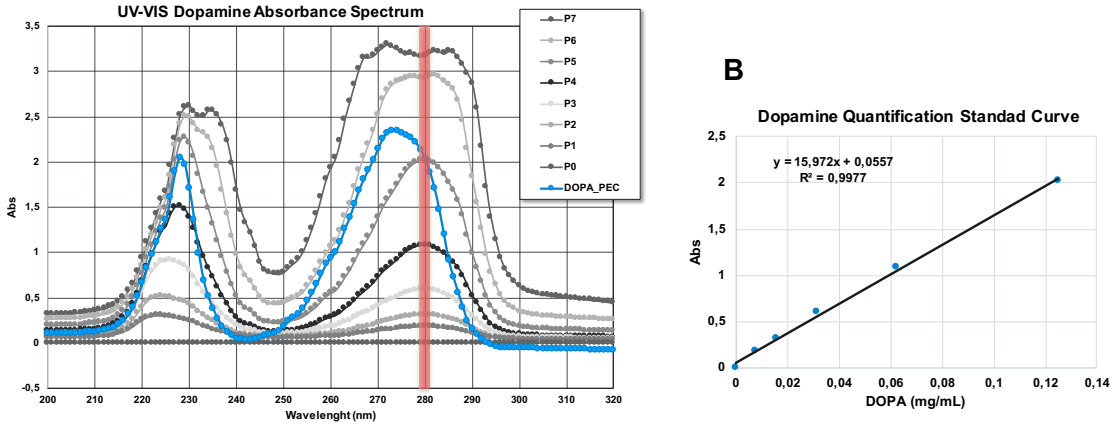

Figure 18. UV-VIS quantification of DOPA. (A) UV-Visible absorbance Dopamine spectrum acquired from 250 to 300 nm and Dopamine quantification determined for absorbance values of 280 nm. (B) Dopamine quantification standard curve according for absorbance readings values at 280 nm.

Using UV-visible absorbance spectrum of the polymer (Fig. 18-A), the amount of dopamine was estimated using the standard curve method for absorbance values of 280 nm (Fig. 18-B). The amount of dopamine in final DOPA_PEC polymer was approximately 12,40 mg per gram of pectin (n=5). Comparatively to the amount of dopamine obtained

for the batches produced during the conditional optimization process, it was significantly higher, and we didn't observe significant variations in the amount of dopamine for each sample (n=5) caused by the filter retention of the polymer (MCE filters).

The successful incorporation of dopamine within pectin structure was also demonstrated by ^{1}H-NMR spectroscopy, through the appearance of new peaks in pectin conjugated with dopamine spectrum, corresponding to characteristic protons of dopamine (Fig. 19). It is important to emphasize the appearance of three peaks, from 7.39 to 6.73 ppm, corresponding to hydrogens of the aromatic ring of dopamine molecule (Fig. 19-a)); and two peaks at 3.28 ppm and 2.92 ppm, characteristic of the hydrogens of the aliphatic chain of dopamine molecule (Fig. 19-b) and c)).

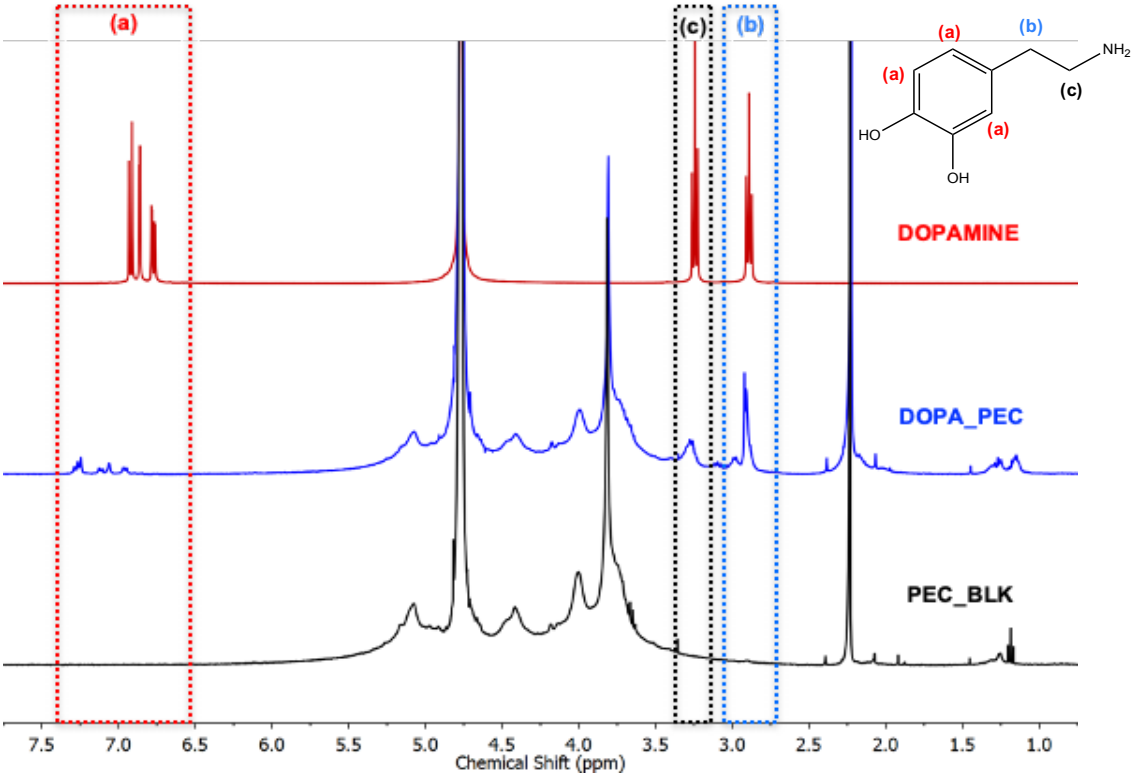

Figure 19. ^{1}H-NMR Spectra of dopamine, pectin (PEC_BLK) and Dopamine conjugated pectin (DOPA_PEC). As showed in the figure the conjugated pectin with dopamine its visible the characteristic peaks of the hydrogens of dopamine molecule. a) Characteristic peaks of hydrogens of the aromatic ring of Dopamine molecule; b) and c) The characteristic peaks of the protons of corresponding to the aliphatic chain of the Dopamine molecule are also visible in the pectin conjugated with dopamine.

The degree of substitution of Dopamine and percentage of Dopamine incorporated on free carboxylic groups of GalA units of pectin, was possible to determine through the comparison of the integral of hydrogens of the aromatic ring of dopamine molecule with the integral of one hydrogen (peak from 4.58 to 4.38 ppm) of the monomeric GalA units of pectin backbone. The degree of substitution estimated was 7.69% of dopamine successfully conjugated with pectin polymer backbone. Considering the total activation of the 63% free carboxylic groups of GalA units of pectin, the

carbodiimide reaction yield was relatively low. Comparatively to other polymers, similar approaches for alginate and Hyaluronic Acid (HA), obtained a degree of substitution of 5.5% [76] and 6% for HA [106], which was consistent with the obtained results for pectin, reinforcing the successful dopamine coupling. The obtained results were probably attributed to the pectin ramified structure which may interfere with the steric conditions required for the coupling reaction occurs, through the induction of chemical repulsive interactions with the neighboring molecules. One the other hand, the autoxidative behavior of dopamine in aqueous environment over time [102], may also contribute to lower conjugation efficiency. Nevertheless, higher conjugation rates may, in the future work affect gelation properties and the viscoelastic behavior of hydrogels, that depends on the free carboxylic groups interaction with Ca^{2+} in the egg-boxes formation [107].

The N-acylurea formation, was evaluated based on the characteristic peak at 2.90 ppm, observed as a singlet, representing the methyl protons of N-acylurea adducts. Unreactive N-acylurea adducts formation rate are temperature and pH dependent [108]. Observing the ^{1}H-NMR spectrum for Pectin conjugated with dopamine, we cannot identify the N-acylurea characteristic peak by the overlapping of the 2.92 ppm peak of the aliphatic chain of the dopamine molecule. Thus, we considered that ^{1}H-NMR was not the most adequate method to evaluate the N-acylurea carbodiimide adduct formation, for the discussed functionalization

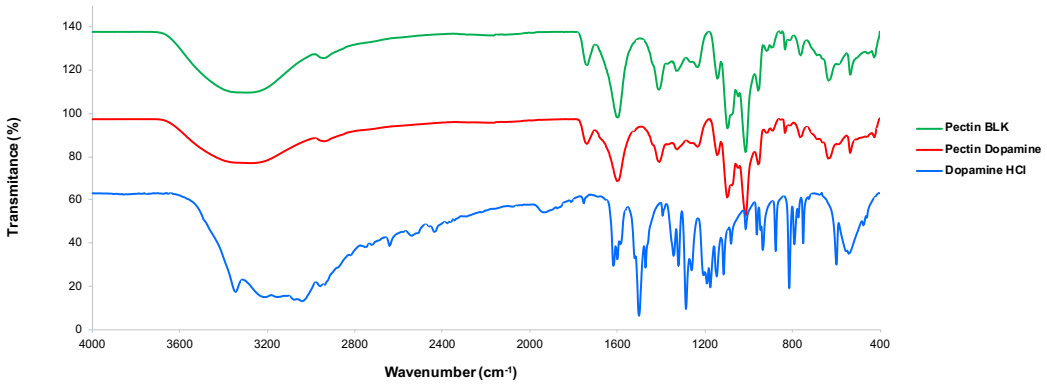

Figure 20. Comparative Fourier Transform Infra-Red (FTIR) spectra of pure Pectin and DOPA functionalized Pectin in comparison with Dopamine.

Structural characterization of the compounds was also performed by ATR-FTIR (Fig. 20). In the pectin spectrum (Pectin-BLK), it is well observed characteristic peaks with strong intensity at: a) 3295 cm^{-1} characteristic of C-OH stretching vibrations from glycosidic ring, b) 2925 cm^{-1}, which can be attributed to -CH_3 stretching vibrations from ester moiety, c) 1725 cm^{-1} corresponding to C=O stretching vibration in carboxylic acids

and esters, b) 1600 and 1410 cm^{-1} assigned to asymmetric and symmetric -C=O vibrations, respectively [109]. The wavelength range between 950 and 1200 cm^{-1} is considered the 'fingerprint' region for carbohydrates, as the peaks appearing in this zone are characteristic of vibration modes from typical chemical groups in polysaccharides [110].

On the other hand, the dopamine spectrum presents a broad peak at 3346-3337 cm^{-1} that is characteristic of -OH and -NH_2 stretching vibrations, together with a peak at 1600 cm^{-1} attributable to the bending vibration mode of primary amines. The strong peak around 1500 cm^{-1} may be attributed to C=C-C stretching vibrations in the aromatic ring, while the one at 1285 cm^{-1} is characteristic of aromatic C-O stretching vibrations [111]. Although the spectrum of modified pectin (Pectin Dopamine) was also performed, no noticeable changes were observed when compared with the one of Pectin BLK, suggesting that probably the functionalization with dopamine occurred in low yield, hampering the detection of significant structural changes through this technique.

Despite the differences in the ATR-FTIR spectrum were not evident comparatively to blank pectin, the absorbance peaks at 280 nm in the UV-Visible spectrum and the appearance of new characteristic peaks corresponding to the aromatic ring of Dopamine molecule in pectin dopamine conjugate $_1$H-NMR spectrum, allowed to conclude the successful incorporation of dopamine in pectin backbone. The accomplishment of the functionalization of pectin with dopamine provides the platform for the development of pectin hydrogels for skin tissue engineering and wound healing applications, with increased mechanical properties and adhesive behavior in wet environmental conditions, such as, heavily exudative chronic wounds.

1.3.3 Rheological characterization ad internal gelation properties of Pectin functionalized hydrogel matrices

The gelation properties of the functionalized pectin hydrogels were optimized based on the internal gelation protocol with $CaCO_3$/GDL, postulated by Neves et al. [44]. The internal gelation protocol was based on the $CaCO_3$/GDL system, in which GDL hydrolyses with time, lowering the pH of the solution, inducing the slow release of calcium from $CaCO_3$ molecules [44].

After stabilization of the viscoelastic properties of the hydrogels within 1h at 37 ºC present a "solid-like behavior", with phase angle (δ) below 10º in less than 1 h, all Ca^{2+} ions present in solution, theoretically bound with pectin forming the "egg-boxes" structure proposed by Fraeye et al. [107]. The "egg-boxes" model suggest that two-fold

symmetrical conformation of pectin, cooperatively bound two neighboring chains to calcium ions, stabilized by hydrogen bounds and Van der Waals interactions [107].

The main goal of this optimization step was the validation of CalEssence® 70 as calcium source and study its impact on gelation properties of pectin hydrogels matrices, such as, viscoelastic behavior and gelation time. Comparatively to traditional $CaCO_3$ powders, CalEssence is nanoparticulated Ca^{2+} powder with enhanced purity, presenting a smallest particle size with high surface area, low density, good suspendability in aqueous medium and high calcium availability.

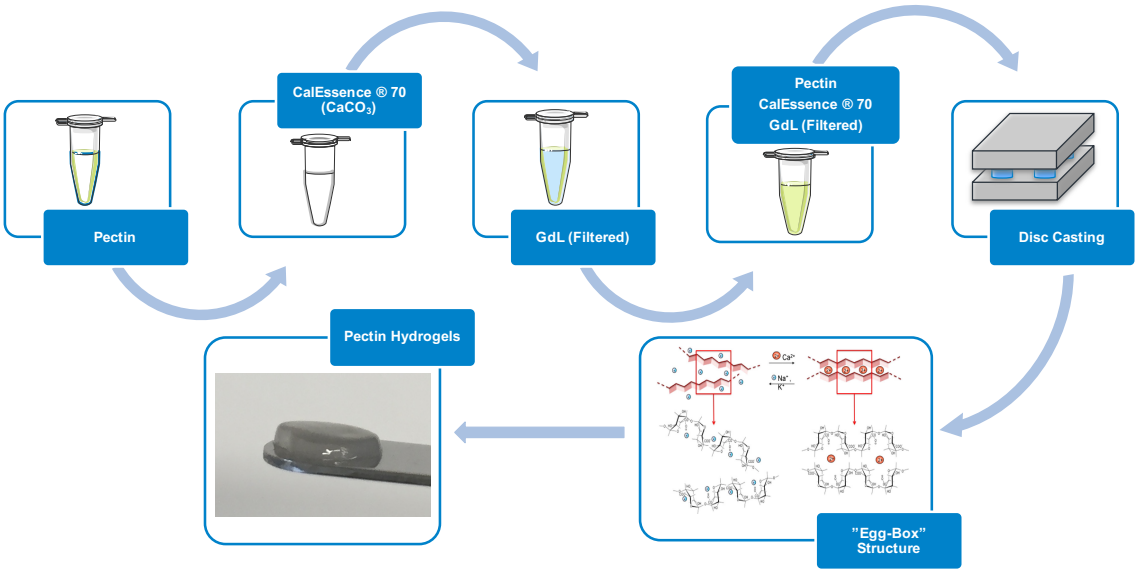

Figure 21. Gelation scheme using the internal gelation methodology. A system of $CaCO_3$(CalEssence ® 70)/GdL was used to induce pectin gelation allowing the casting of 3D hydrogels.

In order to obtain functionalized pectin hydrogels matrices, hydrogels were casted by internal gelation according to section 5 (Fig. 21), and the R-value (ratio between carboxyl groups and calcium ion concentration) was kept at 1, which represents an excess of calcium to guarantee the establishment of “egg-boxes” regions within pectin hydrogel matrices.

The rheological properties of the DOPA_PEC and BLK_PEC gel-precursor solutions and hydrogels were determined in the rheometer at 37ºC in a water-vapor saturated environment ensured by rheometer chamber. For the determination of the linear viscoelastic region (LVR) of DOPA_PEC hydrogels were performed oscillatory measurements with iterative strain amplitude sweeps and frequency sweeps measurements. The evolution of the viscoelastic properties over time (gelation kinetics profile) were assessed using frequency and shear strains values within the LVR, and the time was adjusted to match the time at which GDL was added to pectin.

1.3.3.1 Determination of Linear Viscoelastic Region (LVR) – Amplitude and Frequency Sweeps

In order to determine the linear viscoelastic region of DOPA_PEC hydrogels for further comparison with BLK_PEC hydrogels, using the internal gelation properties, were produced hydrogels discs of both conditions and after stabilization in DMEM in HEPES medium at 37ºC for at least 30 minutes, frequency and amplitude strain sweeps oscillatory measurements were conducted. The frequency sweeps were performed at constant strain of 1% and amplitude strain sweeps at a constant frequency of 0.1 Hz. The oscillatory measurements were performed with pectin hydrogels at concentrations of 1.5 wt.% of DOPA_PEC, BLK_PEC and DOPA_BLK (ratio of equal parts of DOPA_PEC and BLK_PEC) and repeated until we obtain concordant measurements (N≥3). Afterwards, we plotted the graphs (Fig. 22) of the variation of the viscoelastic parameters (elastic component (G') and viscous component (G'') of the shear moduli, and phase angle (δ)) under the previously defined conditions for each condition.

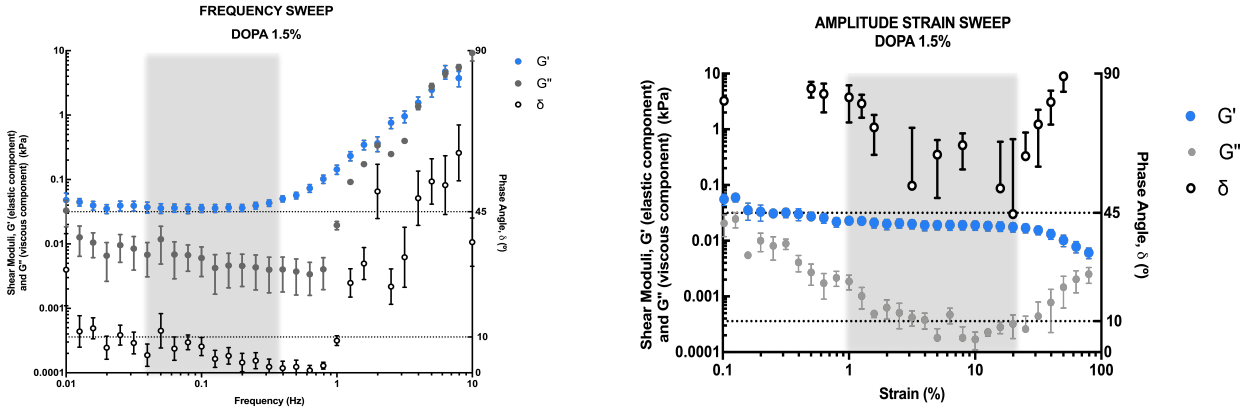

Figure 22. Representative graphs of frequency and amplitude strain sweeps. Linear Viscoelastic Region (LVR) of DOPA_PEC and BLK_PEC hydrogels (1.5 wt%) The frequency sweeps were performed at a constant strain of 1% and the amplitude sweeps were performed at a constant frequency of 0.1 Hz.

The LVR range for the studied conditions were estimated between 0.05 to 0.5 Hz. These results were consistent with previous work published by Neves et al. [44] with pectin hydrogel matrices with same concentration 1.5 wt% prepared by internal gelation with $CaCO_3$/GDL methodology.

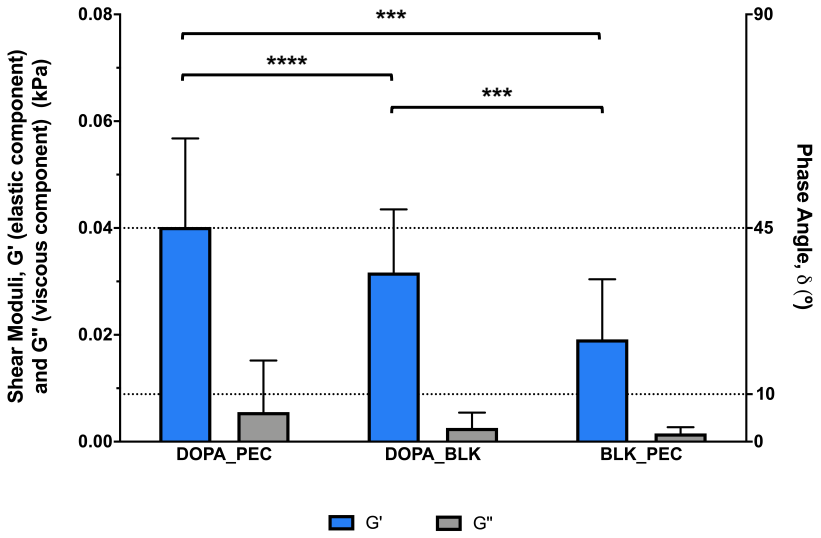

Figure 23. Viscoelastic properties (elastic (G') and viscous (G'') components of the shear moduli of DOPA_PEC , BLK_PEC and DOPA_BLK. Statistically significant differences were marked in the graph between conditions tested as ns ($p > 0.05$), * ($p < 0.05$), ** ($p < 0.01$), *** ($p < 0.001$) and **** ($p < 0.0001$). Denotes no statistically significant differences for G'' in all conditions tested ($p > 0.05$).

The viscoelastic properties of the hydrogels were studied based on the LVR range determined (Fig. 23). As expected, DOPA_PEC hydrogels shear moduli were significantly higher than the BLK_PEC hydrogels ($p<0.001$), especially concerning the elastic component (G'). When we observe the shear moduli of DOPA_BLK formulation, which was composed of a mixture of equal parts of DOPA_PEC and BLK_PEC at 1.5 wt%, we observed decreasing tendency in the shear moduli, particularly in the elastic component (G'). These findings confirmed the influence of the dopamine in pectin mechanical properties, specifically in the elastic component (G') of the hydrogels, allowing fine-tune the mechanical properties by increasing and decreasing the amount of dopamine of the hydrogel matrix.

The rheological analysis confirmed that the presence of dopamine in the polymer structure, produces hydrogels that exhibit a more "solid-like" behavior after gelation. Lee and co-workers, observed similar rheological behavior in catechol alginates presenting a solid-like behavior after gelation and more than 10-fold increase in elastic components (G') of the shear moduli when double the alginate catechol content [76]. Our results show also an increase on 50% from DOPA_PEC and approximately 30% from DOPA_BLK, in comparison to BLK_PEC hydrogels, in the elastic component (G').

Various reports show the influence of the mechanical properties of the substrate (ECM or biomaterials), such as matrix stiffness, as they can modulate the cellular behavior in response to mechanical stimuli [112, 113]. Fibroblasts modulate their cellular mechanical responses according to matrix stiffness, they tend to migrate faster in softer matrices and proliferate preferentially in stiffer ones [114, 115]. In order to obtain optimal

cellular function, biomaterials mechanical parameters are crucial in the development of wound healing solutions or skin tissue engineering constructs.

The functionalization of pectin with dopamine was performed with the purpose of ameliorate the mechanical properties of pectin hydrogels, in the development of injectable hydrogel construct, appropriate for wound healing and also be used as scaffolding methodology for skin tissue engineering applications. With preliminary results, we corroborate the influence of the dopamine conjugated with pectin, in the improvement of the mechanical properties, enabling adjustment of the hydrogels stiffness through the variation of the concentration of dopamine in the hydrogels.

1.3.3.2 Internal gelation kinetics with CalEssence ® 70

In order to evaluate the influence of the usage of the **CalEssence® 70** in the gelation triggering time and whether the functionalization of pectin affects the gelation ability of pectin, the gelation kinetics were assessed for DOPA_PEC and BLK_PEC hydrogels, with crescent concentrations from 1, 1.5 and 2 wt.%. The gelation properties over time were performed at constant frequency and temperature, 0.1 Hz and 37ºC respectively over a period of 1 hour. The data obtained (N≥3) from the shear modulus (the elastic (G') and viscous (G'') components) and phase angle (δ) were represented graphically, and were evaluated the gelation time (t_gel) and the mechanical properties at the end of one hour (Fig. 24) (See Supplementary Material for more data on gelation kinetics).

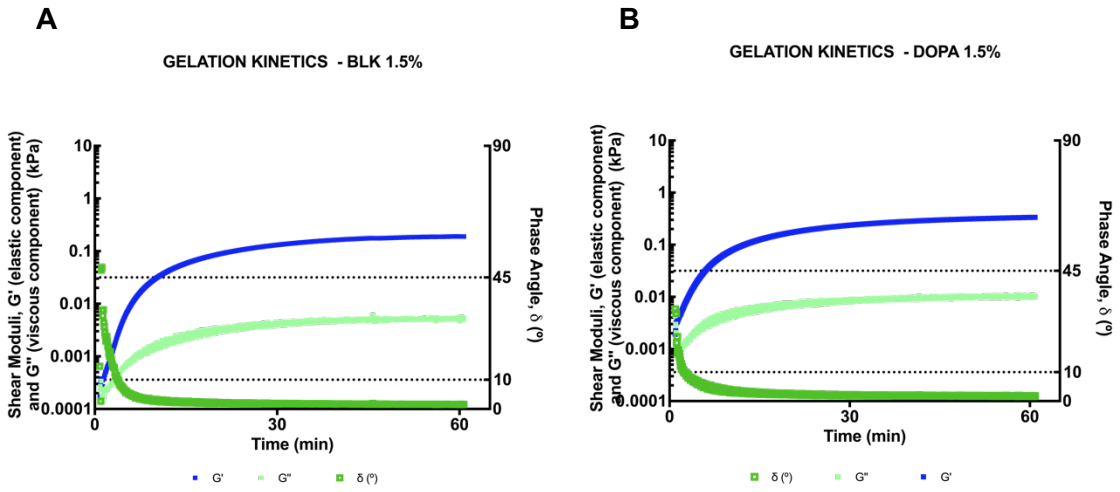

Figure 24. Representative graphs of the Gelation kinetics over time. (A) BLK pectin and (B) dopamine/pectin gelation assays were performed and the precursor solutions were prepared using R=1 between calcium ions (CalEssence ® 70) the and D-Glucone-d-lactone (GDL).

The gelation triggering time corresponds to the time at which δ goes below 45º and there is a crossover between the elastic (G') and viscous (G'') components of the shear modulus. Based on these criteria, we concluded for all the conditions tested (see Supplementary information), the gelation occur instantaneously with **CalEssence® 70** and its impossible to observe the crossover between the components of the shear modulus (G' and G'').

Table 6 - Gelation time and mechanical properties of Dopamine pectin and BLK pectin hydrogels, at different pectin concentrations

CONDITIONS	1 wt%				1.5 wt%				2 wt%			
	t_gel (min)	After 1h			t_gel (min)	After 1h			t_gel (min)	After 1h		
		G' (kPa)	G" (kPa)	δ (º)		G' (kPa)	G" (kPa)	δ (º)		G' (kPa)	G" (kPa)	δ (º)
DOPA_PEC	Instantaneous	0,0564	0,0016	1,5960	Instantaneous	0,3358	0,0102	1,7367	Instantaneous	0,4791	0,0169	2,0167
BLK_PEC	Instantaneous	0,0438	0,0010	1,3400	Instantaneous	0,1899	0,0051	1,5575	Instantaneous	0,3568	0,0116	1,8533

After 1h, as was expected from the previous rheological data, the DOPA_PEC gels present an increased shear modulus with increasing dopamine concentrations in the hydrogels, more significant in the elastic components (G') (Table 6). When we compared both hydrogels, we observe significant differences in shear modulus, particularly in the elastic components (G'), more evident in the higher concentrations of polymer. In the viscous component (G') of the shear modulus and phase angle (δ), the differences between hydrogels with or without dopamine was not significative. Despite both pectin hydrogel formulations present a more "solid-like" behavior over time, the pectin hydrogels with dopamine present an increased stiffness, which may influence the future cell embeddings of hydrogels with HDNFs on one hand, but on the other hand, higher stiffness could facilitate local application in an in vivo setup.

Previously published data, reports gelation triggering time of pectin hydrogels at 1.5 wt% for purified pectin (BLK_PEC) of approximately 2 minutes and higher shear modulus (G' ≈ 0.102 kPa and G'' ≈ 0.009 kPa) [44]. When compared with our results for BLK_PEC at 1.5wt%, the introduction of **CalEssence® 70** in the internal gelation chemistry, provides an instantaneous gelation system without interfere with higher shear modulus of the gels (G' ≈ 0.189 kPa and G'' ≈ 0.005 kPa).

The introduction of **CalEssence® 70** in the internal gelation $CaCO_3$/GDL chemistry as calcium source, was the major breakthrough with these gelation studies in the field of injectable pectin hydrogel systems for tissue engineering. The **CalEssence® 70** nanoparticulated calcium powders characteristics, such as, smallest particle size with high surface area, low density, good suspendability in aqueous medium and high calcium availability, endows the injectable hydrogels system the instantaneous gelation *in-situ*.

Particularly for wound healing applications and skin tissue engineering, our results, established a new approach for the injectable hydrogels systems with the development of instantaneous *in-situ* gelation, which provides a simple and fast application of hydrogel in the wound site.

2 Adhesive Properties

The poor mechanical properties and stability of hydrogels, allied with their poor tissue adhesion in wet environmental, such as, presence of wound exudate or hemorrhage conditions, compromise the application and maintenance of the hydrogel in contact to wound site [78, 79]. The interfacial water molecules, present as a film on tissue surfaces are responsible to initiate hydrogen interactions with functional groups of the hydrogels, impairing significantly the interfacial adhesive strength between the hydrogel and the tissue [78]. Preliminary studies in the group show that pectin hydrogels fail to adhere surgical induced wound beds (unpublished results).

Based on this rationale, we hypothesized that the adhesion strength and performance of the catechol-based pectin hydrogel under environmental wet conditions was significantly higher, by the incorporation of dopamine into pectin structure. Using the Texture Analyzer, we studied the adhesion strength of DOPA_PEC hydrogels, against BLK_PEC hydrogels. The figure 25 represents the experimental setting used for the adhesion studies.

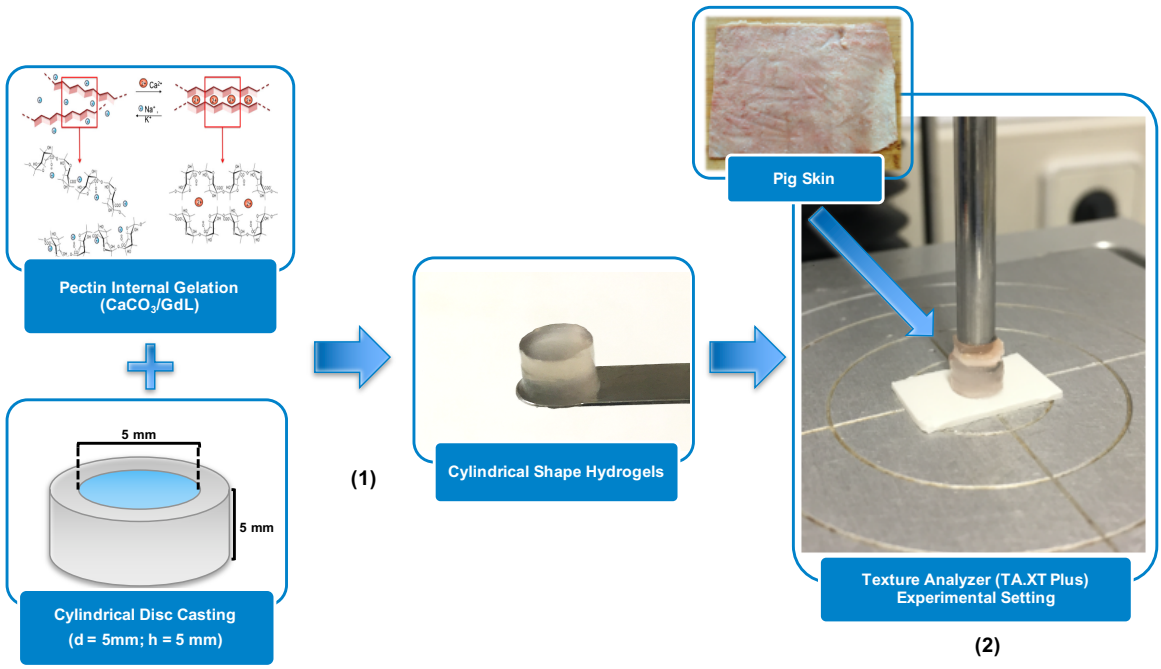

Figure 25. Experimental setting for Adhesion studies. (1) Using internal gelation protocol of $CaCO_3$/GDL and a cylindrical disc casting, discs were produced with5 mm diameter and at least 4 mm of height. (2) For the texture analyzer (TA.XT Plus) experimental setting it was used a cylindrical probe with 5 mm diameter, and the hydrogels were glued to testing platform using double-sided duct tape and superglue, and the surfaces testes (TCPS and pig skin) were glued with double-sided duct tape to testing probe.

The adhesion properties of both hydrogels (DOPA_PEC and BLK_PEC) studied (Adhesiveness (N) and the Work of Adhesion (N.sec)) were studied in an inorganic surface, the TCPS coverslips and organic surface, pig skin (mechanically debrided), used as a wound model (Fig. 25).

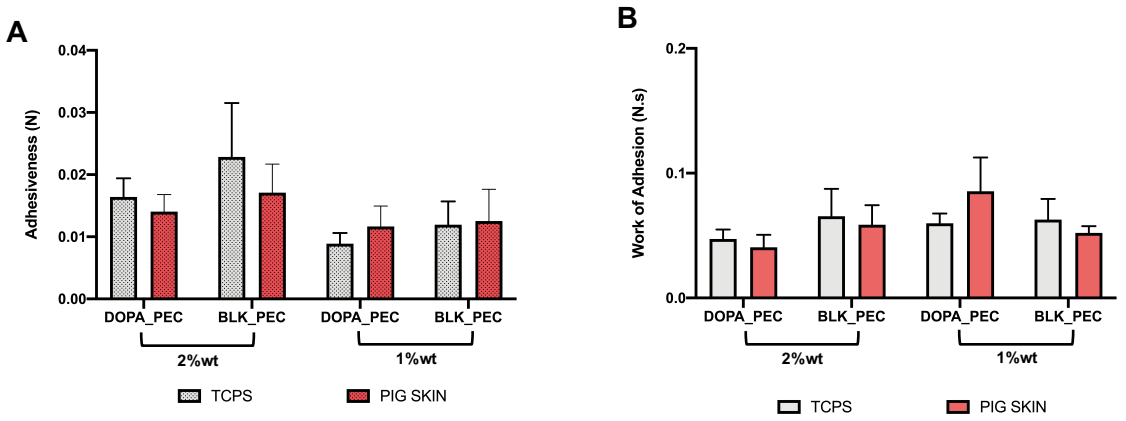

Figure 26. Adhesive properties (Adhesiveness (N) and Work of Adhesion (N.sec)) of DOPA_PEC comparatively to BLK_PEC samples (N=6) with concentrations of 2%wt and 1%wt. (A) Comparative analysis for the Adhesiveness between DOPA_PEC and BLK_PEC in the surfaces tested TCPS (control) and Pig Skin (experimental) (B) Comparative analysis for the Work of Adhesion between DOPA_PEC and BLK_PEC in the surfaces tested TCPS (control) and Pig Skin (experimental). One-way ANOVA (Kruskal-Wallis) Statistical analysis for both parameters denotes no statistically significant differences between samples and concentrations (P>0.01 (ns)).

The obtained results do not show statistically significant changes in the adhesive properties in pectin conjugated with dopamine, independently of the concentration of the dopamine in the polymer (Fig. 26). Furthermore, when compared both formulations, pectin without dopamine (BLK_PEC), overall showed better results for both surfaces. Based on these results, we hypothesized that the developed strategy to evaluate the adhesion strength of DOPA_PEC, probably was not the most suitable approach, taking into account the hydrogels characteristics.

The underlying mechanism of PDA mediated adhesion is the exposure of dopamine molecules engrafted in the polymer to oxidative chemical cross-linking agent [43, 61]. The oxidative process of PDA chains (Fig. 27) in the catechol groups confer tissue adhesiveness to the hydrogel [116]. Thus, several factors may also be contributing to the unexpected results.

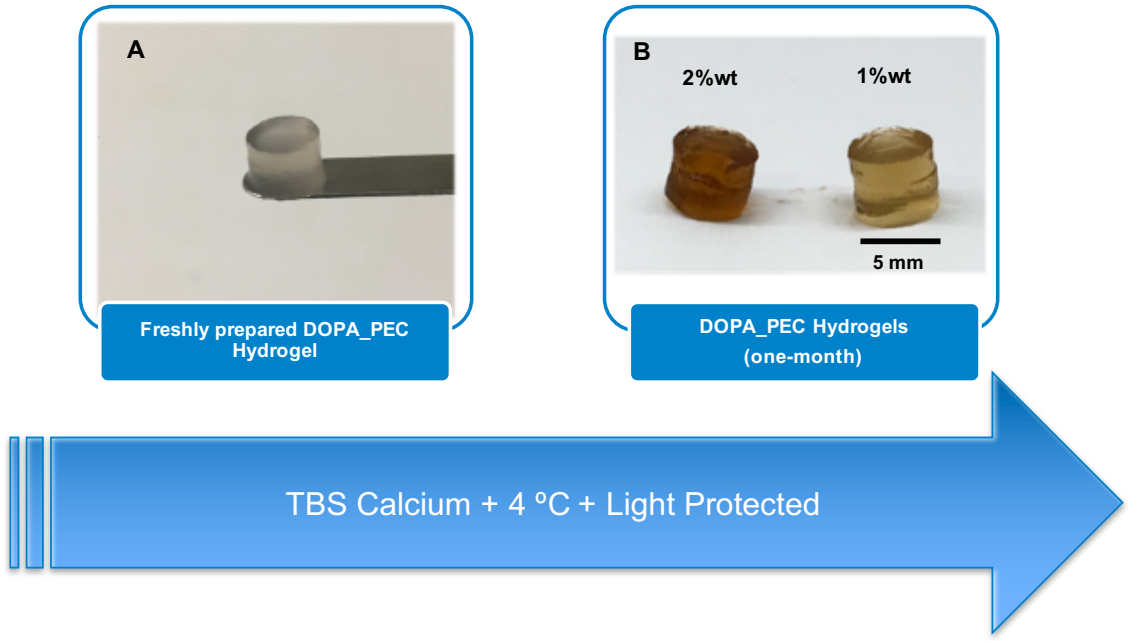

Figure 27. Macroscopic observation of Dopamine/PDA oxidative chemical crosslinking over time. (A) Freshly prepared hydrogels; (B) Hydrogels with 2 wt% and 1 wt% after one-month period of time, immerged in TBS Calcium solution at 4 ºC protected from light (Scale-bar 5 mm).

First, the performed adhesion tests required perfect alignment of the samples when glued to the platform and the surface of hydrogels should be as smooth as possible without uneven surfaces and indentations. The obtained results may have been compromised by the manual, not standardized process of production of the hydrogels samples and preparation of the pig skin wound model surface. On the other hand, pectin is a natural polymer characterized by its complex branched with high molecular weight macromolecule [74]. The ramified nature of pectin, probably exert a protective effect over dopamine molecules grafted in its structure, preventing the exposure of dopamine to oxidation, which compromise the adhesive properties of the functionalized pectin with dopamine. Other hypothesis is that the amount of engrafted DOPA on the pectin backbone is not sufficiently high to increase the adhesiveness of the casted hydrogels.

After one-month period of time, we observed that the macroscopic appearance of the samples, kept immerged in TBS Calcium solution at 4 ºC protected from light, tend to acquire a brownish coloration with increased stiffness (Fig. 27-B), in comparison to freshly prepared ones (Fig. 27-A). Also, the coloration intensity and increased stiffness was observed in hydrogels with higher dopamine concentration. These findings provide the proof of concept that the dopamine molecules grafted in pectin undergoes oxidative cross-linking under certain conditions, however, did not occurs immediately.

These results highlight the need to establish a different approach, in order to improve the oxidative cross-linking of the dopamine molecules in the polymer to optimize the adhesive properties.

3 Morphological and Structural characterization of the functionalized pectin hydrogels with Scanning Electron Microscopy (SEM)

The scanning electron microscopy technology allows the observation, at the pore scale, of liquid containing samples under a frozen state, such as hydrogels, by cryo-scanning electron microscopy (cryo-SEM). The controlled sublimation allows partially removed water from the sample leading to a significantly reduced distortion of sample [117].

The 3D microstructure and porosity of functionalized-pectin hydrogels were assessed by SEM. As we observed (Fig. 28 A-I to A-IV), the size of the discs decreases with increasing concentrations of dopamine within the hydrogel's matrix, with exception of the Blank+DOPA (50/50) which presents a higher diameter in comparison with Blank formulation. As dopamine concentration increases, we would expect a smaller mesh size, with smaller pore diameter, resulting in a more intricate network and denser microstructure of the hydrogel matrix.

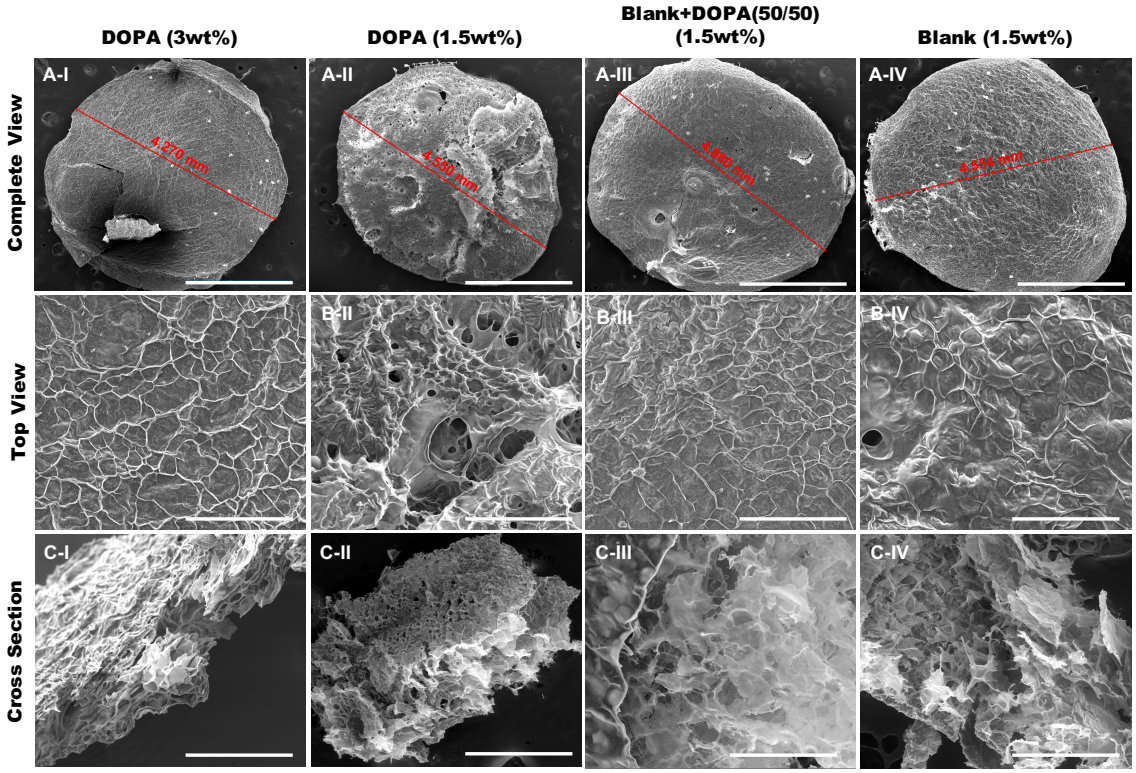

Figure 28. Microstructure of functionalized pectin hydrogel matrices. Macro characterization of different concentrations of DOPA containing hydrogel and Blank pectin hydrogels. Complete View A-I to IV) magnification of 50x and scale bar at 2 mm; Top View B-I to IV) magnification of 500x and scale bar at

200μm; Cross Section C-I and C-IV) magnification of 500x and scale bar at 200μm; C-II) magnification of 200x and scale bar at 500μm; C-III) magnification of 1000x and scale bar at 100μm;

For further analyses and quantification proposes, the pore size should be measured using a more suitable technique (Environmental SEM) in order to establish a more accurate, correlation and measure the contribution of dopamine to microstructure of functionalized-pectin hydrogels.

Regarding the figure 28 (B-I to B-IV), considering that the images present the same magnification and the same scale, we roughly observed that the pore size of the hydrogels tend to decrease with increasing concentrations of dopamine and present a denser microstructure. It is well established in literature that these types of hydrogels may exhibit two types of microstructures, that may exist simultaneously within these gels due different water holding behaviors. One microstructure, not dependent on calcium concentration, is responsible for the long-time stability, such as water holding capacity determined from passive diffusion tests, and the texture stability after long time storage. A second microstructure, which should be dependent on calcium concentration, is responsible for the gel behavior when gels are subjected to external forces, as water holding capacity measured from physical dehydration tests, and the relationship of failure properties to gel composition [118]. Therefore, this complex network may be responsible for the stability of gel structure and the water holding in gels. [118].

4 In vitro cell culture of dopamine modified pectin hydrogels

hDNFs were embedded and cultured under 3D conditions in different formulations of pectin conjugated with dopamine and pectin with RGD. hDNFs are terminally differentiated primary cells, characterized for being anchorage-dependent, with a limited lifespan like every primary cell. Dermal fibroblasts are settled in the skin connective tissue and are responsible for tissue remodeling and wound healing, through the production (fibronectin and collagen) and maintenance of the ECM. The use of primary cells in *in vitro* studies is more reliable since these cells present a similar behavior in culture in their native tissue [119].

The primary goal of using dermal fibroblasts is to evaluate the suitability of the developed wound healing hydrogel and study the behavior of these primary cells when embedded in catechol-based pectin hydrogels 3D matrices. The hydrogels containing hDNFs were tested, focusing on the outcome of cellular activity within the 3D structures. We analyzed the 3D matrices regarding metabolic activity (resazurin assay), proliferation (ki-67 marker) and ECM deposition (fibronectin).

4.1 Viability and metabolic activity of pectin functionalized hydrogels embedded with hDNFs

Concerning cell behavior within the hydrogel's matrix, it is vital to guarantee the survival, the viability of the cells and that they remain metabolically active during the *in vitro* cell culture period. Beyond that, the hydrogel polymeric structure should allow the diffusion of nutrients and gas exchange, throughout the whole disc, therefore, allowing the biological cell activities and processes, such as, cellular proliferation, cell-to-cell interactions, ECM production and deposition [120]. The production of a 3D scaffold addressing these features will allow and potentiate the integration and interaction of the loaded biomaterial with the host tissue in an *in vivo* scenario.

In order to produce this kind of matrices, using the internal ($CaCO_3$/GDL) gelation methodology, precursor solutions of the hydrogel's formulations and cell suspension (cell density $8x10^6$ cells/mL of final solution) were mixed to obtain a final solution of the hydrogels with cells at concentration of 1.5wt%. Approximately 20 µL of solution were dispensed between two teflon plate separated by 500 µm spacers and were incubated for 1hour in cell culture incubator conditions. After 1h incubation period, hydrogels were transferred to cell culture well-plate and incubated in cell culture medium and three timepoints were analyzed over the 14 days in culture (day 3, day 7 and day 14). Due to hydrogels mechanical behavior, the first timepoint was defined after 3 days in culture, enabling the possibility to perform the metabolic activity and further analysis without destroying the samples.

According microscopic observation and metabolic activity resazurin assay (Fig. 28), hDNFs remained viable and metabolically active throughout the 14 days culture in all formulations tested.

In the formulations tested we altered the concentration of RGD with the objective to evaluate the effect of different RGD concentrations on the cell culture, regarding cell viability, morphology and metabolic activity, maintaining the concentration of dopamine to guarantee similar mechanical properties and stiffness of the hydrogels. All formulations of cell-loaded pectin hydrogels discs, were calculated based on the final concentration of 1.5 wt%, with the following concentrations of Dopamine and RGD:

1. DOPA ≈1 M concentration of Dopamine;
2. Blank+DOPA (50/50) ≈ 0.5 M of Dopamine;
3. DOPA+RGD (230µM) ≈ 0.5 M of Dopamine + 230µM of RGD;

4. DOPA+ RGD (200μM) ≈ 0.5 M of Dopamine + 200μM of RGD;
5. Blank – pectin without Dopamine or RGD;
6. Blank+RGD (230μM) ≈ 230μM of RGD;
7. Blank+ RGD (200μM) ≈ 200μM of RGD;

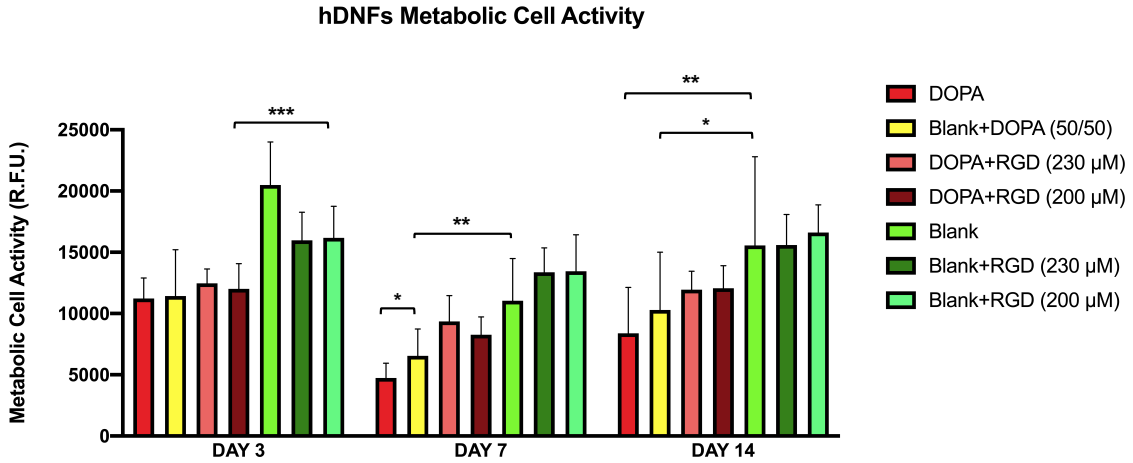

Figure 29. Metabolic Activity (hDNF) embedded within different pectin-functionalized (DOPA and RGD) 3D hydrogel matrices (1.5 %wt) at different timepoints. Statistically most conditions tested present a statistically significant differences with p<0.0001 (****), and the different statistical differences were marked in the graph as ns (p > 0.05), * (p < 0.05), ** (p < 0.01) and *** (p < 0.001).

Despite the structural differences observed overtime, with some exceptions, overall there were no significant differences between the different hydrogel's formulations. The more significant differences observed in metabolic activity of the hDNFs were at day 3, between the formulations DOPA+RGD(200 μM) and Blank+RGD(200 μM); at day 7 between DOPA_PEC(50%)/BLK_PEC(50%) and the formulations DOPA_PEC and BLK_PEC; and finally at day 14, between the Blank and the formulations DOPA and Blank+DOPA(50/50).

Although, the hDNFs metabolic activity was not normalized for DNA content, the significant differences observed at day 3 between DOPA+RGD(200μM) and Blank+RGD(200μM) were consistent with fibroblasts morphology, which already spreading, adopting a spindle-like structure, which was expected due to the interaction between cells and RGD motifs embedded, increasing cell-to-cell network within the hydrogels. These data suggest that this difference was probably attributed to the higher stiffness of the dopamine containing hydrogel (confirmed by the rheological measurements) which interfere with the cell ability to spreading over the pectin functionalized with dopamine 3D matrices. The metabolic activity significant differences at day 7 and day 14 were observed between the formulations in which the amount of dopamine varies. These results were consistent with the previously stated, influence of

the presence dopamine the hydrogel 3D matrices in the stiffness of the hydrogels, which hinders the ability of cells to spread in more stiff matrices.

4.2 Morphology and ECM deposition of hDNFs loaded Pectin Hydrogels

The morphology of the cells reflects its behavior in the interactions when in contact with a specific microenvironment. This parameter provides us important information on the adequacy of a hydrogel as 3D matrices. At the defined timepoints (3, 7 and 14 days) the cell-loaded hydrogels were fixed and stained for filamentous actin (F-actin), fibronectin (FN), and DNA prior to confocal microscopy visualization.

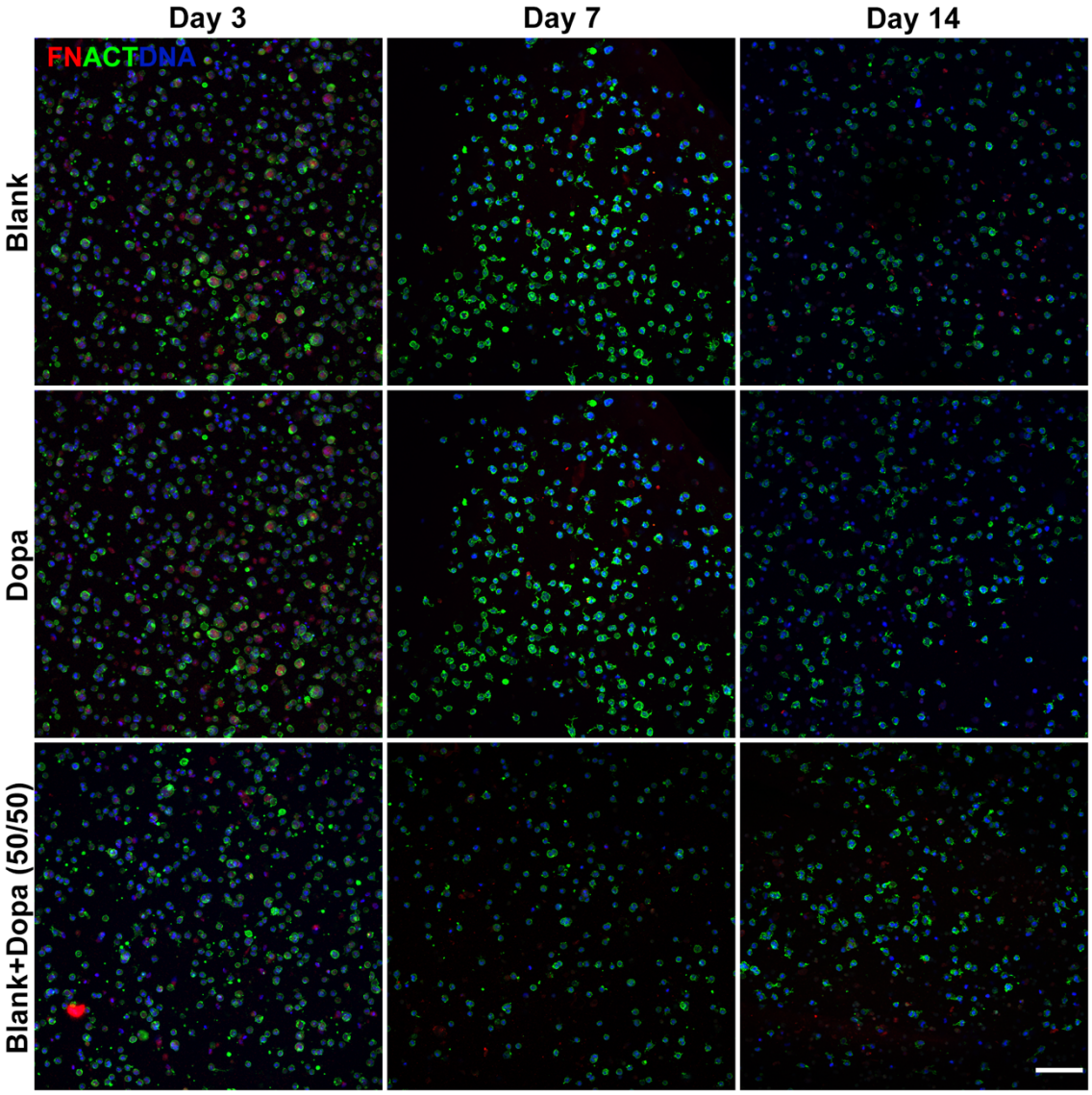

Figure 30. hDNfs morphology when embedded within Blank, DOPA, Blank+DOPA(50/50) hydrogels. Confocal microscopy images depicting the morphology, spatial arrangement and ECM deposition of human Dermal Neonatal Fibroblasts (hDNFs) embedded within DOPA, Blank and Blank+DOPA (50/50) hydrogels after 14 days of culture. The images were captured at the timepoints day 3, 7 and day 14 and the morphology

of hDNFs, stained for nuclei (blue) and f-actin (green) and ECM deposition, stained for fibronectin (red) (scale bar: 100 μm).

After 3 days, a clear difference was observed between hydrogels formulation with RGD motifs and the formulations where RGD was not present. In the formulations without RGD (including pectin with dopamine), the cells presented a more round-shaped and as appear as isolated cells and not depicting any type of cell-to-cell network interactions (Fig. 29).

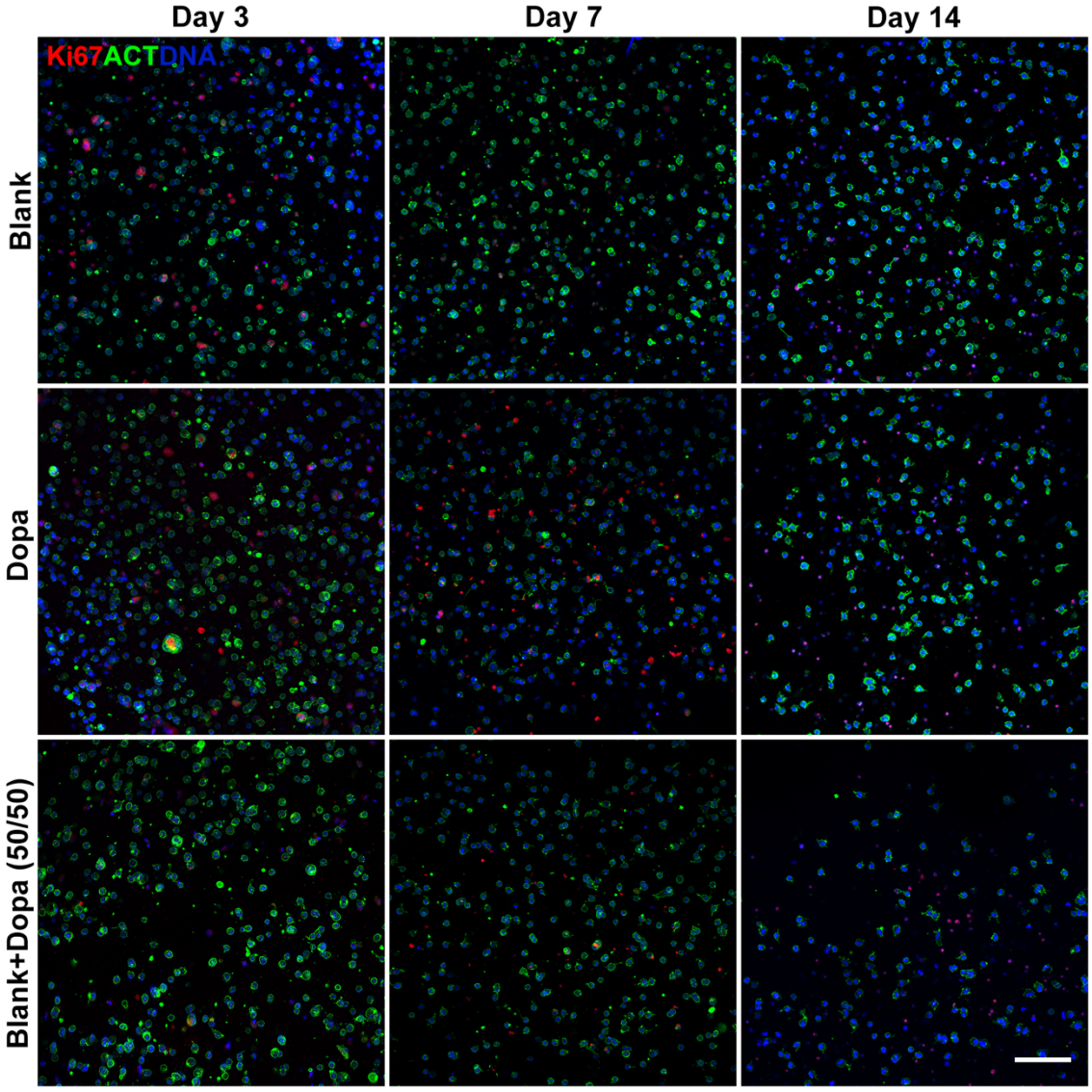

Figure 31. Morphology and cell proliferation of hDNFs when embedded within different concentrations of Blank and DOPA functionalized pectin hydrogels. Confocal microscopy images depicting the morphology, spatial arrangement and cell proliferation of human Dermal Neonatal Fibroblasts (hDNFs) after 3, 7 and 14 days of culture. Morphology of hDNFs, stained for nuclei (blue), f-actin (green) and cell proliferation, stained for ki-67 (red) (scale bar: 100 μm).

Ki-67 is a nuclear protein expressed in all proliferating vertebrate cells, and it is a widely used biomarker to estimate the proportion of dividing cells [121]. This marker was used to evaluate if the cells are able to divide and proliferate within the 3D hydrogel

matrices. As it was expected (Fig. 30), for the functionalized pectin hydrogels, which the dopamine concentrations was varied and blank pectin formulation, we were not able to observe the expression of Ki-67 protein, and the red stained dots were not matched with the nuclei, thus it is considered background during the confocal image acquisition.

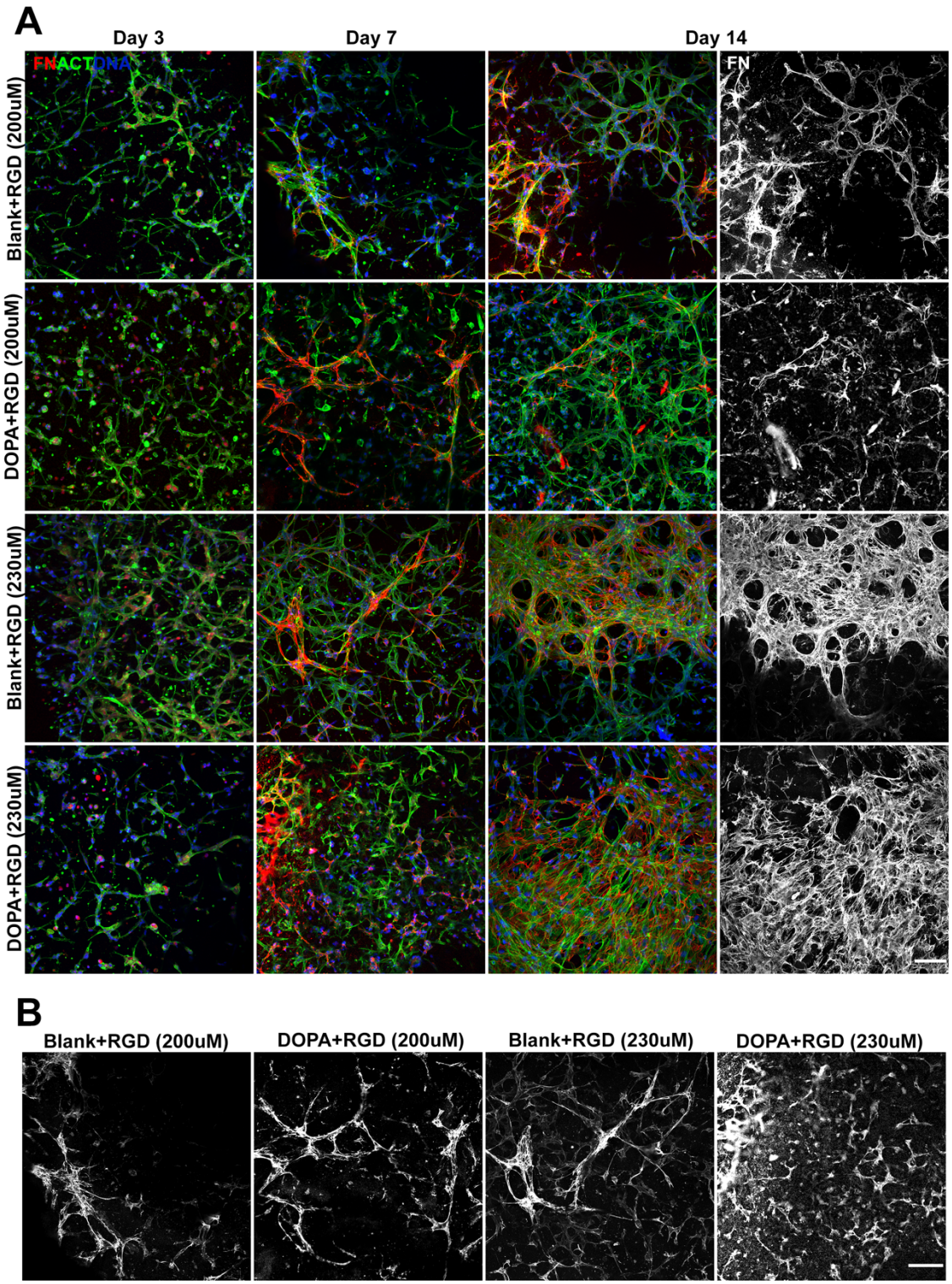

Figure 32. Morphology and ECM deposition of hDNfs when embedded within DOPA and RGD - functionalized pectin hydrogels. Confocal microscopy images depicting the morphology, spatial arrangement and ECM deposition of human Dermal Neonatal Fibroblasts (hDNFs) after 3, 7 and 14 days of

culture. (A) Morphology of hDNFs, stained for nuclei (blue), F-actin (green) and fibronectin deposition by hDNFs (red and gray); (B) Fibronectin deposition after 7 days in culture, (scale bar: 100 μm).

The presence of RGD motif's, has a predominant effect on the cell behavior in the pectin hydrogel 3D microenvironment and cells present the characteristic elongated spindle-like shape, and start to establish intercellular network, confirmed by stained the F-actin cytoskeleton network (Fig. 31-A).

At day 3 we observed a slightly difference in the F-actin cytoskeleton, between the DOPA formulations in comparison with Blank ones, which was denser with increasing concentrations of RGD. Although DOPA formulations present the same RGD concentration (200μM and 230μM) at day 3, they present a less dense F-actin cytoskeleton with the increase of dopamine concentration. These results probably reflect of the effect of Dopamine in the stiffness of the pectin with DOPA hydrogel 3D matrices, that affects the hDNFs cellular behavior and spreading.

After 7 days of culture, we observed the presence of fibronectin in all RGD formulations, which indicates the cellular endogenous ECM production. The FN production was more pronounced at the DOPA with RGD hydrogels formulations (Fig. 31-B), apparently the under lower RGD concentrations the presence of Dopamine has a beneficial effect on the FN production.

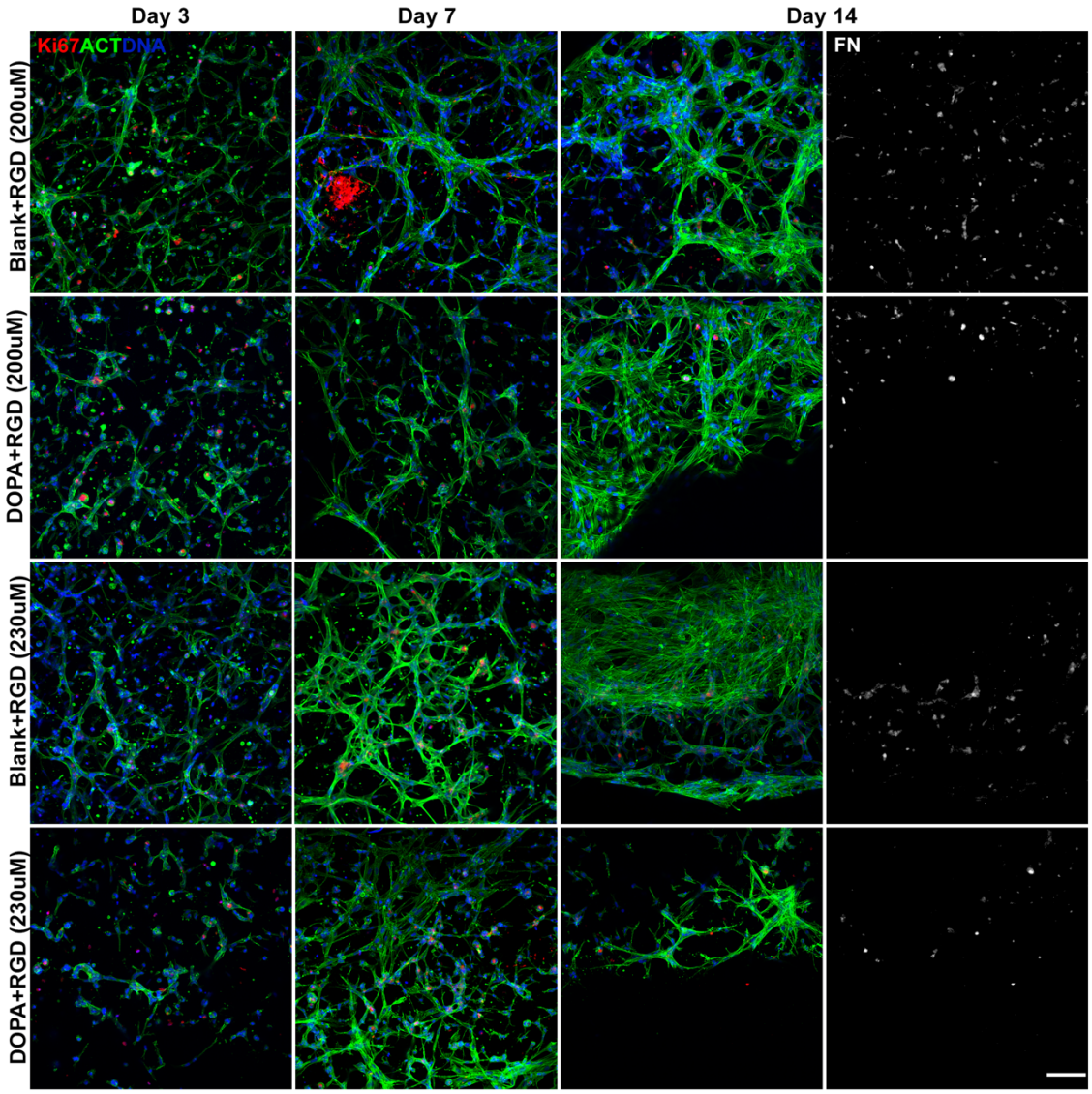

Figure 33. Morphology and cell proliferation of hDNFs when embedded within DOPA and RGD - functionalized pectin hydrogels. Confocal microscopy images depicting the morphology, spatial arrangement and cell proliferation of human Dermal Neonatal Fibroblasts (hDNFs) after 3, 7 and 14 days of culture. Morphology of hDNFs, stained for nuclei (blue), f-actin (green) and cell proliferation, stained for ki-67 (red) and fibronectin (gray scale) (scale bar: 100 μm).

The cell proliferation profile of hDNFs when they were embedded within DOPA and RGD-functionalized pectin hydrogels were also evaluated through the expression of Ki-67 protein. Overall, the hDNFs embedded within DOPA and RGD-functionalized pectin hydrogels, exhibit Ki-67 protein expression (Fig. 32), observed through the red staining of proliferating cells, distributed in cell clusters inside the matrix to facilitate cell division and proliferation. Furthermore, from the ki-67 and FN staining, we observed that apparently the last formulation of DOPA and RGD functionalized pectin hydrogels with 0.5 M of dopamine and 230μM, presents lower number of cells after 14 days of cell culture.

Although, cells remained viable and active over 14 days of culture in all formulations studied, the formulations without RGD within the hydrogel 3D structure, hDNFs overall maintained a round-shaped structure. The RGD formulations after 14 days of culture present a denser cell-to-cell network and it was observed the production of endogenous fibronectin (ECM).

Notwithstanding that the obtained results required further quantification, the findings suggest that hDNFs cellular adhesion and spreading was predominantly influenced by the presence of RGD motifs.

The influence of RGD-modified pectin were previously reported by the work of Neves et al.[44] that stated that the RGD-modified pectin hydrogels were more suitable 3D microenvironment for the establishment of intercellular networks and ECM deposition [44].

However, the presence of dopamine in the formulations with lower concentration of RGD, could display a beneficial effect on the cell ECM production and could be enhancing cellular interactions within the hydrogel 3D microenvironment. A previously published study with Alginate-catechol hydrogels cross-linked without calcium, observed enhanced *in vitro* survival in several human primary cells, including stem cells in 3D alginate catechol hydrogels. Also, the inflammatory response *in vivo* was attenuated in comparison with alginate hydrogels cross-linked with calcium [76]. These findings may support, our observations of the beneficial effect of dopamine on *in vitro* cellular functions.

Conclusions and Future Work

In this work we explored and validate a new functionalization strategy of pectin with dopamine. Our main goal was the improvement of mechanical properties and adhesiveness in wet environmental conditions aiming the development of a pectin-based hydrogel suitable for treatment of acute and chronic wounds. After solving the problems detected during the conditional optimization stage, the final results validate the carbodiimide chemistry protocol for functionalization of pectin with dopamine. With this protocol it was possible to successfully incorporate dopamine in pectin backbone showing that pectin can be multifunctionalized with different moieties to address the different needs in clinical scenario. Taking into account the activation rate of the free carboxylic groups of the GalA of pectin was 100%, the amount of dopamine grafted in the polymer was relatively low. The results suggest that probably the ramified structure of pectin has negative influence (through repulsive interactions) to the reaction yield, hindering the chemical interaction of dopamine with the activated carboxylic groups. In order to study the influence of pectin branched structure in the reaction yield, as future work the coupling reaction should be tested in Polygalacturonic acid (main component of pectin backbone structure) which has a linear structure to test our hypothesis.

As we hypothesized, after gelation of dopamine conjugated pectin using internal gelation chemistry $CaCO_3$/GDL, the hydrogels showed improved mechanical properties in comparison with pectin hydrogels without dopamine. The internal gelation system was successfully optimized, by the substitution of the traditional $CaCO_3$ calcium source for **CalEssence ® 70**. The results of the rheological measurements (gelation kinetics) showed that the gelation of both formulations (pectin with and without dopamine) starts immediately after adding GDL. From previous published work, the pectin internal gelation, with a different calcium source ($CaCO_3$), the gelation triggering time was approximately 2 minutes, for pectin hydrogels at 1.5wt% concentration [44]. The characteristics of **CalEssence ® 70**, allied with the high calcium availability contributes to the instantaneous gelation process, which makes the path for new approaches in development of injectable hydrogels systems, equipped with instantaneous *in-situ* gelation for wound healing. This could represent that when applied in in vivo experiments, animals remain less time under anesthesia.

On the other hand, we obtained inconclusive results when analyzing the adhesive properties of dopamine grafted pectin. Apparently, no increase on the adhesiveness was detected with the inclusion of DOPA as it was previously reported for alginate and Hyaloronic acid, who showed 14±2 kPa and 90±6.7 kPa of adhesive strength,

respectively [122, 123]. Therefore, the inconclusive results make us consider in a future work, the implementation of alternative cross-linking strategy to internal gelation, as it has been proposed in the literature, the exposure to oxidative chemical cross-linking agent (O_2, $NaIO_4$ and H_2O_2, and enzymes, such as peroxidases) [76].

In vitro tests with HDNFs, fibroblasts embedded within the pectin with dopamine hydrogels remained metabolically active for up to 14 days of culture.

The results showed that the establishment of highly intricated intercellular network within the dopamine modified pectin hydrogels, were dependent of the addition of RGD motifs, which promotes the cell adhesion and spreading over the 3D hydrogel matrices and after 7 days culture they migrate outwards the matrix and starts to produce endogenous ECM. Likewise, the presence of dopamine in RGD modified pectin hydrogels with lower concentration, may induce a beneficial effect on ECM production and may enhance cellular interactions within the hydrogel 3D microenvironment, although further experiments are needed.

In a future work should be considered the possibility of embedding the dopamine modified pectin with Human Umbilical Vein Endothelial Cells (HUVEC's), to study the angiogenic effect induced by the presence of dopamine. The literature pointed out the pro-angiogenic effect of dopamine and wound healing, through activation of dopamine D1 receptors [124, 125].

As was mentioned previously, the biomaterials functionalized with dopamine, hold antimicrobial properties, inhibiting and resist to the bacterial growth. Infection and biofilm formation are an extrinsic factor, responsible for delayed wound healing and may lead to wound chronicity. Also, dopamine functionalized hydrogels are potentially associated with anti-inflammatory activity, through the entrapment of ROS. As future work we should considerer to evaluate at which extent the dopamine modified pectin has antimicrobial properties and anti-inflammatory effect through a more profound study of these aspects.

As stated in this thesis, chronic or hard-to-heal wounds are a major problem faced by the health professionals worldwide. Although, there is many available hydrogels options for wound healing, none presents improved mechanical properties an adhesiveness in presence of exudate. A multifunctional hydrogel that meet this criterion, may fulfill this gap.

References

1. Pereira, R.F., et al., *Advances in bioprinted cell-laden hydrogels for skin tissue engineering.* Biomanufacturing Reviews, 2017. **2**(1): p. 1.
2. Kanji, S. and H. Das, *Advances of Stem Cell Therapeutics in Cutaneous Wound Healing and Regeneration.* Mediators Inflamm, 2017. **2017**: p. 5217967.
3. Eming, S.A., P. Martin, and M. Tomic-Canic, *Wound repair and regeneration: mechanisms, signaling, and translation.* Sci Transl Med, 2014. **6**(265): p. 265sr6.
4. Evans, N.D., et al., *Epithelial mechanobiology, skin wound healing, and the stem cell niche.* J Mech Behav Biomed Mater, 2013. **28**: p. 397-409.
5. Yu, J.R., et al., *Current and Future Perspectives on Skin Tissue Engineering: Key Features of Biomedical Research, Translational Assessment, and Clinical Application.* Adv Healthc Mater, 2019: p. e1801471.
6. Wikramanayake, T.C., O. Stojadinovic, and M. Tomic-Canic, *Epidermal Differentiation in Barrier Maintenance and Wound Healing.* Adv Wound Care (New Rochelle), 2014. **3**(3): p. 272-280.
7. Martin, M.T., A. Vulin, and J.H. Hendry, *Human epidermal stem cells: Role in adverse skin reactions and carcinogenesis from radiation.* Mutat Res, 2016. **770**(Pt B): p. 349-368.
8. Ojeh, N., et al., *Stem Cells in Skin Regeneration, Wound Healing, and Their Clinical Applications.* Int J Mol Sci, 2015. **16**(10): p. 25476-501.
9. Fuchs, E., *Epithelial Skin Biology: Three Decades of Developmental Biology, a Hundred Questions Answered and a Thousand New Ones to Address.* Curr Top Dev Biol, 2016. **116**: p. 357-74.
10. Wynn, T.A. and K.M. Vannella, *Macrophages in Tissue Repair, Regeneration, and Fibrosis.* Immunity, 2016. **44**(3): p. 450-462.
11. Driskell, R.R., et al., *Defining dermal adipose tissue.* Exp Dermatol, 2014. **23**(9): p. 629-31.
12. Venus, M., J. Waterman, and I. McNab, *Basic physiology of the skin.* Surgery (Oxford), 2011. **29**(10): p. 471-474.
13. Singer, A.J. and R.A. Clark, *Cutaneous wound healing.* N Engl J Med, 1999. **341**(10): p. 738-46.
14. Demidova-Rice, T.N., M.R. Hamblin, and I.M. Herman, *Acute and impaired wound healing: pathophysiology and current methods for drug delivery, part 1: normal and chronic wounds: biology, causes, and approaches to care.* Adv Skin Wound Care, 2012. **25**(7): p. 304-14.

15. Zeng, R., et al., *Approaches to cutaneous wound healing: basics and future directions.* Cell Tissue Res, 2018. **374**(2): p. 217-232.
16. Eming, S.A., T.A. Wynn, and P. Martin, *Inflammation and metabolism in tissue repair and regeneration.* Science, 2017. **356**(6342): p. 1026-1030.
17. Hesketh, M., et al., *Macrophage Phenotypes Regulate Scar Formation and Chronic Wound Healing.* Int J Mol Sci, 2017. **18**(7).
18. Novak, M.L. and T.J. Koh, *Macrophage phenotypes during tissue repair.* J Leukoc Biol, 2013. **93**(6): p. 875-81.
19. Weidenbusch, M. and H.J. Anders, *Tissue microenvironments define and get reinforced by macrophage phenotypes in homeostasis or during inflammation, repair and fibrosis.* J Innate Immun, 2012. **4**(5-6): p. 463-77.
20. Gurtner, G.C., et al., *Wound repair and regeneration.* Nature, 2008. **453**(7193): p. 314-21.
21. Greaves, N.S., et al., *Current understanding of molecular and cellular mechanisms in fibroplasia and angiogenesis during acute wound healing.* J Dermatol Sci, 2013. **72**(3): p. 206-17.
22. Chang, M., *Restructuring of the extracellular matrix in diabetic wounds and healing: A perspective.* Pharmacol Res, 2016. **107**: p. 243-248.
23. Maeng, Y.S., et al., *Endothelial progenitor cell homing: prominent role of the IGF2-IGF2R-PLCbeta2 axis.* Blood, 2009. **113**(1): p. 233-43.
24. Driskell, R.R., et al., *Distinct fibroblast lineages determine dermal architecture in skin development and repair.* Nature, 2013. **504**(7479): p. 277-281.
25. Demidova-Rice, T.N., M.R. Hamblin, and I.M. Herman, *Acute and impaired wound healing: pathophysiology and current methods for drug delivery, part 2: role of growth factors in normal and pathological wound healing: therapeutic potential and methods of delivery.* Adv Skin Wound Care, 2012. **25**(8): p. 349-70.
26. Kaplani, K., et al., *Wound healing related agents: Ongoing research and perspectives.* Adv Drug Deliv Rev, 2018. **129**: p. 242-253.
27. Fu, X. and H. Li, *Mesenchymal stem cells and skin wound repair and regeneration: possibilities and questions.* Cell Tissue Res, 2009. **335**(2): p. 317-21.
28. Pang, C., et al., *An overview of the therapeutic potential of regenerative medicine in cutaneous wound healing.* Int Wound J, 2017. **14**(3): p. 450-459.
29. Werner, S. and R. Grose, *Regulation of wound healing by growth factors and cytokines.* Physiol Rev, 2003. **83**(3): p. 835-70.
30. Barrientos, S., et al., *Growth factors and cytokines in wound healing.* Wound Repair Regen, 2008. **16**(5): p. 585-601.

31. Motegi, S.I. and O. Ishikawa, *Mesenchymal stem cells: The roles and functions in cutaneous wound healing and tumor growth.* J Dermatol Sci, 2017. **86**(2): p. 83-89.
32. Gorecka, J., et al., *The potential and limitations of induced pluripotent stem cells to achieve wound healing.* Stem Cell Res Ther, 2019. **10**(1): p. 87.
33. Nour, S., et al., *A review of accelerated wound healing approaches: biomaterial-assisted tissue remodeling.* J Mater Sci Mater Med, 2019. **30**(10): p. 120.
34. Yu, J.R., et al., *Current and Future Perspectives on Skin Tissue Engineering: Key Features of Biomedical Research, Translational Assessment, and Clinical Application.* Adv Healthc Mater, 2019. **8**(5): p. e1801471.
35. Atala, A., F.K. Kasper, and A.G. Mikos, *Engineering complex tissues.* Sci Transl Med, 2012. **4**(160): p. 160rv12.
36. Khademhosseini, A. and R. Langer, *A decade of progress in tissue engineering.* Nat Protoc, 2016. **11**(10): p. 1775-81.
37. Chaudhari, A.A., et al., *Future Prospects for Scaffolding Methods and Biomaterials in Skin Tissue Engineering: A Review.* Int J Mol Sci, 2016. **17**(12).
38. Dias, J.R., et al., *In situ crosslinked electrospun gelatin nanofibers for skin regeneration.* European Polymer Journal, 2017. **95**: p. 161-173.
39. Pina, S., et al., *Scaffolding Strategies for Tissue Engineering and Regenerative Medicine Applications.* Materials (Basel), 2019. **12**(11).
40. Bidarra, S.J., C.C. Barrias, and P.L. Granja, *Injectable alginate hydrogels for cell delivery in tissue engineering.* Acta Biomater, 2014. **10**(4): p. 1646-62.
41. Winter, G.D., *Effect of Air Exposure and Occlusion on Experimental Human Skin Wounds.* Nature, 1963. **200**: p. 378-9.
42. Silva, L.P.d., et al., *Hydrogel-Based Strategies to Advance Therapies for Chronic Skin Wounds.* Annual Review of Biomedical Engineering, 2019. **21**(1): p. 145-169.
43. Quan, W.Y., et al., *Mussel-Inspired Catechol-Functionalized Hydrogels and Their Medical Applications.* Molecules, 2019. **24**(14).
44. Neves, S.C., et al., *Biofunctionalized pectin hydrogels as 3D cellular microenvironments.* Journal of Materials Chemistry B, 2015. **3**(10): p. 2096-2108.
45. Stern, D. and H. Cui, *Crafting Polymeric and Peptidic Hydrogels for Improved Wound Healing.* Adv Healthc Mater, 2019. **8**(9): p. e1900104.
46. Chen, J., et al., *Pectin modifications: a review.* Crit Rev Food Sci Nutr, 2015. **55**(12): p. 1684-98.

47. Munarin, F., M.C. Tanzi, and P. Petrini, *Advances in biomedical applications of pectin gels.* International Journal of Biological Macromolecules, 2012. **51**(4): p. 681-689.
48. Munarin, F., et al., *Biofunctional chemically modified pectin for cell delivery.* Soft Matter, 2012. **8**(17): p. 4731-4739.
49. Munarin, F., M.C. Tanzi, and P. Petrini, *Advances in biomedical applications of pectin gels.* Int J Biol Macromol, 2012. **51**(4): p. 681-9.
50. Kaya, M., et al., *Characterization of citrus pectin samples extracted under different conditions: influence of acid type and pH of extraction.* Ann Bot, 2014. **114**(6): p. 1319-26.
51. Neves, S.C., et al., *Biofunctionalized pectin hydrogels as 3D cellular microenvironments (vol 3, pg 2096, 2015).* Journal of Materials Chemistry B, 2015. **3**(42): p. 8422-8422.
52. Munarin, F., et al., *Pectin-based injectable biomaterials for bone tissue engineering.* Biomacromolecules, 2011. **12**(3): p. 568-77.
53. Noreen, A., et al., *Pectins functionalized biomaterials; a new viable approach for biomedical applications: A review.* Int J Biol Macromol, 2017. **101**: p. 254-272.
54. Pandey, N., et al., *Biodegradable Nanoparticles Enhanced Adhesiveness of Mussel-Like Hydrogels at Tissue Interface.* Adv Healthc Mater, 2018. **7**(7): p. e1701069.
55. Rahimnejad, M. and W. Zhong, *Mussel-inspired hydrogel tissue adhesives for wound closure.* RSC Advances, 2017. **7**(75): p. 47380-47396.
56. Zhu, W., et al., *A mussel-inspired double-crosslinked tissue adhesive on rat mastectomy model: seroma prevention and in vivo biocompatibility.* J Surg Res, 2017. **215**: p. 173-182.
57. Fan, C., et al., *A mussel-inspired double-crosslinked tissue adhesive intended for internal medical use.* Acta Biomater, 2016. **33**: p. 51-63.
58. Silverman, H.G. and F.F. Roberto, *Understanding marine mussel adhesion.* Mar Biotechnol (NY), 2007. **9**(6): p. 661-81.
59. Lee, H., et al., *Mussel-inspired surface chemistry for multifunctional coatings.* Science, 2007. **318**(5849): p. 426-30.
60. Lee, H., N.F. Scherer, and P.B. Messersmith, *Single-molecule mechanics of mussel adhesion.* Proc Natl Acad Sci U S A, 2006. **103**(35): p. 12999-3003.
61. Lee, B.P., J.L. Dalsin, and P.B. Messersmith, *Synthesis and gelation of DOPA-modified poly(ethylene glycol) hydrogels.* Biomacromolecules, 2002. **3**(5): p. 1038-47.

62. Yu, J., et al., *Mussel protein adhesion depends on interprotein thiol-mediated redox modulation.* Nat Chem Biol, 2011. **7**(9): p. 588-90.
63. Narkar, A.R., et al., *Effect of Ionic Functional Groups on the Oxidation State and Interfacial Binding Property of Catechol-Based Adhesive.* Biomacromolecules, 2018. **19**(5): p. 1416-1424.
64. Cencer, M., et al., *Effect of pH on the rate of curing and bioadhesive properties of dopamine functionalized poly(ethylene glycol) hydrogels.* Biomacromolecules, 2014. **15**(8): p. 2861-9.
65. Jenkins, C.L., H.J. Meredith, and J.J. Wilker, *Molecular Weight Effects upon the Adhesive Bonding of a Mussel Mimetic Polymer.* ACS Applied Materials & Interfaces, 2013. **5**(11): p. 5091-5096.
66. Mehdizadeh, M., et al., *Injectable citrate-based mussel-inspired tissue bioadhesives with high wet strength for sutureless wound closure.* Biomaterials, 2012. **33**(32): p. 7972-83.
67. Sun, X., et al., *bFGF-grafted electrospun fibrous scaffolds via poly(dopamine) for skin wound healing.* Journal of Materials Chemistry B, 2014. **2**(23): p. 3636-3645.
68. Wang, R., et al., *A Biomimetic Mussel-Inspired ε-Poly-l-lysine Hydrogel with Robust Tissue-Anchor and Anti-Infection Capacity.* Advanced Functional Materials, 2017. **27**(8): p. 1604894.
69. Guo, J., et al., *Click chemistry improved wet adhesion strength of mussel-inspired citrate-based antimicrobial bioadhesives.* Biomaterials, 2017. **112**: p. 275-286.
70. Guo, J., et al., *Synthesis and characterization of anti-bacterial and anti-fungal citrate-based mussel-inspired bioadhesives.* Biomaterials, 2016. **85**: p. 204-17.
71. Fullenkamp, D.E., et al., *Mussel-inspired silver-releasing antibacterial hydrogels.* Biomaterials, 2012. **33**(15): p. 3783-91.
72. Rego, S.J., et al., *Adhesive Bioactive Coatings Inspired by Sea Life.* Langmuir, 2016. **32**(2): p. 560-8.
73. Zhang, S., et al., *Mussel-inspired alginate gel promoting the osteogenic differentiation of mesenchymal stem cells and anti-infection.* Mater Sci Eng C Mater Biol Appl, 2016. **69**: p. 496-504.
74. You, I., et al., *Enhancement of blood compatibility of poly(urethane) substrates by mussel-inspired adhesive heparin coating.* Bioconjug Chem, 2011. **22**(7): p. 1264-9.
75. Ren, Y., et al., *Injectable hydrogel based on quaternized chitosan, gelatin and dopamine as localized drug delivery system to treat Parkinson's disease.* International Journal of Biological Macromolecules, 2017. **105**: p. 1079-1087.

76. Lee, C., et al., *Bioinspired, calcium-free alginate hydrogels with tunable physical and mechanical properties and improved biocompatibility.* Biomacromolecules, 2013. **14**(6): p. 2004-13.
77. Cox, J., *Pressure Injury Risk Factors in Adult Critical Care Patients: A Review of the Literature.* Ostomy Wound Manage, 2017. **63**(11): p. 30-43.
78. Han, W., et al., *Biofilm-inspired adhesive and antibacterial hydrogel with tough tissue integration performance for sealing hemostasis and wound healing.* Bioactive Materials, 2020. **5**(4): p. 768-778.
79. Annabi, N., et al., *Engineering a highly elastic human protein-based sealant for surgical applications.* Sci Transl Med, 2017. **9**(410).
80. Maxwell, E.G., et al., *Pectin - An emerging new bioactive food polysaccharide.* Trends in Food Science & Technology, 2012. **24**(2): p. 64-73.
81. Chen, J., et al., *Pectin Modifications: A Review.* Critical Reviews in Food Science and Nutrition, 2015. **55**(12): p. 1684-1698.
82. Munarin, F., M.C. Tanzi, and P. Petrini, *Advances in biomedical applications of pectin gels (vol 51, pg 681, 2012).* International Journal of Biological Macromolecules, 2013. **55**: p. 307-307.
83. Moreira, H.R., et al., *Injectable pectin hydrogels produced by internal gelation: pH dependence of gelling and rheological properties.* Carbohydr Polym, 2014. **103**: p. 339-47.
84. Numata, K., et al., *Silk-pectin hydrogel with superior mechanical properties, biodegradability, and biocompatibility.* Macromol Biosci, 2014. **14**(6): p. 799-806.
85. Skjak-Braek, G., E. Murano, and S. Paoletti, *Alginate as immobilization material. II: Determination of polyphenol contaminants by fluorescence spectroscopy, and evaluation of methods for their removal.* Biotechnol Bioeng, 1989. **33**(1): p. 90-4.
86. Konovalova, M.V., et al., *Preparation and biocompatibility evaluation of pectin and chitosan cryogels for biomedical application.* J Biomed Mater Res A, 2017. **105**(2): p. 547-556.
87. Markov, P.A., et al., *Mechanical properties, structure, bioadhesion, and biocompatibility of pectin hydrogels.* J Biomed Mater Res A, 2017.
88. Prabhudev, H. and A.H. Sneharani, *Extraction and characterization of pectin methylesterase from muskmelon biowaste for pectin remodeling.* J Food Biochem, 2020: p. e13237.
89. Khedmat, L., et al., *Recent advances in extracting pectin by single and combined ultrasound techniques: A review of techno-functional and bioactive health-promoting aspects.* Carbohydr Polym, 2020. **229**: p. 115474.

90. Umana, M.M., et al., *Effects of acoustic power and pH on pectin-enriched extracts obtained from citrus by-products. Modelling of the extraction process.* J Sci Food Agric, 2019. **99**(15): p. 6893-6902.
91. Stone, M.T. and M. Kozlov, *Separating proteins with activated carbon.* Langmuir, 2014. **30**(27): p. 8046-55.
92. Wang, W., et al., *Ultrasound-assisted heating extraction of pectin from grapefruit peel: optimization and comparison with the conventional method.* Food Chem, 2015. **178**: p. 106-14.
93. Munarin, F., et al., *Sterilization treatments on polysaccharides: Effects and side effects on pectin.* Food Hydrocolloids, 2013. **31**(1): p. 74-84.
94. Maxwell, E.G., et al., *Pectin – An emerging new bioactive food polysaccharide.* Trends in Food Science & Technology, 2012. **24**(2): p. 64-73.
95. Pereira, R.F., et al., *Cell-instructive pectin hydrogels crosslinked via thiol-norbornene photo-click chemistry for skin tissue engineering.* Acta Biomater, 2018. **66**: p. 282-293.
96. Ruoslahti, E. and M.D. Pierschbacher, *New perspectives in cell adhesion: RGD and integrins.* Science, 1987. **238**(4826): p. 491-7.
97. Pierschbacher, M.D. and E. Ruoslahti, *Cell attachment activity of fibronectin can be duplicated by small synthetic fragments of the molecule.* Nature, 1984. **309**(5963): p. 30-3.
98. Hou, J., et al., *Enzymatically crosslinked alginate hydrogels with improved adhesion properties.* Polymer Chemistry, 2015. **6**(12): p. 2204-2213.
99. Olde Damink, L.H., et al., *Cross-linking of dermal sheep collagen using a water-soluble carbodiimide.* Biomaterials, 1996. **17**(8): p. 765-73.
100. Lai, J.Y., L.J. Luo, and D.H. Ma, *Effect of Cross-Linking Density on the Structures and Properties of Carbodiimide-Treated Gelatin Matrices as Limbal Stem Cell Niches.* Int J Mol Sci, 2018. **19**(11).
101. Iuga, C., J.R. Alvarez-Idaboy, and A. Vivier-Bunge, *ROS initiated oxidation of dopamine under oxidative stress conditions in aqueous and lipidic environments.* The journal of physical chemistry. B, 2011. **115**(42): p. 12234-12246.
102. Umek, N., et al., *Dopamine Autoxidation Is Controlled by Acidic pH.* Front Mol Neurosci, 2018. **11**: p. 467.
103. Posati, T., et al., *Polydopamine Nanoparticle-Coated Polysulfone Porous Granules as Adsorbents for Water Remediation.* ACS Omega, 2019. **4**(3): p. 4839-4847.

104. Liu, Y., K. Ai, and L. Lu, *Polydopamine and its derivative materials: synthesis and promising applications in energy, environmental, and biomedical fields.* Chem Rev, 2014. **114**(9): p. 5057-115.
105. Cheng, C., et al., *The hydrodynamic permeability and surface property of polyethersulfone ultrafiltration membranes with mussel-inspired polydopamine coatings.* Journal of Membrane Science, 2012. **417-418**: p. 228-236.
106. Lee, M.S., et al., *Target-specific delivery of siRNA by stabilized calcium phosphate nanoparticles using dopa-hyaluronic acid conjugate.* J Control Release, 2014. **192**: p. 122-30.
107. Fraeye, I., et al., *Fine-tuning the properties of pectin–calcium gels by control of pectin fine structure, gel composition and environmental conditions.* Trends in Food Science & Technology, 2010. **21**(5): p. 219-228.
108. Montalbetti, C.A.G.N. and V. Falque, *Amide bond formation and peptide coupling.* Tetrahedron, 2005. **61**(46): p. 10827-10852.
109. Bichara, L.C., et al., *Structural and spectroscopic study of a pectin isolated from citrus peel by using FTIR and FT-Raman spectra and DFT calculations.* Infrared Physics & Technology, 2016. **76**: p. 315-327.
110. Urias-Orona, V., et al., *A novel pectin material: extraction, characterization and gelling properties.* International journal of molecular sciences, 2010. **11**(10): p. 3686-3695.
111. Klosterman, L. and C.J. Bettinger, *Calcium-Mediated Control of Polydopamine Film Oxidation and Iron Chelation.* Int J Mol Sci, 2016. **18**(1).
112. Georges, P.C. and P.A. Janmey, *Cell type-specific response to growth on soft materials.* J Appl Physiol (1985), 2005. **98**(4): p. 1547-53.
113. Discher, D.E., P. Janmey, and Y.L. Wang, *Tissue cells feel and respond to the stiffness of their substrate.* Science, 2005. **310**(5751): p. 1139-43.
114. Ghosh, K., et al., *Cell adaptation to a physiologically relevant ECM mimic with different viscoelastic properties.* Biomaterials, 2007. **28**(4): p. 671-679.
115. Chen, S., et al., *Study of stiffness effects of poly(amidoamine)-poly(n-isopropyl acrylamide) hydrogel on wound healing.* Colloids Surf B Biointerfaces, 2016. **140**: p. 574-582.
116. Han, L., et al., *Tough, self-healable and tissue-adhesive hydrogel with tunable multifunctionality.* NPG Asia Materials, 2017. **9**(4): p. e372-e372.
117. Sriamornsak, P., et al., *Cryo-scanning electron microscopy (cryo-SEM) as a tool for studying the ultrastructure during bead formation by ionotropic gelation of calcium pectinate.* Int J Pharm, 2008. **352**(1-2): p. 115-22.

118. Mao, R., J. Tang, and B.G. Swanson, *Water holding capacity and microstructure of gellan gels.* Carbohydrate Polymers, 2001. **46**(4): p. 365-371.
119. Hayflick, L., *The Limited in Vitro Lifetime of Human Diploid Cell Strains.* Exp Cell Res, 1965. **37**: p. 614-36.
120. Lee, S.Y., et al., *Microscale diffusion measurements and simulation of a scaffold with a permeable strut.* Int J Mol Sci, 2013. **14**(10): p. 20157-70.
121. Sobecki, M., et al., *Cell-Cycle Regulation Accounts for Variability in Ki-67 Expression Levels.* Cancer Res, 2017. **77**(10): p. 2722-2734.
122. Pandey, N., et al., *Biodegradable Nanoparticles Enhanced Adhesiveness of Mussel-Like Hydrogels at Tissue Interface.* Advanced healthcare materials, 2018. **7**(7): p. e1701069-e1701069.
123. Zhou, D., et al., *Dopamine-Modified Hyaluronic Acid Hydrogel Adhesives with Fast-Forming and High Tissue Adhesion.* ACS Applied Materials & Interfaces, 2020. **12**(16): p. 18225-18234.
124. Vaughn, A.R., et al., *A Concise Review of the Conflicting Roles of Dopamine-1 versus Dopamine-2 Receptors in Wound Healing.* Molecules, 2017. **23**(1).
125. Shome, S., P.S. Dasgupta, and S. Basu, *Dopamine regulates mobilization of mesenchymal stem cells during wound angiogenesis.* PLoS One, 2012. **7**(2): p. e31682.
126. Gantwerker, E.A. and D.B. Hom, *Skin: histology and physiology of wound healing.* Facial Plast Surg Clin North Am, 2011. **19**(3): p. 441-53.
127. Singh, S., A. Young, and C.-E. McNaught, *The physiology of wound healing.* Surgery (Oxford), 2017. **35**(9): p. 473-477.
128. Harries, R.L., D.C. Bosanquet, and K.G. Harding, *Wound bed preparation: TIME for an update.* Int Wound J, 2016. **13 Suppl 3**: p. 8-14.
129. Schultz, G.S., et al., *Wound bed preparation: a systematic approach to wound management.* Wound Repair Regen, 2003. **11 Suppl 1**: p. S1-28.
130. Klein, S., et al., *Evidence-based topical management of chronic wounds according to the T.I.M.E. principle.* J Dtsch Dermatol Ges, 2013. **11**(9): p. 819-29.
131. Madhok, B.M., K. Vowden, and P. Vowden, *New techniques for wound debridement.* Int Wound J, 2013. **10**(3): p. 247-51.
132. Wilkins, R.G. and M. Unverdorben, *Wound cleaning and wound healing: a concise review.* Adv Skin Wound Care, 2013. **26**(4): p. 160-3.
133. Jones, R.E., D.S. Foster, and M.T. Longaker, *Management of Chronic Wounds-2018.* JAMA, 2018. **320**(14): p. 1481-1482.
134. Han, G. and R. Ceilley, *Chronic Wound Healing: A Review of Current Management and Treatments.* Adv Ther, 2017. **34**(3): p. 599-610.

135. Li, H.Z., et al., *Negative pressure wound therapy for surgical site infections: a systematic review and meta-analysis of randomized controlled trials.* Clin Microbiol Infect, 2019. **25**(11): p. 1328-1338.
136. Vikatmaa, P., et al., *Negative pressure wound therapy: a systematic review on effectiveness and safety.* Eur J Vasc Endovasc Surg, 2008. **36**(4): p. 438-48.
137. Webster, J., et al., *Negative pressure wound therapy for surgical wounds healing by primary closure.* Cochrane Database Syst Rev, 2019. **3**: p. CD009261.
138. Peinemann, F. and A. Labeit, *Negative pressure wound therapy: A systematic review of randomized controlled trials from 2000 to 2017.* J Evid Based Med, 2019. **12**(2): p. 125-132.
139. Dai, C., S. Shih, and A. Khachemoune, *Skin substitutes for acute and chronic wound healing: an updated review.* J Dermatolog Treat, 2018: p. 1-33.
140. Vig, K., et al., *Advances in Skin Regeneration Using Tissue Engineering.* International journal of molecular sciences, 2017. **18**(4): p. 789.
141. MacNeil, S., *Progress and opportunities for tissue-engineered skin.* Nature, 2007. **445**(7130): p. 874-80.
142. Boyce, S.T. and A.L. Lalley, *Tissue engineering of skin and regenerative medicine for wound care.* Burns Trauma, 2018. **6**: p. 4.
143. Lalieu, R.C., et al., *Hyperbaric Oxygen Therapy for Non-Ischemic Diabetic Ulcers: A Systematic Review.* Wound Repair Regen, 2019.
144. Harries, R.L., D.C. Bosanquet, and K.G. Harding, *Wound bed preparation: TIME for an update.* International Wound Journal, 2016. **13**: p. 8-14.
145. Snyder, R.J., C. Fife, and Z. Moore, *Components and Quality Measures of DIME (Devitalized Tissue, Infection/Inflammation, Moisture Balance, and Edge Preparation) in Wound Care.* Advances in Skin & Wound Care, 2016. **29**(5): p. 205-215.
146. Clark, R.A., K. Ghosh, and M.G. Tonnesen, *Tissue engineering for cutaneous wounds.* J Invest Dermatol, 2007. **127**(5): p. 1018-29.
147. Krishnaswamy, V.R., D. Mintz, and I. Sagi, *Matrix metalloproteinases: The sculptors of chronic cutaneous wounds.* Biochim Biophys Acta Mol Cell Res, 2017. **1864**(11 Pt B): p. 2220-2227.
148. Ligi, D., et al., *Chronic venous disease - Part II: Proteolytic biomarkers in wound healing.* Biochim Biophys Acta, 2016. **1862**(10): p. 1900-8.
149. Eming, S.A., T. Krieg, and J.M. Davidson, *Inflammation in wound repair: molecular and cellular mechanisms.* J Invest Dermatol, 2007. **127**(3): p. 514-25.
150. Leoni, G., et al., *Wound repair: role of immune-epithelial interactions.* Mucosal Immunol, 2015. **8**(5): p. 959-68.

151. Zubair, M. and J. Ahmad, *Role of growth factors and cytokines in diabetic foot ulcer healing: A detailed review.* Rev Endocr Metab Disord, 2019.
152. Scalise, A., et al., *Microenvironment and microbiology of skin wounds: the role of bacterial biofilms and related factors.* Semin Vasc Surg, 2015. **28**(3-4): p. 151-9.
153. James, G.A., et al., *Biofilms in chronic wounds.* Wound Repair Regen, 2008. **16**(1): p. 37-44.
154. Wu, Y.K., N.C. Cheng, and C.M. Cheng, *Biofilms in Chronic Wounds: Pathogenesis and Diagnosis.* Trends Biotechnol, 2019. **37**(5): p. 505-517.
155. Omar, A., et al., *Microbial Biofilms and Chronic Wounds.* Microorganisms, 2017. **5**(1).
156. Gompelman, M., S.A. van Asten, and E.J. Peters, *Update on the Role of Infection and Biofilms in Wound Healing: Pathophysiology and Treatment.* Plast Reconstr Surg, 2016. **138**(3 Suppl): p. 61S-70S.

Supplementary Material

1. Gelation Kinetics of *in vitro* formulations tested

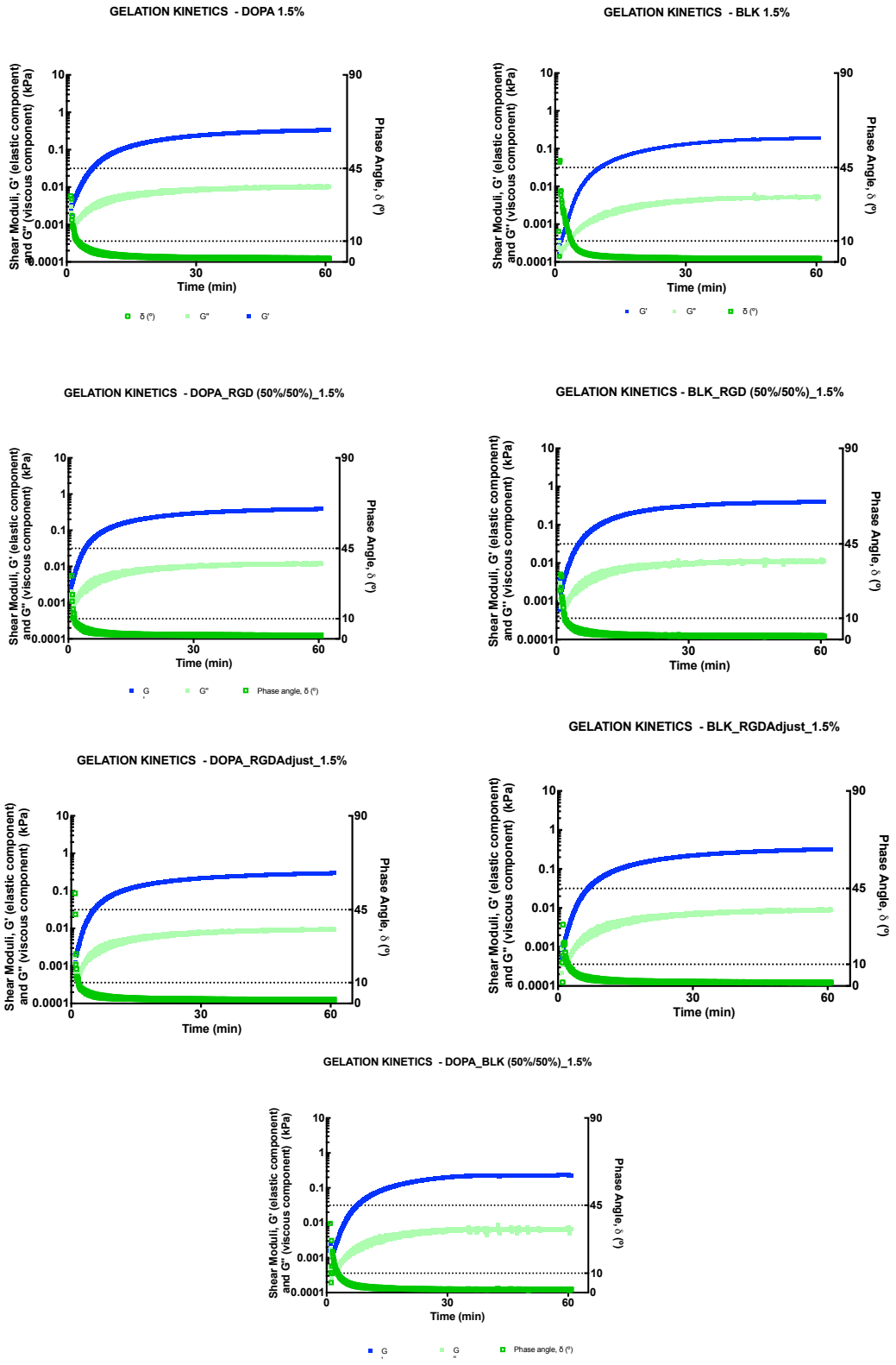

Figure S1. Representative graphs of the Gelation kinetics over time of the all *in vitro* conditions tested. solutions using R=1 (according to the eq. $R_{Ca/GDL}$ = 2 $[Ca^{2+}]/[GDL]$) between calcium ions (CalEssence ® 70) the and D-Glucone-d-lactone (GDL) content

Annexes

ANNEX I- Important Factors Influencing Wound Healing

ANNEX II- Wound Local Treatment - Wound Bed Preparation

ANNEX III- Adjuvant Wound Treatment Therapies

ANNEX IV- Chronic Wound healing

ANNEX I

Important Factors Influencing Wound Healing

Several factors will contribute actively for the final outcome of wound healing which is characterized by the rapidly recovery of skin tissue homeostasis and wound closure. This includes factors considered internal or external to wound healing and wound microenvironment, impacting the successful progression towards each stage of wound healing. Intrinsic factors include age, immune status, chronic diseases, psychophysiological stress and genetics, such as healing impaired hereditary diseases and hypertrophic scarring and keloids.[126, 127] The extrinsic factors include nutrition, infection, hypoxia, smoking, cancer, radiation, chemotherapy and medication. [126, 127] From this group of extrinsic and intrinsic factors, it's important to mention the impact of age, nutrition, hypoxia, smoking, infection, immunosuppression, chronic disease, wound management and genetics. [127]

Age

Elderly patients have a thinner epidermal layer and slower inflammatory, migratory and proliferation responses. Elderly patients are more prone to chronic illness, which in combination with the age-related skin features translates into a slower and less effective wound healing and higher risk of wound complications. [127]

Nutrition

The nutritional status of the patient can positively or negatively influence wound healing. Malnutrition and specially protein insufficiency (blood albumins less than 1.5 mg/dL) has a profound negative effect on wound healing. In cases of protein insufficiency, the inflammatory phase is prolonged and inhibition of fibroblast function occurs. Furthermore, there is the reduction of angiogenesis and collagen deposition, due to high demands of proteins for collagen synthesis.[126, 127]. Poor reserves of carbohydrates (collagen synthesis), lipids (omega-3 fatty acids modulate inflammatory activity via arachidonic acid pathway), vitamins (vitamin A involved in epidermal growth) and minerals (zinc important cofactor for wound healing), translate also into an impaired healing [126, 127].

Hypoxia

Wounds presents disrupted local vascular supply which leads to some degree of hypoxia. Despite a degree of hypoxia being necessary to the re-epithelization and has a chemoattractant effect over neutrophils and macrophages, sufficient perfusion and oxygenation are key ingredients, and the two most common causes of impaired wound healing [126, 127]. Other mechanisms involved in Wound healing that are oxygen dependent are inflammation, bactericidal activity, angiogenesis, epithelization and collagen deposition.[126]

Smoking

Smoking has a deleterious effect on the inflammatory phase wound healing affecting chemotaxis, migratory function and oxidative bactericidal mechanisms, reduce fibroblast migration and proliferation, immune function and downregulated collagen synthesis and deposition [126, 127].

Infection

Wound infection is prevented by developing a group of strategies, such as debridement of necrotic tissue, exudate management, reducing the bacterial colonization. The presence of a bacterial load higher than 10^5 per gram of tissue is an indicator for infection and delayed healing. One major goal of wound management strategies is to control factors that can lead to wound infection and retain the bacterial load below the critical threshold [126].

Immunosuppression

Patient immune status, specially any degree of immunosuppression (HIV, cancer and malnutrition) can lead to impaired wound healing. [127] Furthermore, the usage of drugs, such as steroids or immunosuppressants, the chemotherapy (downregulation of VEGF) and radiation (tissue ischemia) treatments impair the inflammatory response, with a consequent reduction in cytokines concentrations and collagen deposition, essential for wound healing responses.[126, 127]

Chronic disease

Chronic diseases affecting the cardio-respiratory system may compromise the demands of oxygen and nutrients required for adequate wound healing. Diabetic patients present poor wound healing rates. Higher glucose levels affect the leukocytes activity leading to an immune dysfunction, altered MMP expression and function, and long-term microvascular damage (neuropathy) which is related to slower collagen synthesis and

accumulation, decreased angiogenesis, poor tensile wound strength leading to deficiencies in wound healing. [126, 127]

Genetics

Hypertrophic scars and keloids are the final outcome of enhanced proliferative phase and diminished collagen lysis, characterized by an overgrowth of scar tissue, composed mainly by type III collagen (immature) and ECM (water and glycoprotein) deposition.[126] Although it can appear in individuals of all races, hypertrophic scars and keloids has a strong genetic component, manifesting more predominantly in darker-pigmented individuals and appear more commonly in body areas comprising shoulders, arms or upper chest and are rare below the waist.[126, 127]

ANNEX II

Wound Local Treatment - Wound Bed Preparation

Most of the wounds progress normally through the physiological wound healing process and rapidly heal, although a significant portion fail to progress towards wound healing process, resulting in chronic wound with high morbidity and increasing health costs [128].

The wound bed preparation concept, first published by Schultz et al., describes a structured approach to manage non-healing wounds, based on the knowledge of the wound pathophysiology and patient related factors [129]. These systematic approach to non-healing wounds precedes the foundations for the T.I.M.E. concept definition. The TIME concept takes together four fundamental principles, systematizing chronic wound care principles: **Tissue management**, **Infection/inflammation** control, **Moisture imbalance** and **Edge of wound** [130]. This systematic wound assessment should be part of the global health patient status assessment and should include the underlying pathology and patient comorbidities, important to optimize the wound care diagnostics and treatment strategy [128].

Tissue management involves the assessment for the presence of non-viable or necrotic tissue, including callus, foreign bodies, exudate, biofilm or slough. The main goal of this evaluation is to establish a proper wound cleansing and debridement strategy, according to type tissue present [128].

Infection/inflammation includes the evaluation of the etiology of wound and sources, signs and symptoms of infection or inflammation not related to infection. The addressed interventions include the application of topical antimicrobials and systemic antibiotics if necessary [128].

Moisture imbalance includes the assessment of the amount of fluid/exudate present in the wound, defining interventions towards the fluid/exudate management/control. (REF)

Edge of the wound involves assessing the characteristics of the wound edges, surrounding skin and epithelial edge advancement, developing interventions with the objective to control non-advancing or undermining wound edges. (REF)

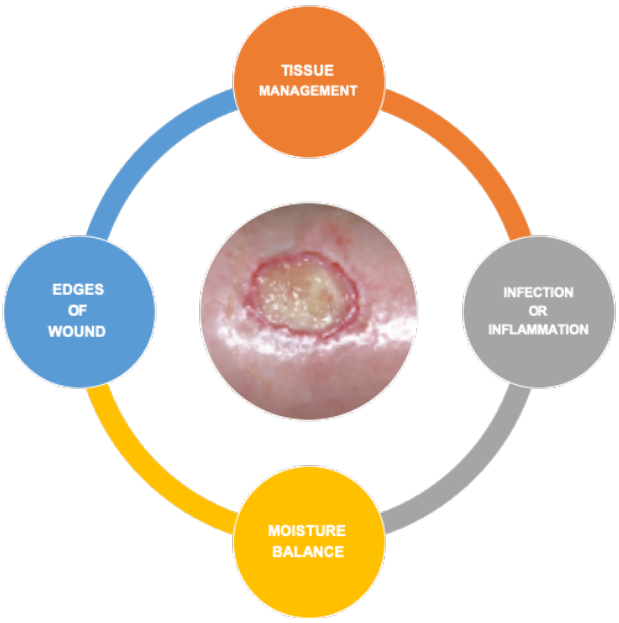

Figure 1. Schematic representation of TIME Concept for wound local treatment. The TIME concept represents the evaluation and treatment of the wound according to the Tissue Management, presence of Inflammation or Infection, Moisture Balance management and edges of the wound and wound contraction,

Tissue Management

Debridement is a key step both in acute and chronic wound management. Chronic wounds are frequently characterized by the presence of necrotic tissue, due to underlying pathogenic abnormalities leading to a continuous production of necrotic tissue. The surplus of necrotic tissue requires constant debridement to reduce necrosis and promote wound healing [129]. Tissue management involves debridement interventions to remove devitalized structures, such as, necrotic tissue, slough (or other wound coatings), foreign bodies, elimination of dead space harboring bacteria and drainage of pus, preparing the ground for wound healing.[131] The main goal of debridement is the removal of wound infected tissue or wound components that promotes a chronic inflammatory state, via proinflammatory cytokines and chemokines. [128, 130, 131]

Debridement consists in a wide variety of techniques, specifically surgical debridement, autolytic, enzymatic, chemical, mechanical, larval, hydrosurgery and ultrasonic (Table 1)

Surgical debridement is the gold standard technique and is recommended whenever is possible. Choosing the appropriate debridement technique relies on various factors: patient specificities, wound appearance, environmental factors and experience of health professional [128].

Table 1 – Currently available debridment techniques. (Adapted from [129, 130])

Debridement Method	Description
Surgical (or sharp)	Invasive method using either a curette or scalpel can be used. It includes the removal of callus, non-viable tissue, biofilm, slough and/or foreign bodies as well as debridement of wound edges and base down to healthy bleeding tissue. Surgical debridement is the gold-standard form of debridement; however, it requires skilled health professionals to perform it and appropriate local anesthesia since it carries a risk bleeding or tissue damage.
Autolytic	Uses moisturization to allow degradation by phagocytic cells, softening of necrotic tissue and liquefaction of slough. It includes moist dressings such as hydrocolloid and alginate dressings, honey dressings, hydrogels and polyacrylates. High exudative wounds may not be appropriate for this method to be used.
Enzymatic	Uses topical application of exogenous enzymes to the wound surface where they work synergistically with endogenous enzymes to debride the surface. There are several agents available in market including fibinolysin/desoxyribonuclease (fibriolysin/DNase), collagenase and papain/urea [129]. Enzymatic debridement processes are pH-dependent and the enzymes may have limited or no activity at a given pH of wound [130].
Chemical	Use of antiseptics such as silver, povidone-iodine, chlorhexidine, PHMB or octenidine can achieve debridement. Hydrogen peroxide or sodium hydrochloride can be used but have a limited role because of the toxic effects and pain experienced with their use.
Biological (Larval)	Larval therapy is a form of atraumatic selective removal of moist slough using larvae from the green bottle fly (*Lucilia sericata or Lucilia cuprina*); they can ingest pathogenic organisms but cannot remove callus.
Mechanical	Mechanical debridement uses wet to dry gauze that adhere to the top layer of the wound bed on drying, with debridement taking place on the removal of the dressing.

Hydrosurgery	Hydrosurgery consists of wound lavage through a pressurized hand piece or whirlpool. It is relatively painless and has been shown to reduce bioburden.
Ultrasonic	Low-frequency, low-dose ultrasonic-assisted debridement can be undertaken with either contact or non-contact devices. Contact devices work by cavitation and acoustic streaming, which directly agitates the wound bed. Non-contact devices work in conjunction with atomized saline. They are relatively painless, but the equipment can be expensive and not readily available.

An appropriate debridement technique should be selected based on the amount of devitalized tissue to be debrided from the wound bed, the infection status and patient status (pain sensitivity, anticoagulants therapy and risk factors). The current evidence suggests the surgical debridement as the most cost-effective methodology, and supports the usage of hydrogels, more suitable for autolytic debridement [130].

Infection and Inflammation Control

Nonhealing wounds/chronic wounds presents an unbalanced state between the different wound healing intermediates, such as inflammatory cells, cytokines, growth factors and proteases (MMPs). This could induce a continuous inflammatory phase and inability to progress to normal wound healing stages. Furthermore, current microscopic techniques reveal that, the majority of chronic wounds presents wound biofilm (60 – 90%), which is responsible for persistent infection and inflammation [128].

All chronic wounds present some grade of colonization with bacteria. However, the presence of bacteria in wound does not necessarily means that infection is present, or that it will lead to wound healing impairment [129]. Low levels of wound contamination have been attributed to a positive effect in wound microenvironment, facilitating healing through the production of proteolytic enzymes, which contribute to wound debridement and stimulation of neutrophilic leukocytes [130].

Through wound cleansing, surface contaminants, bacteria and foreign bodies are removed from the wound surface and surrounding skin. If properly applied, wound cleaning is responsible for reducing wound bioburden and delaying the development of wound biofilm, improving the wound environment and accelerating healing [132].

Besides potable tap water, which is and alternative for rapid decontamination, specially at the home care setting, there are a wide range of commercially available wound-cleansing solutions for clinical use – sterile water, sterile saline solution (Sodium

Chloride 0,9%), Ringer's solution and antiseptic solutions like polyhexanide with betaine (PHMB), octenidine dihydrochloride and iodine solutions, such as povidone-iodine and iodine cadexomer [128]. Although recent data demonstrate no difference using tap water in comparison with saline solutions and are both ineffective in reduction of wound bacteria and ameliorating wound healing rates. Still, tap water and saline solution are feasible alternatives for rapid wound decontamination [132].

The usage of topical antibiotics is contraindicated, based on the possibility of inducing antibiotic resistance and pathogen selection. Wound dressings impregnated with topical antimicrobials such as, ionic silver dressings and medical grade honey, combined with proper debridement and cleaning solutions, may be used in alternative to topical antibiotics and sufficient to treat localized infection [128, 130]. Adjuvant antibiotic treatment with oral or intravenous antibiotics should be considered, if there is visible signs of systemic infection, spreading cellulitis or lymphangitis [128].

Table 2 resumes the most important features of the antiseptic solutions and antimicrobial agents available in clinical setting.

Table 2 – Currently available wound cleansing and antiseptic solutions.

Wound Cleaning Solutions	**Indications and delivery**	**Implications in wound healing and infection rates**
Saline Solution	Wound cleansing	No significant improve in wound healing and infection rates [130].
Povidone-iodine	Antiseptic solution, dressing or ointment, with a well-defined action spectrum in comparison with other antiseptics [23, 128, 130, 132].	Not well established positive wound healing positive effects [132]. Loss of effectiveness in the presence of protein components from wound exudate [130].
Polyhexadine/Betaine (PHMB)	Wound cleaning solution or gel and acts in negatively charged phospholipid bilayers inducing leaks into bacterial cell membrane and ultimately causes cell	High biocompatibility and low toxicity. Improves healing rate by reduction of wound size, odor and exudate. Associated with improvement of patients

	death. Antibactericidal effects with decreasing wound pH [132].	quality of life because of pain reduction effect [132].
Octenidine	Antiseptic solution for wound cleansing.	High biocompatibility index[1], although, there are descriptions of unwanted side effects with edema and tissue necrosis when used under pressure or wound cavities [130].
Silver	Dressing or ointment effective against a broad spectrum of microbes, viruses and gram-positive and gram-negative bacteria.	No evidence of improvement of wound healing rates [132]. Evidence of tissue toxicity and cytotoxicity in vivo and in vitro [130].
Chlorhexidine	Solution for wound irrigation and cleaning	Evidence of toxicity and lack of evidence about efficacy correlated with the concentration [132].
Medical Grade Honey	In-vitro studies shows bactericidal properties of honey against *Pseudomonas aeruginosa, Enterococcus faecium* and MRSA [130].	No significant differences in wound healing rates and infection rates in chronic venous leg ulcers [130].

Moisture Imbalance

Exudate plays a crucial role in wound healing, responsible for activating and recruiting components of the complement immune system, ultimately assisting the autolytic debridement through phagocyte's cells attraction to wound site [128]. Excessive or reduced exudate production may compromise wound healing. Excessive amounts of exudate either can damage the surrounding skin (maceration) or potentially become a nutrient source for biofilm formation. Likewise, insufficient exudate production is responsible for eschar formation, inhibiting cellular wound healing processes [128].

[1] Biocompatibility Index – ratio between the antimicrobial effectiveness and tissue tolerance.

The moisture management within the wound bed is vital for several processes including granulation tissue formation, epithelization, degree of maceration, the susceptibility for infection and patient comfort and quality of life [130]. Managing wound exudate to optimum levels includes appropriate dressing choices that provides adequate moisture balance, avoid peri-wound skin maceration, prevent exudate leakage, easy to apply, adapting to wound dimensions and atraumatic in removal [128].

There are many different dressing materials for moisture management according to wound type and wound characteristics, such as exudate amount. They can be divided up into different generic classes: hydrocolloids, alginates, hydrogels and foams [130].

The following table (Table 3) defines the general features for each class of moisture management dressings.

Table 3 - Moisture management wound dressings characteristics (Adapted from [130])

Class	Indications, delivery and implications in wound healing rates
Hydrocolloids	Dressing composed by sodium carboxymethyl cellulose with secondary dressing. In contact with wound exudate is jellified maintaining the wound moisture. Comparative studies demonstrate that using hydrocolloids has no significant differences in healing rates when used in diabetic leg and foot ulcers, when compared with gauze dressing soaked with saline, foam dressings or silver-impregnated wound dressings.
Alginates	Alginates in contact with fluid forms gels in calcium alginate with deposition of calcium ions in the alginate structure. Meta-analysis comparing alginates with the alternative wound dressings in treatment of diabetic and venous leg ulcers, reveal no significant improve in the healing rate.
Hydrogels	Hydrogels are polymeric structures responsible for guarantee a balanced moisture environment of a dry wound bed. Comparatively to other wound healing strategies, such as dry gauze or soaked in saline solution, the healing rates of hydrogels are significant higher in diabetic ulcers. Drug delivery hydrogels (growth factors, antimicrobials, ...), that presents controlled release, depending on wound conditions, may have an increasing role in the topical therapy of chronic wounds.

Foams	Foams are widely used in clinic, as wound tamponade. Composed of polyurethane, foams enable the ingrowth of granulation tissue through their pores and present a relative permeability, allowing gas exchange. Combined with acrylates or other superabsorbers compounds, may increase the lower wound exudate absorption ability of the foams. Depending on the pore size of the foam, granulation tissue formation rate, and infection wound status, dressing changes may be extended within a week, reducing the risk of traumatic removal of granulation tissue infiltrates within the foam. No consistent comparative studies support the benefit of using foams instead of traditional saline moistened gauze dressings.

Edges of the Wound

The edges of the wound are a reliable indicator of wound contraction, tissue epithelization and treatment effectiveness. A reduction of 20 to 40 % of the total wound area after 2 to 4 weeks of treatment are considered a reliable predictor of positive outcome regarding wound healing status.[128] Wound bed granulation tissue formation is the prerequisite for cellular migration and the beginning of the epithelial tissue formation (reepithelization) from the wound edges or skin appendages. During this phase is important to assess the condition of the surrounding skin for the presence of dry or macerated edges in order to guarantee a balanced moisture environment and compensate the lack of moisture with appropriate dressings.[130] The amount of wound exudate tends to continuously decrease with the progression of granulation tissue formation and often contributes to failure of the epithelization in chronic wounds. [130]

The main strategies to tackling these problems include: proper debridement techniques, the usage of bioactive skin substitutes, autologous skin grafts and adjunctive therapies, such as, Negative Pressure Wound Therapy (NPWT) phototherapy, electromagnetic or laser therapy, to promote the epidermal tissue proliferation [128]. The current bioactive skin substitutes include cryoconserved allogenic keratinocytes, allogenic fibroblasts and full-thickness allogenic constructions of keratinocytes and fibroblasts on a collagen matrix [130].

ANNEX III

Adjuvant Wound Treatment Therapies

Wound management of complex acute (major trauma, surgical defects or burns) or chronic wounds, includes the selection of an adequate wound dressing that fulfills the wound's clinical assessment, meeting the needs to promote a rapid and proper healing. Current clinical evidence supports complementary treatment with adjuvant (advanced) wound healing options, such as NPWT, application of skin substitutes in the skin defects or Hyperbaric Oxygen therapy [133].

Negative Pressure Wound Therapy - NPWT

The NPWT is based on the principle of applying continuous or intermittent pressure, promotes the wound closure by maintaining a balanced moist environment, optimize blood flow and continuously remove exudate, reducing MMPs levels within the wound bed (Fig. 1) [128, 134]. These combined features present in NPWT devices are able to minimize some deleterious and uncontrolled factors presented in chronic or complicated wounds, such as abdominal surgical wound defects, and when compared with standard wound care are associated with reduced wound infection incidence [134, 135].

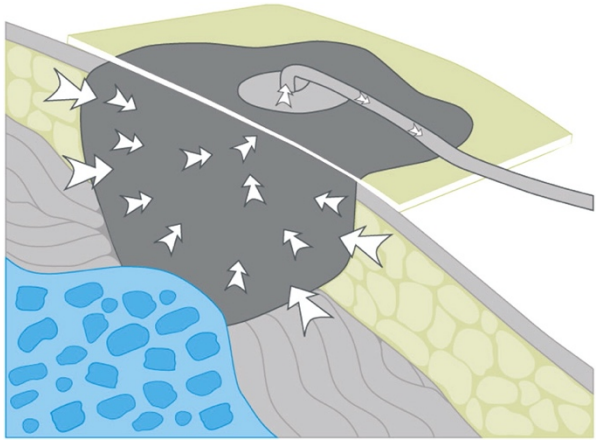

Figure 1. Schematic representation of topical Negative Pressure Wound Treatment. The wound cavity is filled with a high porosity foam (gray) that distributes constant negative pressure exerted on all tissue layers. (Adapted from Vikatmaa, P. et al [136])

Although NPWT is associated with lower infection rates, especially in surgical site infection, and improved healing rates, when compared with standard wound care in systematic reviews and meta-analysis, the evidence did not show a clear advantage of NPWT, probably attributed to some bias in RCTs [137, 138]. There's a need to establish

guidelines, defining wound clinical indications and application criteria of NPWT, in order to standardize procedures applying NPWT in patients that might benefit from it and ultimately saving unnecessary health-related costs.

Skin Substitutes

Autologous skin grafts have been widely used in significant surgical defects or burns, when it's necessary the replacement of large surface areas of skin tissue. Skin tissue engineering allowed the development of bioprosthetic skin substitutes alternatives to traditional autologous skin grafts [134].

Skin substitutes combines skin cells, such as fibroblasts and keratinocytes with biomaterials capable of mimicking the skin ECM structure [134]. Depending on the type of skin tissue present, skin substitutes can be divided into epidermal, dermal and composite (both epidermal and dermal components), according to composition and biomaterial, skin substitutes can be subdivided into autologous, xenogenic, allograft and synthetic sources (Fig. 2) [139, 140].

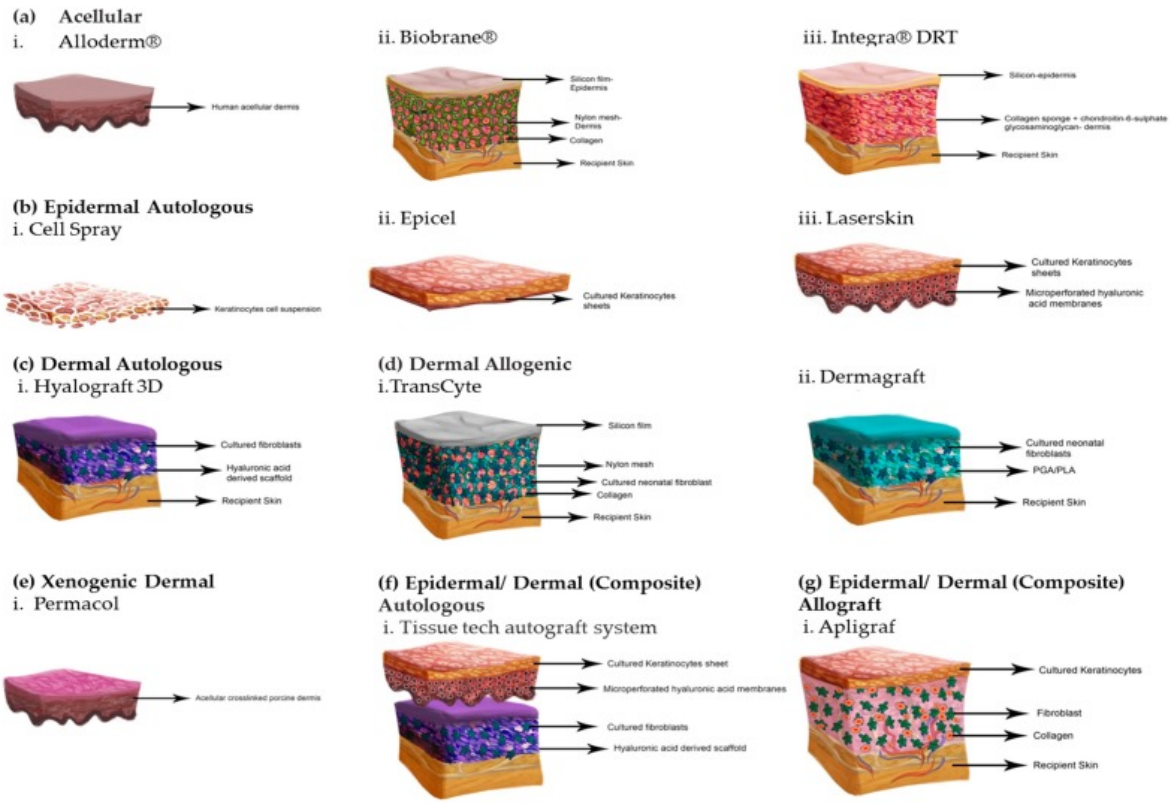

Figure 2. Tissue engineered skin substitutes types (a) Acellular (b) Epidermal Autologous (c) Dermal autologous (d) Dermal Allogenic (e) Dermal Xenogenic (f) Autologous Epidermal/Dermal (Composite) (g) Allograft Epidermal/Dermal (Composite) (Adapted from [140])

Current commercially available skin substitutes present some limitations, such as risk of infection, reduced vascularization, poor mechanical integrity, failure in host tissue integration, scarring, immune rejection [141] and lack in the ability to produce differentiated structures, such as hair, sweat glands and skin innervation. [140, 142] The development of skin substitutes is an expensive and time-consuming process involving 2-3 weeks of cell culture before its ready to use. Further investigation is necessary to fulfill the gaps of the current available skin tissue substitutes, in order to improve its clinical applications, large-scale production and reduce production costs [140].

Hyperbaric Oxygen Therapy

Hyperbaric oxygen therapy (HBOT) relies on the principle that high oxygen concentrations under atmospheric pressures greater than sea level, induce fibroblast proliferation, enhance immune function and leukocyte activity, stimulate angiogenesis, improves collagen deposition and reduces edema [134, 143].

Concerning chronic wounds, local tissue hypoxia is one of the major characteristics, therefore, the aim of HBOT is to increase oxygen supply to the wound, improving healing, and thus, preventing major wound related complications[128, 143].

Figure 3. Hyperbaric Oxygen wound therapy chamber (Adapted from Han et al [134])

Despite these potential benefits, the application of HBOT still controversial. It requires the availability of hyperbaric chamber, it's a time-consuming treatment and presents high risk of significant side effects, such as oxygen toxicity affecting the brain and pneumothorax [128, 134, 143].

Recent evidence in diabetic foot ulcers, suggests that the HBOT, either doesn't contribute to higher wound healing rates, nor prevent limb amputation, which is the major

diabetic foot ulcer complication. There's a need to perform additional research, establishing patient selection criteria, in order to identify which group of patients might benefit from this therapy [143].

ANNEX IV

Chronic Wound Healing

Wound healing is a complex, highly regulated process, depending on intricate interaction between skin cells, immune cells and growth factors, critical to maintain the barrier function of the skin [134].

A minority of wounds fail to progress normal wound healing (figure 1) resulting in chronic wounds with associated morbidity and high costs in treatments with long hospital stays and long-term outpatient follow-up visits. Patients experience pain, anxiety, loss of productivity and decreased quality of life [144, 145]. Wound etiology and patients health status are major contributing factors in wound treatment and healing [25, 145]. Chronic wounds exhibit unbalanced biochemistries, high bacterial loads, drug-resistant biofilms and hyperproliferative wound edges, producing prolonged or excessive inflammatory phase and disable cells responses to reparative stimuli [145].

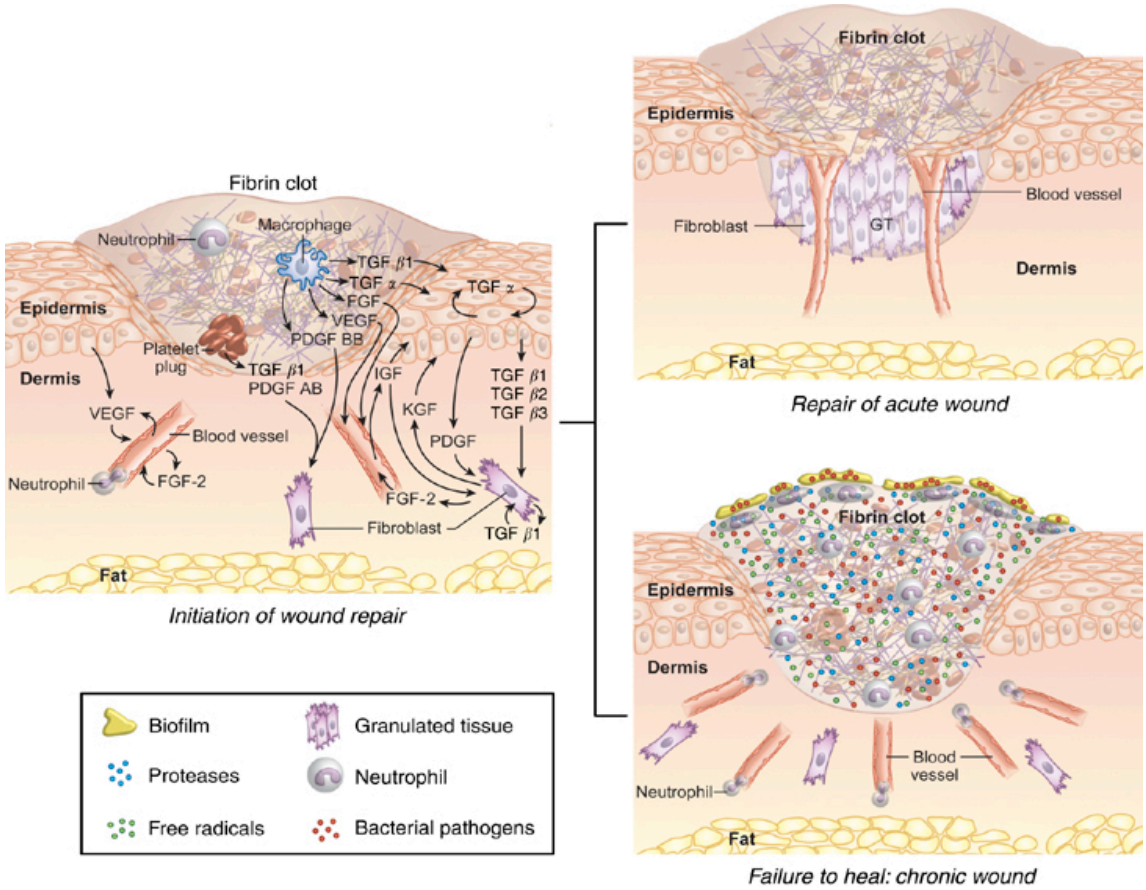

Figure 1 – Wound healing phases in acute wound repair and chronic wound. (Adapted from Clark et al. [146]

Contrasting with acute wounds, chronic wounds arise from a deviation of the physiologic wound healing mechanisms [5]. Chronic wounds are defined as break in epithelial layer continuity greater than 42 days of duration or have a frequent recurrence [21]. Chronic wound can be classified into vascular leg ulcers (VLU), such as venous or arterial leg ulcers, diabetic foot ulcers (DFU) and pressure ulcers (PU) [14].

Although these different types of chronic wounds present a different etiological motive, they also share some common features including unbalanced proteolytic activity combined with exposure of subepithelial and ECM structures, This altogether creates a propitious environment for bacterial colonization immediately after the wound formation [147, 148].

The combination of patient specific systemic factors (diabetes, vascular insufficiency, age and malnutrition) and local tissue factors (increase proteolytic activity and bacterial load) induce a persistent pathological inflammation, persistent infections, with formation of drug-resistant microbial biofilms and inability of dermal and/or epidermal cells to respond to healing stimuli, leading to wound chronicity [14, 149].

Despite the wide range of variation between the underlying mechanism of wound chronicity, the deviation of the natural physiological wound healing has locally a multifactorial cause, including factors such as, defects in blood supply (peripheral vascular diseases), compromised immune function (immunosuppression or immune deficiency), metabolic diseases (diabetes), medications, or previous local tissue injury, such as excessive moisture, sustained pressure and temperature [134].

Therefore, main characteristics of chronic wound are an unbalanced proteolytic activity inducing an excessive and prolonged inflammatory phase, along with an increased risk of wound infection, resulting in the inability of the tissue to respond to the reparative stimuli, leading to a chronically inflamed wound bed and failure to heal [21, 149].

Inflammation in Chronic Wounds

Inflammation plays a pivotal role in wound repair. Uncontrolled and prolonged inflammation impairs tissue regeneration, leading to the development of chronic wounds [150]. The prolonged inflammatory stimuli present in chronic wounds contributes to the uninterrupted recruitment of resident neutrophils into inflamed tissue (normally diminished after 24-72 hours in acute healing), perpetuating inflammatory response [150].

The imbalance between pro- and anti-inflammatory stimuli in chronic wounds is responsible for activation of keratinocytes, fibroblasts, endothelial

cells, neutrophils and macrophages, presenting increased protease expression (mainly the activation of cathepsin G, urokinase Plasminogen Activator Receptor (uPAR) and neutrophil elastase) and higher levels of ROS [21]. Reactive Oxygen Species not only are produced by leukocytes and neutrophils in response to wound bacterial load, but also senescent endothelial cells and fibroblasts, inducing damage to ECM proteins and direct cell membrane injury [21, 149]. Additionally, ROS affect selectively the signaling pathways inducing the activation of transcription factors, responsible for the controlled expression of pro-inflammatory chemokines, cytokines (IL-1, IL-6, TNF-α) and proteolytic enzymes (MMPs and serine proteases) [21, 151].

Proinflammatory cytokines are considered potent inducers, leading to unbalanced excessive activity of MMPs. Proinflammatory cytokines induction in chronic wounds, upregulates the activity of MMPs, including collagenases (MMP-1, MMP-8), stromelysins (MMP-3, MM-10 and MMP-11) and membrane type MMP (MT1-MMP), downregulating the expression of tissue inhibitors of MMPs [149].

The excessive inflammatory environment of chronic wounds, along with the increased proteolytic microenvironment of the wound bed, important mediators' determinant for wound repair are degraded by proteases. The most important targets of MMPs activity, includes protease inhibitors', α1-proteinase inhibitor, α2-macroglobulin, components of the provisional wound matrix (fibronectin and vitronectin), and growth factors responsible for wound repair (PDGF and VEGF), which are degraded or inactivated by protease activity [149].

The unbalance between oxidant and antioxidant effect observed within chronic wound microenvironment, is considered a major factor responsible for the amplification of the unrestrained and persistent inflammatory state of non-healing wounds. Therefore, the development of target therapies, effective in the disruption of the proinflammatory cycle observed within the chronic wounds, and the protection of regenerative tissue from the damage induced by chronically inflamed microenvironment, are a promising field for future therapeutic interventions [149].

Infection and Biofilms Formation in Chronic Wounds

Wound infection is considered an extrinsic factor and the most preventable factor in wound treatment. Infection is responsible for the delaying of wound healing, leading to wound chronicity, with consequent increase of morbidity (e.g. limb amputation) and mortality risk (sepsis).[14] Adult skin microbiota is composed by a wide range of commensal bacteria, fungi, viruses and parasites, which replication and growing are controlled through the interaction with host immune defenses, maintaining balance and

normally avoiding host infection [152]. Wounds are the result of the disruption of skin-barrier integrity, thus are considered contaminated. However, bacterial count higher than 10^5 viable bacteria is considered to be detrimental for wound healing and causes wound infection [14, 134, 152]. The number of bacteria itself it's a poor indicator of the impact of the bacterial load into the wound healing process, thus the medical terminology to characterize the degree of infection is based on the bacterial virulence and the host's immunological response (Table 1.)

Table 1 – Infection stages in wound healing. (Adapted from [152])

Classification	Wound characteristics
Contamination	Presence of bacteria without active proliferation.
Colonization	Presence of multiplying bacteria without triggering host immune response.
Critical Colonization	Bacterial proliferation overcomes the host immune responses.
Infection	Expanding bacterial quantity with host immune reaction in progress.

The presence of bacteria has a negative effect into the wound microenvironment, including disturbances of the lactate deposition, pH (tendency to alkalization) and the expression of cytokines and MMPs, developing a chronic pro-inflammatory state, observed in infected wounds. Persistent inflammation, leads to prolonging the presence of macrophages and neutrophils into the wound bed, changing the wound microenvironment, increasing the levels of ROS, toxins and proteases, resulting in the degradation of growth factors and inhibits the assembling of matrix components, creating a proteinaceous debris that deposit in the wound bed forming a pseudoeschar [152].

The research data from the past 2 decades, pointed out that many chronic wound infections are attributed to the biofilm mode of microbial growth [153]. Approximately 60% of chronic wounds requiring debridement have been demonstrated to be related to biofilms in comparison to acute wounds in which the biofilm was identified in only 6% of the cases [154].

Biofilms are a dynamic microenvironment, formed by multiple group of bacteria, frequently with different phenotypes, held together by extracellular polymeric substances (EPS) (approximately 90% of biofilm volume) [154]. The biofilm EPS are mainly constituted by polysaccharides, which promotes adhesion, aggregation, providing the formation of a protection barrier, and proteins along with humic substances, that

facilitates metabolic activities within the biofilm matrix [154]. This structure confers to biofilm matrix, high resistance to mechanical, chemical, immune and antimicrobial attacks. Biofilm is highly resistant to external removal attempts and demonstrate high tolerance to antimicrobial treatment, even when biofilms structure are damaged, it has self-regenerative capacity [152, 155, 156].

The microorganism population within the biofilm matrix acquires a signaling network (quorum sensing), via small organic molecules, assuming an organization similar to multicellular organism, which regulates biofilm formation, adaptation and response to injury [152].

Biofilm-related infections are characterized as persistent infections with a slow onset and progression, overwhelming the host's immune responses, unable antimicrobial effectiveness and characterized by the inability of antimicrobials to complete penetrate into the biofilm [153, 155].

Page intentionally left in blank